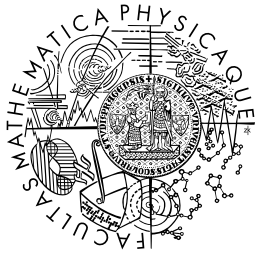

FACULTY
OF MATHEMATICS
AND PHYSICS
Charles University

MASTER THESIS

Jiří Veselý

Charged Particles in Spacetimes with an Electromagnetic Field

Institute of Theoretical Physics

Supervisor of the master thesis: RNDr. Martin Žofka, Ph.D.
Study programme: Physics
Study branch: Theoretical physics

Prague 2017

I declare that I carried out this master thesis independently, and only with the cited sources, literature and other professional sources.

I understand that my work relates to the rights and obligations under the Act No. 121/2000 Sb., the Copyright Act, as amended, in particular the fact that the Charles University has the right to conclude a license agreement on the use of this work as a school work pursuant to Section 60 subsection 1 of the Copyright Act.

Prague, 20th July 2017 Jiří Veselý

Title: Charged Particles in Spacetimes with an Electromagnetic Field

Author: Jiří Veselý

Institute: Institute of Theoretical Physics

Supervisor: RNDr. Martin Žofka, Ph.D., Institute of Theoretical Physics

Abstract: The subject of study of this thesis is the Kerr–Newman–(anti-)de Sitter space-time, a rotating and charged exact black-hole solution of the Einstein–Maxwell equations with a non-zero cosmological constant. In the first part of the thesis we examine admissible extremal configurations, present the corresponding Penrose diagrams, and investigate the effects of frame-dragging. In the second part, we follow the motion of charged particles via the Lagrangian formalism, focusing on the equatorial plane and the axis where we arrived at some analytic results concerning the trajectories. Static particles, effective potentials and – in the case of the equatorial plane – stationary circular orbits are examined. We also perform numerical simulations of particle motion to be able to check our analytic results and also to foster our intuition regarding the behaviour of the test particles. The last part concerns quantum tunnelling of particles through the space-time's horizons, specifically the null geodesic method. The main goal of these computations is to obtain horizon temperatures, in which we succeed up to a constant multiplicative factor. We discuss various pitfalls of the method and stake out a possible approach when applying it to the extreme horizons present in KN(a)dS.

Keywords: electrogeodesics, Kerr–Newman–(anti-)de Sitter, extreme black holes, geodetic structure, black hole horizons, quantum tunnelling, Hawking radiation, horizon temperature

First and foremost, I would like to thank my supervisor RNDr. Martin Žofka, Ph.D. for his patient guidance and for our many helpful and lengthy discussions on the subject, without which creating a work of this magnitude would not be possible. I am also immensely grateful to my fellow student Bc. Jakub Káninský for introducing me to the wonders of figure making in LaTeX, allowing me to effortlessly unify the graphical style of the work. Last but not least, my thanks go to all those who read the thesis...

Contents

Introduction

This year marks the centennial of Albert Einstein's introduction of the cosmological constant Λ into his general theory of relativity. At that time the large-scale structure of the universe was assumed to be static, but the original 1915's field equations did not permit a static cosmological model Einstein desired – a problem remedied by the very addition of the cosmological constant. While later developments in astronomy persuaded him to abandon this cosmological model and the constant itself, recent years have turned Einstein's self-perceived mistake into another of his achievements, as cosmologists have found another use for the constant: not to make the universe static, but to make it *less static* than it was considered to be for the most of the twentieth century, in accordance with observations concluding that the expansion of the universe is accelerating for seemingly no good reason.

Soon after the cosmological term was added to the equations, Dutch mathematician, physicist, and astronomer Willem de Sitter discovered the de Sitter space-time, also reaching its hundredth anniversary this year. It is an exact solution to the vacuum Einstein field equations with a positive cosmological constant. As it was suggested by Einstein himself that the value of the constant is positive, de Sitter did not consider an analogue with a negative cosmological constant. Therefore, this so-called anti-de Sitter solution did not emerge until years later. Interestingly, it seems as if it appeared from nowhere, since its discovery cannot be traced anywhere in the literature, possibly due to the formal similarity of the space-time with the original de Sitter one.

This thesis, however, deals with a more general space-time then that of de Sitter, specifically the Kerr–Newman–(anti-)de Sitter space-time. It is an exact solution to the Einstein–Maxwell equations with a non-zero cosmological constant of either sign and involves a massive, rotating and charged black hole. It can be considered an amalgamation of the aforementioned (anti-)de Sitter background with the asymptotically flat Kerr–Newman black hole, which was discovered in 1965 by American physicist Ezra T. Newman as an electrically-charged variant of the previous 1963's rotating solution bearing the name of Roy Kerr, a mathematician from New Zealand. By setting different parameters of the metric equal to zero, it is possible to obtain each of the solutions above from the examined general one as a limiting case, as well as the oldest nontrivial exact space-time and the "mother of all black holes": the 1916's Schwarzschild solution, discovered by German physicist and astronomer Karl Schwarzschild; its charged extension: the Reissner–Nordström metric, found independently by German aeronautical engineer Hans Reissner in 1916, German mathematician, theoretical physicist and philosopher Hermann Weyl in 1917 and Finnish theoretical physicist Gunnar Nordström in 1918; and their counterparts with a non-zero cosmological constant. Finally, by eliminating all parameters, the most radical limit leads to the Minkowski space-time – the stage of special relativity –, named after German mathematician Hermann Minkowski.

However beautiful and interesting they may be, exact solutions are merely an approximation to realistic physical situations found in the universe, since we must keep in mind the non-linearity of the Einstein equations, but they certainly offer

us a deeper insight into the theory of relativity. One important example is the Kerr space-time, as it can be used to model the vicinity of rotating astrophysical objects. Moreover, even the simpler Schwarzschild solution can be used to explain one of the fundamental mysteries incompatible with classical mechanics, showing the need for a better theory, namely the perihelion precession of Mercury – even though Einstein's original explanation relied on his own approximate solution to the field equations. Our space-time, being a generalisation of both Schwarzschild and Kerr solutions, can be also used in such a context. However, one must keep in mind that electric charge is usually considered negligible in real black holes, as macroscopic objects tend to be neutral (a limit that can be performed easily in the chosen metric). As for the cosmological constant, even though a positive cosmological constant corresponds to current observations, its observed value is small and its effects only dominate the influence of the black hole itself over larger distances. However, far from the black hole one cannot assume that the model poses a viable approximation of real situations, because one cannot neglect the influence of other astrophysical matter there, exerting gravitational effects of its own. Nonetheless, adding the cosmological constant is a step towards higher precision of the model regardless of the distance from the singularity.

Although the cosmological constant is considered to be positive, for the sake of completeness we shall not prefer one sign over the other in our investigations. Considering a cosmological constant of the opposite sign may have its uses as well, for example in the so-called AdS/CFT correspondence in string theory [1, 2].

The thesis is divided into three parts followed by three appendices. While the main topic of the work is motion of charged test particles in the examined space-time, in the first part of the presented thesis we study some general properties of the metric itself: Firstly, we verify that the Einstein–Maxwell field equations are indeed satisfied. Then, we delve into the problem of extremal scenarios when generally different horizons merge. We manage to find the conditions the parameters of the metric must satisfy in order to produce a certain horizon arrangement, we draw conformal diagrams of the extremal scenarios and compare our results with those for extremal Kerr–Newman black hole. We close the chapter by observing some effects of frame-dragging.

In the second part, we primarily examine motion of charged test particles in the Lagrangian formalism. Problems of motion of charged particles in the Kerr–Newman solution and of uncharged particles in the Kerr–(anti-)de Sitter space-time have recently been studied [3, 4], albeit using the Hamilton–Jacobi equation. We aim to undertake the next logical step of bringing both charged particles and a non-vanishing cosmological constant into play, focusing solely on the equatorial plane and the space-time's axis. After establishing the formalism and determining the integrals of motion, we first study the problem of static particles. Next, we examine stationary circular orbits and the effective potential for equatorial motion. The chapter ends with radial motion on the axis, where we manage to find an interesting alternative effective potential to describe the turning points. For photon motion, we utilise the near-horizon approximation to find null geodesics in a horizon's neighbourhood.

In the considerably shorter third part, we set out to investigate the null geodesic tunnelling method as proposed by Maulik K. Parikh and Frank Wilczek [5]. The method models black hole radiation using a semi-classical approx-

imation of quantum mechanics. Unlike the earlier works by Stephen W. Hawking based on the quantum field theory [6, 7], this approach enforces the conservation of energy through the back-reaction of the metric and can, therefore, lead to more relevant results. As an added bonus, the calculations required by the tunnelling method are also much simpler than those in Hawking's works. After introducing the method, we shall try to apply it to the horizons in the Kerr–Newman–(anti-)de Sitter space-time in hopes of determining their temperatures, pointing out various inconsistencies plaguing the literature along the way.

Finally, the first two appendices are dedicated to alternative approaches to the studied problem of motion: One analyses an (almost) equivalent Lagrangian and the other derives the Carter constant using the Hamilton–Jacobi equation without further drawing any consequences for particle motion. Last but not least, the final appendix is mathematical, introducing methods of determining the number of positive roots a polynomial has.

Tensor & unit formalism

Tensors are used to describe physical quantities in the general theory of relativity. We shall make use of the standard tensor index notation, where the upper indices are contravariant ("vector") and the lower are covariant ("covector").

As usual, Greek indices range from 0 to 3 and Latin indices from 1 to 3, the zeroth index corresponding to the time-like coordinate. For the sake of clarity, in specific cases we shall write the symbol denoting the given coordinate, not the corresponding number.

In the presented formulae we work with the usual Einstein summation convention where one should automatically assume summation over two opposite identical indices in a tensor or a product of tensors unless specifically stated otherwise.

The used signature of the metric tensor is $(-+++)$. Time-like vectors, therefore, have negative magnitude.

This thesis uses the geometrized unit system in which the speed of light c and the gravitational constant G are set equal to unity. When assigning specific values to physical quantities, we shall either express them as a multiple of another quantity of the same dimension, or we shall make use of an arbitrary unit of length denoted u.

1. The space-time

The space-time we shall be investigating is the Kerr–Newman–(anti-)de Sitter solution with the standard Boyer-Lindquist-type coordinates [8]. The line element reads

$$\begin{aligned} \mathrm{d}s^2 = -\frac{\Delta_r}{\Xi^2\rho^2}\left(\mathrm{d}t - a\sin^2\theta\,\mathrm{d}\phi\right)^2 + \frac{\rho^2}{\Delta_r}\mathrm{d}r^2 + \frac{\rho^2}{\Delta_\theta}\mathrm{d}\theta^2 + \\ + \frac{\Delta_\theta \sin^2\theta}{\Xi^2\rho^2}\left(a\mathrm{d}t - (r^2+a^2)\mathrm{d}\phi\right)^2 , \end{aligned} \tag{1.1}$$

where

$$\begin{aligned} \rho^2 &= r^2 + a^2\cos^2\theta\,, \\ \Delta_r &= (r^2+a^2)(1-\tfrac{1}{3}\Lambda r^2) - 2mr + q^2\,, \\ \Delta_\theta &= 1 + \tfrac{1}{3}\Lambda a^2\cos^2\theta\,, \\ \Xi &= 1 + \tfrac{1}{3}\Lambda a^2\,. \end{aligned} \tag{1.2}$$

This space-time describes a rotating electrically-charged black hole with mass m, angular momentum per unit energy[1] a and charge q in a background universe with a non-zero cosmological constant Λ. The space-time has a ring singularity located at $r = 0$, $\theta = \pi/2$. It is a stationary and axially-symmetrical electrovacuum solution of the Einstein–Maxwell equations with the four-potential[2]

$$A = -\frac{qr}{\Xi\rho^2}\left(\mathrm{d}t - a\sin^2\theta\,\mathrm{d}\phi\right)\,. \tag{1.3}$$

In order to retain the Lorentzian signature of the metric for all $\theta \in [0,\pi]$, we require

$$\tfrac{1}{3}\Lambda a^2 > -1 \Leftrightarrow \Xi > 0\,. \tag{1.4}$$

$\Delta_\theta(\theta)$ is then always positive. If $\Lambda > 0$, this condition is irrelevant as it is fulfilled for any a.

These coordinates make it very easy to see that setting a particular set of parameters equal to zero indeed yields a simpler "household-name" space-time: e.g. one gets the Reissner–Nordström solution by considering $\Lambda = a = 0$.

The solution can contain up to four distinct horizons, which can be found as the roots of $\Delta_r(r)$. Aside from the inner and outer black hole horizons R_I and R_O, which can be found in space-times of the Kerr and Reissner–Nordström families even for a vanishing Λ, for a positive Λ two so-called cosmological horizons $R_{\mathrm{C}-}$ and $R_{\mathrm{C}+}$ appear. If all four horizons are present, it holds that

$$R_{\mathrm{C}-} < 0 < R_\mathrm{I} < R_\mathrm{O} < R_{\mathrm{C}+}\,. \tag{1.5}$$

However, for a particular combination of the space-time's parameters, certain horizons may merge, leading to extremal scenarios, or disappear altogether.

[1] The orientation of the ϕ coordinate is chosen in such a way that angular momentum a is positive.

[2] [8] erroneously states that the inclusion of a non-zero cosmological constant to the Kerr–Newman solution does not require any changes in the four-potential, while, in fact, it needs to be divided by $\Xi(\Lambda)$. In the case of $\Lambda = 0$, it holds that $\Xi = 1$ and we correctly obtain the original Kerr–Newman four-potential.

The addition of the cosmological constant to the Kerr–Newman solution is a much more dramatic change than the transition from the Kerr to the Kerr–Newman space-time by adding charge, not only because of the addition of the two horizons for $\Lambda > 0$. Due to the presence of the cosmological term, this solution is not asymptotically flat. Current observations [9] suggest that we live in a universe with a positive cosmological parameter

$$\Omega_\Lambda \equiv \frac{\Lambda c^2}{3H_0^2} = 0.6911 \pm 0.0062\,, \tag{1.6}$$

where $H_0 = (67.74 \pm 0.46)$ km s^{-1} Mpc^{-1} is the present-day Hubble parameter. From there, we get

$$\Lambda = (1.11 \pm 0.02)\, 10^{-52}\ \mathrm{m}^{-2}\,. \tag{1.7}$$

However, the most massive astrophysical black holes ever observed have masses of the order of [10]

$$M_{\mathrm{max}}^{\mathrm{BH}} = 10^{10} M_\odot \approx 1.5 \times 10^{13}\,\mathrm{m}\,. \tag{1.8}$$

As astrophysical black holes satisfy $a \lesssim m$, then

$$\Lambda a^2 \lesssim \Lambda m^2 \lesssim \Lambda\Big(M_{\mathrm{max}}^{\mathrm{BH}}\Big)^2 \approx 2.5 \times 10^{-26} \ll 1 \tag{1.9}$$

and Λ can therefore be treated locally as a perturbation of the Kerr–Newman metric. Nonetheless, its addition has far-reaching consequences for the space-time. For it to have a measurable effect, we need $\Lambda r^2 > 1$, which occurs for sufficiently large radii.

Unlike the standard Euclidean spherical coordinates, the Boyer-Lindquist radial coordinate r is extended into negative values. These are hidden behind the black hole horizons (if there are any) within the inner region of the black hole. It is natural for us to assume that we live in the outer region[3]. We shall, therefore, place greater emphasis on positive values of r.

The equatorial plane, which lies at $\theta = \pi/2$, is the plane of reflection symmetry of the space-time: In the corresponding symmetry transformation, the spatial components of x^μ transform as $\vec{x} = (r, \theta, \phi) \to \vec{x}' = (r, \pi - \theta, \phi)$. The only functions of θ that $g_{\mu\nu}$ and A_μ contain are $\cos^2\theta$ and $\sin^2\theta$. As both of these functions are even with respect to the symmetry in question, the whole space-time is indeed symmetric as well.

Later on, when charts with spatial slices of the space-time begin to appear, the axes will be labelled with coordinates obtained using the standard Cartesian transformation relations[4]

$$\begin{aligned} x &= r\sin\theta\cos\phi\,,\\ y &= r\sin\theta\sin\phi\,,\\ z &= r\cos\theta\,. \end{aligned} \tag{1.10}$$

Typically, we shall be interested in the equatorial plane at $\theta = \pi/2$ with

$$\begin{aligned} x &= r\cos\phi\,,\\ y &= r\sin\phi\,,\\ z &= 0\,, \end{aligned} \tag{1.11}$$

[3] A static observer in the area with negative r would be, among other things, always subjected to a naked singularity.

[4] We shall only draw charts of the area with $r > 0$.

or slices with constant ϕ: Due to the axial symmetry of the space-time, we can take $\phi = 0$ and use

$$\begin{aligned} x &= r \sin\theta \,, \\ y &= 0 \,, \\ z &= r \cos\theta \,. \end{aligned} \tag{1.12}$$

In fact, in this case x corresponds to the cylindrical radial coordinate, i.e. it determines the distance from the axis of symmetry.

1.1 Verification of the Einstein–Maxwell equations

Being an exact solution of the Einstein–Maxwell equations, the Kerr–Newman–(anti-)de Sitter space-time should satisfy both Einstein's equations of the gravitational field with the cosmological term

$$G_{\mu\nu} + \Lambda g_{\mu\nu} = 8\pi T_{\mu\nu} \tag{1.13}$$

and Maxwell's equations

$$F^{\mu\nu}{}_{;\nu} = 4\pi J^{\mu} \,, \tag{1.14}$$

$$F_{[\mu\nu;\rho]} = 0 \,. \tag{1.15}$$

The latter of Maxwell's equations is satisfied immediately from the definition of the electromagnetic field tensor $F_{\mu\nu} \equiv A_{\nu;\mu} - A_{\mu;\nu}$. For the four-potential given by (1.3), the only non-vanishing independent elements of the electromagnetic tensor are

$$\begin{aligned} F_{tr} &= \frac{q}{\Xi\rho^4}\left(-r^2 + a^2\cos^2\theta\right) , & F_{t\theta} &= \frac{q}{\Xi\rho^4}\left(ra^2 \sin 2\theta\right) , \\ F_{\phi r} &= \frac{q}{\Xi\rho^4}\left((r^2 - a^2\cos^2\theta)a\sin^2\theta\right) , & F_{\phi\theta} &= \frac{q}{\Xi\rho^4}\left(-r(r^2+a^2)a\sin 2\theta\right) . \end{aligned} \tag{1.16}$$

Since the Kerr–Newman–(anti-)de Sitter space-time represents an electrovacuum, its stress-energy tensor is the electromagnetic one,

$$T_{\mu\nu} \equiv \frac{1}{4\pi}\left(F_{\mu}{}^{\alpha}F_{\nu\alpha} - \frac{1}{4}g_{\mu\nu}F^{\alpha\beta}F_{\alpha\beta}\right) . \tag{1.17}$$

When substituted into, Einstein's equations (1.13) for our space-time hold true and Maxwell's equation (1.14) gives us a vanishing four-current J^{μ}. This correctly corresponds to electrovacuum – the source of gravity and the electromagnetic field is located within the singularity (which cannot be reasonably described using tensors such as J^{μ}) and, as such, there should be no currents in the "outer" space-time. All things considered, the Kerr–Newman–(anti-)de Sitter space-time and the corresponding electromagnetic field (1.16) is indeed an exact solution of the Einstein–Maxwell equations.

1.2 Extremal horizons

Before we move on to study electrogeodesics, it may be worthwhile to study the allowed extremal scenarios. Not only can these special conditions make our pursuit of electrogeodesics mathematically easier since their parameters are constrained and the resulting expressions can be reduced in some cases, but also – and more importantly – they offer us a less complicated view of the examined space-time, which might in turn help us understand the more general cases. A black hole becomes extremal only under a certain combination of its parameters, which reduces the number of degrees of freedom of the space-time. The description of an extremal black hole is then simpler than that of a non-extremal black hole or a naked singularity, which may lead to the anticipated simplification of the equations of motion. Extremal black holes can be recognised from the behaviour of their horizons: in extremal situations at least two of the originally separate horizons merge. Therefore, in order to construct extreme black holes out of the Kerr–Newman–(anti-)de Sitter space-time, we first need to analyse the horizons.

The horizons of the studied space-time are the roots of $\Delta_r(r) = 0$ with $\Delta_r(r)$ given by (1.2). A form that is somewhat more convenient for our purposes is

$$\Delta_r(r) = -\frac{\Lambda}{3}\left(r^4 + \left(a^2 - \frac{3}{\Lambda}\right)r^2 + \frac{6m}{\Lambda}r - \frac{3(a^2+q^2)}{\Lambda}\right). \tag{1.18}$$

Since $\Delta_r(r)$ is a polynomial of degree four, $\Delta_r(r) = 0$ is a quartic equation with up to four different complex roots.

The absolute term, a^2+q^2, is greater than zero for all real a, q except $a = q = 0$. The leading term's coefficient, $-\Lambda/3$, determines the polynomial's behaviour and the coefficient's sign gives the polynomial's sign for $r \to \pm\infty$. For $\Lambda > 0$ the polynomial tends to $-\infty$ and – because all polynomials are continuous – it has at least one positive and at least one negative root. However, for $\Lambda < 0$ the polynomial tends to $+\infty$ and it may not have any real roots. The case of $\Lambda = 0$ shall not be discussed in this work. The properties of the Kerr–Newman solution are well known and its electrogeodesics have already been examined [3].

In order to get the conditions the parameters need to satisfy for the space-time to become that of a specific extremal black hole, it is useful to compare (1.18) with the required factorisation of the polynomial. The most general one would be

$$\Delta_r(r) = -\frac{\Lambda}{3}(r-A)(r-B)(r-C)(r-D), \tag{1.19}$$

where A, B, C and D are a set of generally but not necessarily different complex numbers, which, if real, would represent the horizons. After multiplying all the factors together, the coefficients in the resulting polynomial must be equal to those in the original one. We then get four equations, one for every power of r (not counting a trivial one for r^4), which should impose four conditions on the "unknowns": the positions of the horizons and the four parameters of the space-time – mass m, angular momentum per unit energy a, charge q and the cosmological constant Λ. The number of variables varies depending on our desired choice of horizon multiplicities, with every distinct horizon position representing a new variable. The total count of variables is at least five (for a single horizon of multiplicity four) and at most eight (for four horizons of multiplicity one).

Since we only have four conditions, every solution will contain at least one free parameter. The free parameters will be chosen separately for every case in such a way that allows for the most elegant description of results[5]. However, even these parameters may need to satisfy certain requirements (in the form of inequalities, not equalities) in order to represent physically acceptable results.

Such a general factorisation as the one above (especially with complex variables) does not impose any conditions on the physical parameters of the metric at all, we need to be more specific. Optimally, we would be able to express A, B, C and D using all the space-time parameters as free parameters and then study the values of the parameters that would allow A, B, C and D to be real and therefore represent physical horizons. For our space-time, however, such a task proves to be significantly more difficult than it is useful, as we are – for the time being – not interested in non-extremal black holes. That being said, this does not mean there is nothing to be gained from it. Should we only take the very first step and compare the coefficient at r^3 in the general factorisation with the corresponding coefficient in (1.18), we immediately get

$$A + B + C + D = 0\,, \tag{1.20}$$

a simple condition that the roots of Δ_r need to satisfy. This relation holds no matter whether the roots are real (and therefore represent the horizons) or not. As stated previously, our intention to study extremal black holes implies that there will be fewer horizons, but some will be of higher multiplicity than one. In this case, if the roots are real, the last equation translates to

$$\sum_i m_i R_i = 0\,, \tag{1.21}$$

where R_i is the position of horizon i and m_i is its multiplicity. It is interesting to note that this relation does not depend on the parameters of the space-time as long as we study the Kerr–Newman–(anti-)de Sitter solution.

Now, let us begin investigating specific scenarios. We shall investigate every single type of extremal black hole with no disappearing horizons[6]: 4, 3+1, 2+2 and 2+1+1. Afterwards, we shall proceed to examine extremal models with at least one horizon disappearing. These models include horizons 3, 2+1 and 2. The effects of parameter perturbations will be investigated next, followed by conformal diagrams of the extremal scenarios. The section ends with a brief comparison of our extremal models with those of the Kerr–Newman family with emphasis on the astrophysically-relevant cases.

1.2.1 The inadmissible scenarios: horizons 4 & 2+2

First, for the sake of completeness, we shall list the unphysical extremal black holes of the Kerr–Newman–(anti-)de Sitter space-time, beginning with the most extremal black hole, where all the four horizons merge. The corresponding factorisation is then considerably simpler than the general one,

$$\Delta_r(r) = -\frac{\Lambda}{3}(r - A)^4 = -\frac{\Lambda}{3}(r^4 - 4Ar^3 + 6A^2r^2 - 4A^3r + A^4)\,, \tag{1.22}$$

[5] That being said, it is preferable to keep Λ as a free parameter, because from the astrophysical point of view its value is known and fixed.

[6] We shall adopt a simple labelling convention of the situations, where $m_{i_1}+m_{i_2}+...$ represents a scenario of horizons with multiplicities m_{i_1}, m_{i_2}, ...

where A is the unknown position of the assumed extremal horizon, a real number. Comparing the coefficients with (1.18), we get the following equations

$$\begin{aligned} r^3 &: -4A = 0\,, \qquad & r^2 &: 6A^2 = a^2 - \tfrac{3}{\Lambda}\,, \\ r^1 &: -4A^3 = \tfrac{6m}{\Lambda}\,, & r^0 &: A^4 = -\tfrac{3(a^2+q^2)}{\Lambda}\,. \end{aligned} \tag{1.23}$$

Solving these equations, we find out that this particular extremal black hole would only occur when $m = 0$, $a^2 = 3/\Lambda$ and $q^2 = -3/\Lambda$ with Λ as the sole remaining free parameter. The horizon would then be located at $A = 0$, which is consistent with (1.21) and quite dubious in itself. The conditions above can never actually be met: for $\Lambda > 0$ charge q is purely imaginary whereas for $\Lambda < 0$ it is angular momentum a that is purely imaginary, which contradicts our common experience and is not easy to interpret. Hence, this extremal black hole never occurs.

A similar situation arises in the case of two horizons both of multiplicity two, where complex numbers are unavoidable as well. The factorisation is

$$\begin{aligned} \Delta_r(r) &= -\frac{\Lambda}{3}(r-B)^2(r-C)^2 = \\ &= -\frac{\Lambda}{3}\left(r^4 - 2(B+C)r^3 + (B^2+4BC+C^2)r^2 - 2BC(B+C)r + B^2C^2\right)\,. \end{aligned} \tag{1.24}$$

In the same way as before we can find out that, using Λ and a as the free parameters, this scenario requires $m = 0$ and

$$q^2 = -\frac{\Lambda}{12}\left(\frac{3}{\Lambda} + a^2\right)^2\,. \tag{1.25}$$

The horizons would then be located at

$$B = \sqrt{\frac{3}{2\Lambda} - \frac{a^2}{2}} = -C\,, \tag{1.26}$$

assuming $B > C$ without loss in generality, which is possible due to the symmetry of the factorisation with respect to B and C. From these last two results we can easily see that this black hole is unphysical too – for B and C to be real, we inevitably need Λ to be positive. However, q^2 would then be negative, which means that q would be, once again, purely imaginary.

1.2.2 Horizons 1+3

A scenario that leads to real results is that of two horizons, one of multiplicity one (denoted R_1) and the other of multiplicity three (R_3). The factorisation is

$$\begin{aligned} \Delta_r(r) &= -\frac{\Lambda}{3}(r-R_1)(r-R_3)^3 = \\ &= -\frac{\Lambda}{3}\left(r^4 - (3R_3+R_1)r^3 + 3(R_3^2+R_1R_3)r^2 - (R_3^3+3R_1R_3^2)r + R_1R_3^3\right)\,. \end{aligned} \tag{1.27}$$

By comparing this formula with (1.18) in the same manner as before we obtain these results:

$$\begin{aligned} a^2 &= \frac{3}{\Lambda} - 6R_3^2\,, \quad R_3 = \sqrt[3]{\frac{3}{4}\frac{m}{\Lambda}}\,, \\ q^2 &= \Lambda R_3^4 - a^2\,, \quad R_1 = -3R_3 \end{aligned} \tag{1.28}$$

with m and Λ being the free parameters. Note that the condition (1.21) is satisfied, $R_1 + 3R_3 = 0$. For arbitrary[7] real $m > 0$ and $\Lambda \neq 0$ both horizons are real. However, an additional condition needs to be imposed on the ratio of m and Λ to make sure that a and q are both real: it must hold true that $a^2 \geq 0$ and $q^2 \geq 0$, which means

$$0 \leq \frac{3}{\Lambda} - 6\left(\frac{3}{4}\frac{m}{\Lambda}\right)^{\frac{2}{3}} \leq \Lambda\left(\frac{3}{4}\frac{m}{\Lambda}\right)^{\frac{4}{3}}\,. \tag{1.29}$$

The first inequality is equivalent to

$$0 < \Lambda \leq \frac{2}{9}\frac{1}{m^2} \approx 0.22/m^2\,, \tag{1.30}$$

while the second one to

$$\Lambda \geq \frac{16(26\sqrt{3}-45)}{3}\frac{1}{m^2} \approx 0.18/m^2\,. \tag{1.31}$$

Fortunately, both conditions are compatible. Hence, for any $m > 0$ the corresponding range of acceptable values of Λ is

$$\Lambda \in \left[\frac{16(26\sqrt{3}-45)}{3m^2}, \frac{2}{9m^2}\right]\,, \tag{1.32}$$

or, inversely,

$$m^2 \in \left[\frac{16(26\sqrt{3}-45)}{3\Lambda}, \frac{2}{9\Lambda}\right]\,. \tag{1.33}$$

Now that we know $\Lambda > 0$ it is clear that R_3 is positive and R_1 negative.

On the following page, in *The Little Prince*-esque figure 1.1 one can see the course of $\Delta_r(r)$ in the vicinity of the horizons for a set of space-time parameters satisfying the conditions above.

Having considered Λ and m as the free parameters, we were actually not prohibited from using any other pair of the space-time parameters to fulfil this function, even though it may have led to more complicated expressions. For example, in order to compare the space-time with the non-extremal Kerr solution, it may be advantageous to have m and a as free parameters, because these also are the free parameters in the Kerr solution. Let us then reformulate the 1+3 horizon problem using m and a as the free parameters:

To do so, we shall use formulae (1.28). From the top right one we get

$$\Lambda = \frac{3}{4}\frac{m}{R_3^3}\,, \tag{1.34}$$

[7] If the mass is equal to zero, we get one horizon of multiplicity four, which, as we have already discussed, is not an acceptable solution.

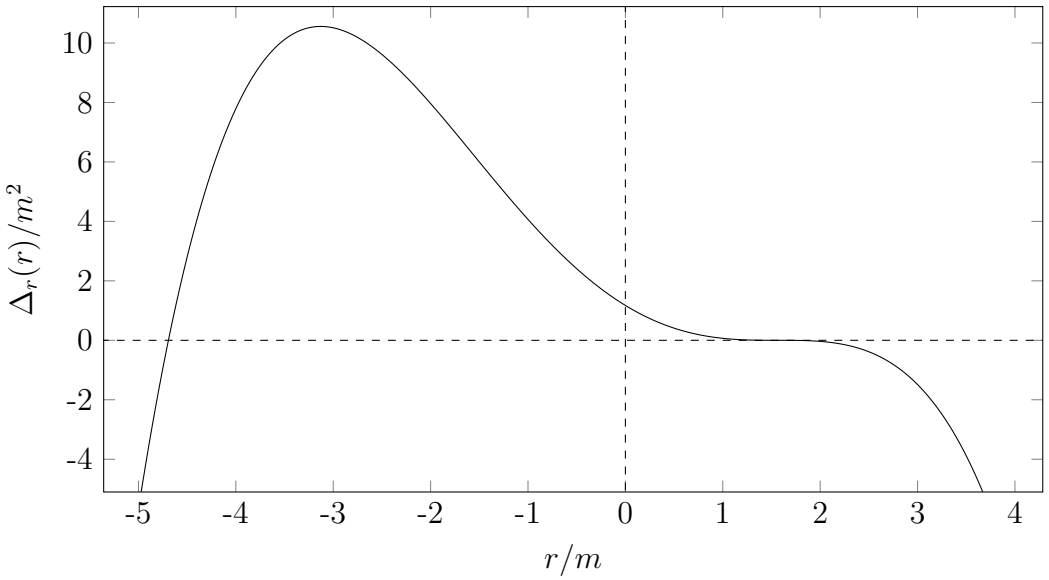

Figure 1.1: The course of $\Delta_r(r)$ corresponding to the 1+3 scenario with parameters $\{\underline{\Lambda}, \underline{m}, a, q\} = \{10^{-3}\,\mathrm{u}^{-2}, 14\,\mathrm{u}, 11.09\,\mathrm{u}, 10.34\,\mathrm{u}\}$. The values of the free parameters (underlined) are precise, the values of the dependent parameters are rounded to two decimal places.

and, after substituting this Λ into the top left formula, we obtain an equation for R_3 as a function of m and a

$$R_3^3 - \frac{3}{2}mR_3^2 - \frac{1}{4}ma^2 = 0\,, \tag{1.35}$$

which clearly has a positive root (Λ is, therefore, positive as well, consistently with the previous approach). It can be found using Cardano's formula[8],

$$R_3 = \frac{m}{2}\left(x + 1 + x^{-1}\right) \tag{1.36}$$

with

$$x = \frac{m^{2/3}}{(m^2 + a^2 + a\sqrt{2m^2 + a^2})^{1/3}}\,. \tag{1.37}$$

Again, the bottom two equations in (1.28),

$$\begin{gathered} q^2 = \Lambda R_3^4 - a^2 = \frac{3}{4}mR_3 - a^2\,, \\ R_1 = -3R_3\,, \end{gathered} \tag{1.38}$$

allow us to find q^2 and R_1, this time as functions of m and a, after substituting for R_3 from the expression above. Once more, an additional condition needs to imposed on the free parameters to make sure that q is indeed real,

$$a^2 \in \left[0, \frac{3}{16}(3 + 2\sqrt{3})m^2\right] \tag{1.39}$$

for arbitrary $m > 0$. Interestingly, for a vanishing a (i.e. an extremal Reissner–Nordström–de Sitter black hole) it holds that $x = 1$ and the position of the triple

[8]The other roots are not real.

horizon is simply $R_3 = \frac{3}{2}m$, which is closer to the singularity than the horizon of the Schwarzschild black hole of the same mass at $2m$, but farther away than that of an extremal Reissner–Nordström black hole at m. As for all $a = 0$ limits, in this case the singularity reduces into a point and it is not possible to travel between the regions of positive and negative r.

The values used in figure 1.1 satisfy all of the relations above.

1.2.3 Horizons 1+1+2

Another physical scenario is that of three horizons, two of which are of multiplicity one (denoted R_1 and R_1'), while the last is of multiplicity two (R_2). The corresponding factorisation is then

$$\Delta_r(r) = -\frac{\Lambda}{3}(r - R_1)(r - R_1')(r - R_2)^2 \,. \tag{1.40}$$

After expanding the polynomial and comparing it with (1.18) we find out that for fixed free parameters a, q and Λ (within their respective allowed ranges), there are multiple different sets $\{R_1, R_1', R_2, m\}$ that solve the equations. Due to the symmetry of the equations with respect to R_1 and R_1', it is possible to interchange these values in any of the following. The symmetrical counterparts of a given solution will be discarded without loss in generality. It is possible to express the results in terms of the four following functions of the free parameters:

$$\begin{aligned} \alpha_\pm &= \sqrt{\frac{\Lambda}{3}\left(6 - 2a^2\Lambda \pm \sqrt{9 - 42a^2\Lambda + a^4\Lambda^2 - 36\Lambda q^2}\right)}\,, \\ \beta_\pm &= \operatorname{sgn}(\Lambda)\sqrt{\frac{\Lambda}{6}\left(3 - a^2\Lambda \pm \sqrt{9 - 42a^2\Lambda + a^4\Lambda^2 - 36\Lambda q^2}\right)}\,. \end{aligned} \tag{1.41}$$

Using these functions, the four independent results are listed in table 1.1

#	ΛR_1	$\Lambda R_1'$	ΛR_2	$3\Lambda^2 m$
1	$\alpha_+ + \beta_-$	$-\alpha_+ + \beta_-$	$-\beta_-$	$-\alpha_+^2\beta_-$
2	$\alpha_+ - \beta_-$	$-\alpha_+ - \beta_-$	$+\beta_-$	$+\alpha_+^2\beta_-$
3	$\alpha_- + \beta_+$	$-\alpha_- + \beta_+$	$-\beta_+$	$-\alpha_-^2\beta_+$
4	$\alpha_- - \beta_+$	$-\alpha_- - \beta_+$	$+\beta_+$	$+\alpha_-^2\beta_+$

Table 1.1: Horizons 1+1+2

Every solution fulfils (1.21), $R_1 + R_1' + 2R_2 = 0$.

As in the previous cases further conditions need to be imposed on the free parameters to make sure that the results describe physically acceptable situations: we need the arguments of the square roots in (1.41) to be greater than or equal to zero while keeping the parameters real at the same time. This ensures that the results are real as well. Moreover, we demand m to be non-negative, $m \geq 0$, as negative mass contradicts our common experience[9]. We also need to dismiss the

[9]Nevertheless, the existence of exotic matter with negative mass is allowed by the Einstein–Maxwell equations, although it would have some unusual properties. While it can be frequently encountered in theoretical work regarding wormholes, both exotic matter (in macroscopic quantities) and the wormholes themselves are yet to be proven to exist.

case of $\alpha_\pm = 0$ as that would result in creating another horizon of multiplicity two at $R_1 = R_1'$. Two horizons of multiplicity two have already been discussed and rejected before. This requirement clearly means that $\Lambda \neq 0$. Of course, $\Lambda = 0$ would reduce (1.18) to a quadratic polynomial, which cannot have three different roots we now desire.

The first two solutions contain only α_+ and β_-, while the second two only α_- and β_+, which means we must study the appropriate parameter ranges separately for each pair of solutions. As $\forall \beta_\pm \neq 0 : \mathrm{sgn}(\beta_\pm) = \mathrm{sgn}(\Lambda)$, it follows from the condition $m \geq 0$ that the odd-numbered solutions represent space-times with negative Λ and the even-numbered ones represent positive Λ. When $\beta_\pm$ vanishes, so does the difference between the two solutions in each pair $1, 2$ and $3, 4$. These special cases of solutions satisfying $\beta_\pm = 0$ represent a massless black hole regardless of the sign of Λ.

After examining the above-mentioned requirements it turns out that Λ has to be positive, because negative Λ prevent α_+ and β_+ from being real. For instance, for α_+ to be real, the following inequality needs to be satisfied:

$$\frac{\Lambda}{3}\left(6 - 2a^2\Lambda + \sqrt{9 - 42a^2\Lambda + a^4\Lambda^2 - 36\Lambda q^2}\right) > 0\,. \tag{1.42}$$

If we consider a negative Λ, the term in the parentheses must now be negative for the whole expression to be positive,

$$6 - 2a^2\Lambda + \sqrt{9 - 42a^2\Lambda + a^4\Lambda^2 - 36\Lambda q^2} < 0\,. \tag{1.43}$$

However, the left-hand side of the inequality is now clearly positive, as $-2a^2\Lambda > 0$ for a negative Λ, which means this condition cannot be satisfied. A very similar argument holds for β_+ as well, except it is now acceptable to have $\beta_+ = 0$. We then get

$$3 - a^2\Lambda + \sqrt{9 - 42a^2\Lambda + a^4\Lambda^2 - 36\Lambda q^2} \leq 0\,. \tag{1.44}$$

The left-hand side is once again a sum of positive numbers – including a positive constant – and, as such, it is necessarily greater than zero. Thus, for a negative Λ, we cannot consider any solutions containing α_+ and/or β_+. However, a quick look at table 1.1 shows that the first two solutions contain α_+, while the second pair contains β_+. Negative Λ are thus inadmissible in any of the solutions.

Furthermore, since Λ is positive, the odd-numbered solutions can only be realised when the corresponding $\beta_\pm$ vanish (so that $m \geq 0$), but – as there is no difference between an odd-numbered solution and its corresponding even-numbered one when $\beta_\pm = 0$ – we can disregard these solutions for now, since they would already be contained as limits in the physical solutions #2 and #4.[10]

Next, let us focus on q^2 for a fixed positive Λ and a fixed allowed a^2, which shall be discussed afterwards. The "inner" square root of $\alpha_\pm$ and $\beta_\pm$ is the same for all the functions,

$$\sqrt{9 - 42a^2\Lambda + a^4\Lambda^2 - 36\Lambda q^2}\,. \tag{1.45}$$

[10] $\beta_- = 0$ requires $a = q = 0$, which is indeed an extreme case of solution #2. However, β_+ does never vanish, and solution #3 is unphysical no matter the parameters.

It also happens to contain the only term with q^2 in any of the functions. To see that q^2 is well behaved, we only need to make sure that the argument of the square root is non-negative, which is satisfied for

$$q^2 \in \left[0, \frac{9 - 42a^2\Lambda + a^4\Lambda^2}{36\Lambda}\right] . \tag{1.46}$$

Analysing the last remaining parameter a^2 is somewhat more tricky. We shall begin as we did with q^2. The "inner" square root gives us the condition

$$a^2 \in \left[0, \frac{21 - 6\sqrt{12 + \Lambda q^2}}{\Lambda}\right] \cup \left[\frac{21 + 6\sqrt{12 + \Lambda q^2}}{\Lambda}, \infty\right) . \tag{1.47}$$

Since we have already included the interdependency of q^2 and a^2 in the range of q^2, let us eliminate q^2 in the range of a^2 by considering the largest interval possible,

$$a^2 \in \left[0, \frac{21 - 12\sqrt{3}}{\Lambda}\right] \cup \left[\frac{21 + 12\sqrt{3}}{\Lambda}, \infty\right) \tag{1.48}$$

for $q^2 = 0$. For these a^2, any q^2 satisfying (1.46) are acceptable. Unlike q^2, a^2 does appear in $\alpha_\pm$ and $\beta_\pm$ outside the examined square root as well, so we may need to further reduce the allowed range of a^2 to make sure that $\alpha_\pm$ and $\beta_\pm$ are real. For solution #2 we require α_+ and β_- to be concurrently real, which leads to a system of two inequalities,

$$\begin{aligned} 6 - 2a^2\Lambda + \sqrt{9 - 42a^2\Lambda + a^4\Lambda^2 - 36\Lambda q^2} > 0 \,, \\ 3 - a^2\Lambda - \sqrt{9 - 42a^2\Lambda + a^4\Lambda^2 - 36\Lambda q^2} \geq 0 \,. \end{aligned} \tag{1.49}$$

Summing these, we obtain a remarkably simpler inequality

$$9 - 3a^2\Lambda > 0 \,, \tag{1.50}$$

whence

$$a^2 \in \left[0, \frac{3}{\Lambda}\right) . \tag{1.51}$$

For solution #4, the initial set of inequalities only differs in the sign of the square root. Therefore, the square root is eliminated in the process of summing as well, and the admissible range of a^2 remains the same.

Both conditions (1.48) and (1.51) combined, considering that

$$21 - 12\sqrt{3} < 3 < 21 + 12\sqrt{3} \,, \tag{1.52}$$

we obtain

$$a^2 \in \left[0, \frac{21 - 12\sqrt{3}}{\Lambda}\right] . \tag{1.53}$$

To summarise, the only two physical solutions #2 and #4 both require the space-time parameters to be

$$\begin{aligned} &\Lambda > 0 \,, \\ &a^2 \in \left[0, \frac{21 - 12\sqrt{3}}{\Lambda}\right] , \\ &q^2 \in \left[0, \frac{9 - 42a^2\Lambda + a^4\Lambda^2}{36\Lambda}\right] . \end{aligned} \tag{1.54}$$

A particular choice of solution is determined by the value of the remaining parameter m,

$$\begin{aligned} m_{\#2} &= \frac{\alpha_+^2 \beta_-}{3\Lambda^2}\,, \\ m_{\#4} &= \frac{\alpha_-^2 \beta_+}{3\Lambda^2}\,. \end{aligned} \tag{1.55}$$

Take note that for $a = q = 0$ it holds that

$$m_{\#2}\Big|_{a=q=0} = 0\,, \tag{1.56}$$

meaning we obtain the de Sitter space-time. Hence, if we are interested in an *extremal* solution, we should avoid setting both of these parameters equal to zero in scenario #2, but setting any one of them to zero is allowed. For solution #4 it is possible to have $a = q = 0$, as then

$$m_{\#4}\Big|_{a=q=0} = \frac{1}{3\sqrt{\Lambda}} \tag{1.57}$$

and we obtain the extremal Schwarzschild–de Sitter space-time with the expected mass [8]. Take note that in this limit the singularity reduces into a point and it is not possible to travel between the regions of positive and negative r.

Last but not least, we shall discuss the relative positions of the horizons in solutions #2 and #4. For a (necessarily) positive Λ it holds that $\alpha_\pm > 0$ and $\beta_\pm \geq 0$. It immediately follows that in both solutions the double horizon's position R_2 is non-negative[11],

$$R_2 = \frac{\beta_\mp}{\Lambda} \geq 0\,, \tag{1.58}$$

while R_1' is negative,

$$R_1' = -\frac{\alpha_\pm + \beta_\mp}{\Lambda} < 0\,. \tag{1.59}$$

The remaining horizon,

$$R_1 = \frac{\alpha_\pm - \beta_\mp}{\Lambda}\,, \tag{1.60}$$

is so far a mystery to us. We do not know its sign, nor whether it is greater than R_2 or not. As of now, we are only certain that $R_1 > R_1'$.

Let us first deal with the relation of R_1 and R_2. If we want these positions to be equal, we need to satisfy $\alpha_\pm = 2\beta_\mp$, which leads to

$$\pm\sqrt{9 - 42a^2\Lambda + a^4\Lambda^2 - 36\Lambda q^2} = \mp 2\sqrt{9 - 42a^2\Lambda + a^4\Lambda^2 - 36\Lambda q^2}\,. \tag{1.61}$$

For either of the solutions this means that the square root is equal to zero, which happens for

$$q^2 = \frac{9 - 42a^2\Lambda + a^4\Lambda^2}{36\Lambda}\,, \tag{1.62}$$

with Λ and a^2 satisfying (1.54). For this choice of q^2, $R_1 = R_2 \equiv R_3$ are the same for both solutions,

$$R_3 = \sqrt{\frac{3 - a^2\Lambda}{6\Lambda}}\,, \tag{1.63}$$

[11] In what follows, if there are signs "$\pm$" or "$\mp$" present in any of the expressions, the upper sign holds for solution #2 and the lower for #4.

and the other horizon is located at $R_1' = -3R_3$. It should be noted that this result is consistent with (1.28) for two horizons of multiplicities one and three, albeit expressed in terms of different free parameters. Expressing R_3 as a function of m and Λ is a matter of rewriting m appropriately using values from table 1.1:

$$m = \frac{\alpha_\pm^2 \beta_\mp}{3\Lambda^2} = \frac{4}{3}\frac{\beta_\mp^3}{\Lambda^2} = \frac{4}{3}\Lambda R_3^3\,, \tag{1.64}$$

where we used that $\alpha_\pm = 2\beta_\mp$ and $R_2 \equiv R_3 = \beta_\mp/\Lambda$. One can now easily see that

$$R_3 = \sqrt[3]{\frac{3}{4}\frac{m}{\Lambda}}\,. \tag{1.65}$$

As expected, this result is the same as (1.28). It is also clear that $R_1 \equiv R_3$ is now non-negative.

If we want R_1 to be greater than R_2, we require $\alpha_\pm > 2\beta_\mp$. This leads to an analogy of (1.61), only with a "$>$" sign. As the square root is non-negative, it is obvious that $R_1 > R_2$ holds for solution #2. For this solution, that means R_1 is surely positive, but its upper boundary is yet unknown to us. Similarly, $R_1 < R_2$ is true for solution #4 only, but that does not tell us whether R_1 may be negative.

For solution #2, determining the largest R_1 possible for a fixed $\Lambda > 0$ can be done by computing the derivatives of R_1 with respect to a^2 and q^2. For parameters satisfying (1.54), both derivatives are negative, which means that in order to get the largest R_1, we need to set $a = q = 0$. For this choice of parameters, we get $R_1^{\max} = \sqrt{3/\Lambda}$, the horizon position in the de Sitter solution [8]. Consequently, with Λ approaching zero, we can see that $\lim_{\Lambda\to 0^+} R_1^{\max} = \infty$.

Focusing on solution #4, $R_1 = 0$ requires $\alpha_- = \beta_+$, which is (disregarding the case $\Lambda = 0$) equivalent to $a^2 = -q^2$, the only real solution of which is $a = q = 0$, a limit allowed in this scenario, leading to the extremal Schwarzschild–de Sitter space-time with the double horizon at $R_2 = \sqrt{1/\Lambda}$ as expected [8]. A negative R_1 would require $\alpha_- < \beta_+ \Leftrightarrow a^2 < -q^2$, which is impossible to satisfy. Thus, R_1 can never be negative in either of the solutions.

To conclude, the possible range of the values of R_1 for solution #2 is

$$R_{1,\#2} \in [R_2, \infty)\,, \tag{1.66}$$

whilst for #4,

$$R_{1,\#4} \in [0, R_2]\,, \tag{1.67}$$

where $R_{1,\#4} = 0 \Leftrightarrow a = q = 0$. For both solutions, $R_1 = R_2$ is realised when

$$q^2 = \frac{9 - 42a^2\Lambda + a^4\Lambda^2}{36\Lambda}\,. \tag{1.68}$$

On the following page, figure 1.2 shows the course of $\Delta_r(r)$ near the horizons for a set of parameters corresponding to solution #2 and #4 respectively. Both figures are consistent with our analytical results.

1.2.4 Extremal black holes with disappearing horizons

To complete our discussion of extremal Kerr–Newman–(anti-)de Sitter black holes, we need to consider scenarios with disappearing horizons when at least

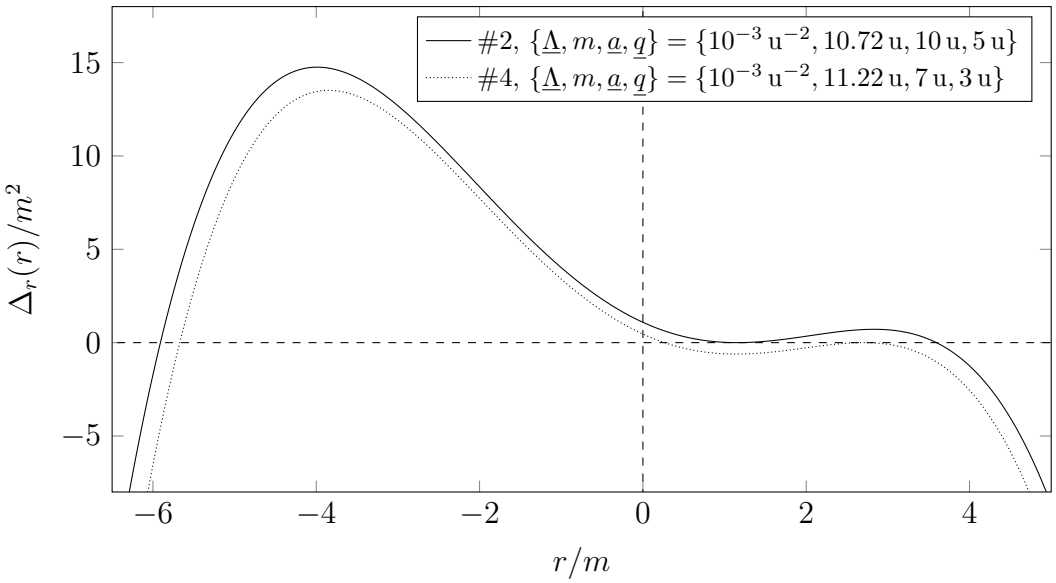

Figure 1.2: The course of $\Delta_r(r)$ corresponding to the two $1+1+2$ horizon scenarios. The values of the free parameters (underlined) are precise, the value of m is rounded to two decimal places.

two of the non-disappearing horizons merge. There may be up to three extremal scenarios of this type: a single horizon of multiplicity three, a single horizon of multiplicity two, and horizons 2+1. While physical horizons are given as real roots of Δ_r, disappearing horizons are complex roots. This single piece of information allows us to eliminate two of the three scenarios we set out to investigate. Recall that before we delved into individual cases of extremal black holes, we had discovered a simple relation that the roots of Δ_r need to satisfy: their sum must be equal to zero, (1.20). This means that it is not possible to have a black hole with a single disappearing horizon, as a sum of three real numbers and a complex one can only be equal to zero when the imaginary part of the complex number is zero as well, which is not possible for a disappearing horizon. Consequently, the extremal black holes of types 3 and 2+1 never occur, as they shed only one horizon. The last scenario of a single horizon of multiplicity two, however, needs to be investigated further.

Perhaps the easiest approach to studying this situation is to return to the 1+1+2 scenario. The factorisation we used, (1.40), is the most general factorisation for our current problem as well, as long as we allow the generally different R_1 and R_1' to have complex values. The four sets of solutions are listed in table 1.1. The structure of these expressions is quite helpful to our cause: if $\alpha_\pm$ is complex with $\beta_\mp$ real at the same time, R_2 is real and the remaining roots R_1 and R_1' have a non-zero imaginary part. Looking at the definition of these functions (1.41),

$$\begin{aligned}\alpha_\pm &= \sqrt{\frac{\Lambda}{3}\left(6 - 2a^2\Lambda \pm \sqrt{9 - 42a^2\Lambda + a^4\Lambda^2 - 36\Lambda q^2}\right)}\,,\\ \beta_\pm &= \mathrm{sgn}(\Lambda)\sqrt{\frac{\Lambda}{6}\left(3 - a^2\Lambda \pm \sqrt{9 - 42a^2\Lambda + a^4\Lambda^2 - 36\Lambda q^2}\right)}\,,\end{aligned} \tag{1.41}$$

we can see that the inner square root of both of these functions must be real for

$\beta_\pm$ to be real. As it is not complex, a complex $\alpha_\pm$ must be purely imaginary as a square root of a negative number. This implies that the black hole mass m, proportional to $\alpha_\pm^2$ as given in table 1.1, is a real number. It is therefore worthwhile to occupy ourselves with this scenario as it can represent a physically reasonable situation. However, this does not necessarily mean that it is mathematically possible to fulfil the conditions...

Let us first discuss the case of a positive Λ. Recall that both physical solutions #2 and #4 for horizons 2+1+1 required a positive Λ. We also determined a range of parameters for which both $\alpha_\pm$ and $\beta_\mp$ are simultaneously real, (1.54). Looking back on how we derived these conditions, we can see that trying to find the conditions leading to $\alpha_\pm^2 < 0$ and $\beta_\mp > 0$ follows the same line of reasoning until (1.49) for solutions containing α_+ and β_- (that is, #1 and #2) or its variant with the opposite signs by the square root for #3 and #4. Changing the sign of the first inequality in both cases (i.e. requiring $\alpha_\pm^2 < 0$), however, renders both sets of inequalities unsolvable for real parameters. Therefore, this type of extremal black hole forbids a positive Λ.

For a negative Λ, the situation is quite different. We already know that a negative Λ never allows both $\alpha_\pm$ and $\beta_\mp$ to be real at the same time. We have also found out that β_+ unavoidably requires a positive Λ in order to be real, which instantly eliminates solutions #3 and #4 as they contain β_+. All that remains is to analyse β_- and α_+ assuming a negative Λ. It is obvious that we need not worry about the inner square root, as its argument is now certainly positive for arbitrary a and q. Real β_- requires

$$\frac{\Lambda}{6}\left(3 - a^2\Lambda - \sqrt{9 - 42a^2\Lambda + a^4\Lambda^2 - 36\Lambda q^2}\right) \geq 0\,, \tag{1.69}$$

which is for $\Lambda < 0$ equivalent to

$$3 + a^2|\Lambda| - \sqrt{9 + 42a^2|\Lambda| + a^4|\Lambda|^2 + 36|\Lambda|q^2} \leq 0\,, \tag{1.70}$$

where we replaced Λ with $-|\Lambda|$ for the sake of clarity. After transferring the square root to the right side and taking the square of the inequality (which is possible as both sides as positive), we get

$$(a^2 + q^2)|\Lambda| \geq 0\,, \tag{1.71}$$

which is satisfied for all a and q. As far as α_+ is concerned, the inequality that would cause α_+ to be purely imaginary is

$$-\frac{|\Lambda|}{3}\left(6 + 2a^2|\Lambda| + \sqrt{9 + 42a^2|\Lambda| + a^4|\Lambda|^2 + 36|\Lambda|q^2}\right) < 0\,, \tag{1.72}$$

which is evidently again true for arbitrary a and q. Apart from these (remarkably permissive) constraints that arose from our desire to create an extremal black hole of this type, we must not forget that the more fundamental condition (1.4) needs to be met for any Kerr–Newman–anti-de Sitter space-time with $\Lambda < 0$, including this one. Hence, an extremal black hole with a single horizon 2 is achievable for a negative Λ, arbitrary q and $a^2 \in [0, 3/|\Lambda|)$. The corresponding solution with a non-negative mass m is #2. For it, the mass is given as

$$m = \frac{\alpha_+^2\beta_-}{3\Lambda^2}\,, \tag{1.73}$$

and both α_+^2 and β_- are now non-positive. The double horizon's position,

$$R_2 = \frac{\beta_-}{\Lambda} = \sqrt{\frac{3 - a^2\Lambda - \sqrt{9 - 42a^2\Lambda + a^4\Lambda^2 - 36\Lambda q^2}}{6\Lambda}}\,, \tag{1.74}$$

is non-negative and is equal to zero only when $a = q = 0$. Similarly as before, this limit corresponds to the anti-de Sitter space-time with $m = 0$, which is not a proper extremal KN(a)dS scenario. At least one of the parameters must be non-zero if we want to obtain the examined extremal scenario.

As always, figure 1.3 shows the course of $\Delta_r(r)$ in the vicinity of the horizon for a set of parameters fulfilling the conditions above.

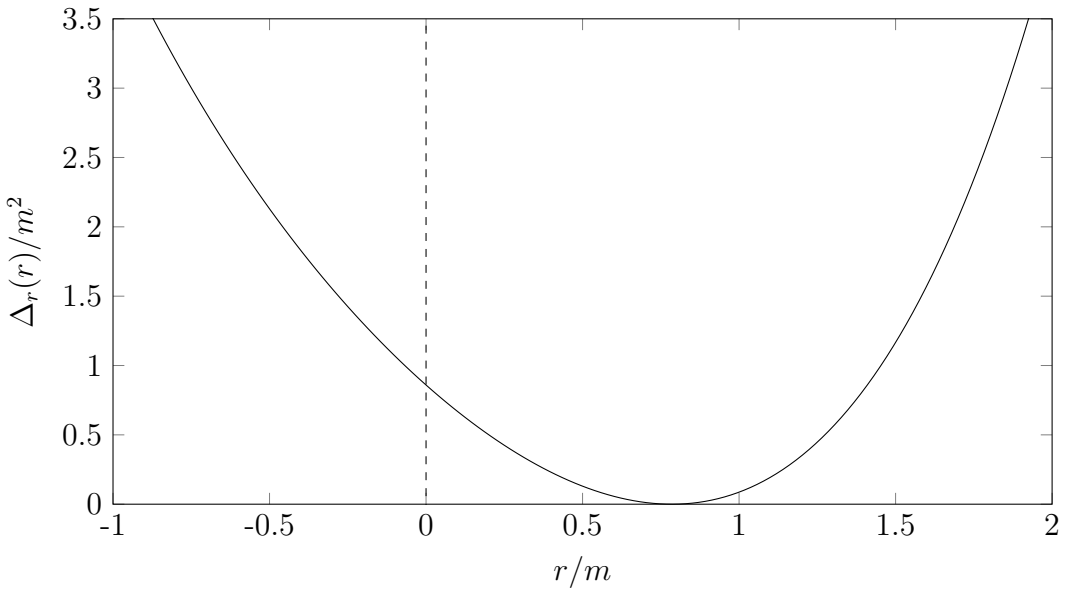

Figure 1.3: The course of $\Delta_r(r)$ in the vicinity of the horizon for a space-time with parameters $\{\underline{\Lambda}, m, \underline{a}, \underline{q}\} = \{-10^{-3}\,\mathrm{u}^{-2}, 24.12\,\mathrm{u}, 10\,\mathrm{u}, 20\,\mathrm{u}\}$ corresponding to the scenario of a single horizon of multiplicity two. The values of the free parameters (underlined) are precise, the value of m is rounded to two decimal places.

1.2.5 Extremal naked singularities

A naked singularity is a singularity that lies in the causal past of a future null infinity. For practical purposes, our interpretation is that it is a singularity visible by a reasonable observer, which means there is no event horizon between the observer and the singularity. For an asymptotically flat space-time, "a reasonable observer" usually is a static observer in flat spatial infinity. However, our examined space-time is not asymptotically flat and for $\Lambda > 0$ it does not even allow for a static observer in infinity, as this observer's four-velocity would become space-like for a negative Δ_r, which can be easily seen from the metric (1.1). For our purposes, a reasonable observer shall rest at the farthermost area with positive r where Δ_r is positive.[12]

[12]Except for some cases with $a = q = 0$, Δ_r is also positive around the singularity at $r = 0$. As it is the innermost area of the black hole, it is obvious we shall not place our static observer

It could be deemed inappropriate to talk about naked singularities without any mention of the cosmic censorship hypothesis. This hypothesis, which postulates that singularities need to be "clothed" in horizons in order to preserve the deterministic nature of the universe, refuses to accept the very concept of naked singularities.

In simpler cases (e.g. the Kerr–Newman solution), a naked singularity typically has no horizons. However, in the Kerr–Newman–(anti-)de Sitter solution we may find a naked singularity with horizons. In the following we shall discuss the even more special case of extremal naked singularities.

The one extremal black hole that seems offhand suspicious of this indecent exposure is the scenario of horizon 2 with $\Lambda < 0$, as it already lacks two of the four horizons. However, the singularity at $r = 0$ is hidden behind a double horizon $R_2 > 0$ for arbitrary a and q with the exception of the degenerate case of $a = q = 0$ when $R_2 = 0$. Furthermore, the reasonable observer (as discussed before) can be situated in the area containing radial infinity, as for a negative Λ, Δ_r is surely positive for $r \to \infty$. Therefore, apart from the mentioned singular case, the cosmic censorship hypothesis – which to date remains to be a conjecture, not an undisputed fact – is not violated.

Nevertheless, we have already encountered two naked singularities according to our definition above. In scenarios 1+3 and 1+1+2 (with the double horizon being the outermost one), we have found out that the singularity is contained in the only stationary area and shall never be hidden behind a horizon for the reasonable observer. Therefore, according to the cosmic censorship conjecture, the only astrophysically-relevant extremal Kerr–Newman–(anti-)de Sitter black holes are scenarios 1+2+1 (with the double horizon in the middle) and 2.

1.2.6 Extremal black holes: summary

To sum up, we have found out that is it possible to construct four types of extremal black holes out of the Kerr–Newman–(anti-)de Sitter space-time, namely $(-1 \oplus 3-)$, $(-1 \oplus 2 + 1-)$, $(-1 \oplus 1 - 2-)$ and $(\oplus 2+)$. The updated designations of the models now also show the alignment of the horizons in order of increasing r and the $\pm$ signs tell us whether the area between given horizons (or, a horizon and positive or negative infinity) is stationary $(+)$ or not $(-)$. As has already been stated, stationarity is determined by the sign of $\Delta_r(r)$. The asymptotics of the polynomial is given by its leading term $-\Lambda r^4/3$ and as such its sign in radial infinity of either sign is $-\mathrm{sgn}(\Lambda)$. Upon reaching a root of odd multiplicity the polynomial's sign changes, while upon reaching a root of even multiplicity it remains the same. That presents us with a simple key to find the stationary areas of a given scenario[13]. Moreover, a circle denotes the location of the singularity at $r = 0$. By comparing a given scenario with the most general one $(-1 \oplus 1 - 1 + 1-)$, where the horizons are $R_{\mathrm{C}-} < 0 < R_{\mathrm{I}} < R_{\mathrm{O}} < R_{\mathrm{C}+}$, it is easy to see which horizons merge and which disappear, if any. In the following, functions $\alpha_\pm$ and

there, because from this hypothetical observer's perspective, any black hole – even the most general one with four different horizons – would be a naked singularity. We position the observer farther away from the singularity in order to have the maximum possible number of horizons dividing them.

[13]The $\pm$ signs for a given scenario are also evident from the chart of $\Delta_r(r)$ in the corresponding section.

$\beta_\pm$ are defined as[14]

$$\begin{aligned}\alpha_\pm &= \sqrt{\frac{1}{3\Lambda}\left(6 - 2a^2\Lambda \pm \sqrt{9 - 42a^2\Lambda + a^4\Lambda^2 - 36\Lambda q^2}\right)}\,,\\ \beta_\pm &= \sqrt{\frac{1}{6\Lambda}\left(3 - a^2\Lambda \pm \sqrt{9 - 42a^2\Lambda + a^4\Lambda^2 - 36\Lambda q^2}\right)}\,.\end{aligned} \tag{1.75}$$

Scenario $(-\mathbf{1} \oplus \mathbf{3}-)$ (naked)

Free parameters Λ & m

Horizon positions:

$$\begin{aligned}R_1 &= -3R_3\,,\\ R_3 &= \sqrt[3]{\frac{3}{4}\frac{m}{\Lambda}}\,.\end{aligned} \tag{1.76}$$

Corresponding space-time parameters:

$$\begin{aligned}&\Lambda > 0\,,\\ &m^2 \in \left[\frac{16(26\sqrt{3}-45)}{3\Lambda}, \frac{2}{9\Lambda}\right]\,,\\ &a^2 = \frac{3}{\Lambda} - 6R_3^2\,,\\ &q^2 = \Lambda R_3^4 - a^2\,.\end{aligned} \tag{1.77}$$

Free parameters m & a

Horizon positions:

$$\begin{aligned}R_1 &= -3R_3\,,\\ R_3 &= \frac{m}{2}\left(x + 1 + x^{-1}\right)\,,\end{aligned} \tag{1.78}$$

with

$$x = \frac{m^{2/3}}{(m^2 + a^2 + a\sqrt{2m^2 + a^2})^{1/3}}\,. \tag{1.79}$$

Corresponding space-time parameters:

$$\begin{aligned}&m > 0\,,\\ &a^2 \in \left[0, \frac{3}{16}(3 + 2\sqrt{3})m^2\right]\,,\\ &\Lambda = \frac{3}{4}\frac{m}{R_3^3}\,,\\ &q^2 = \frac{3}{4}mR_3 - a^2\,.\end{aligned} \tag{1.80}$$

Scenario $(-\mathbf{1} \oplus \mathbf{2} + \mathbf{1}-)$

Horizon positions:

$$\begin{aligned}R_{1-} &= -\alpha_+ - \beta_-\,,\\ R_2 &= \beta_-\,,\\ R_{1+} &= +\alpha_+ - \beta_-\,.\end{aligned} \tag{1.81}$$

[14]Please note that knowing $\mathrm{sgn}(\Lambda)$ beforehand, we have slightly redefined the functions in order to further simplify the resulting expressions.

Corresponding space-time parameters:

$$\begin{aligned} &\Lambda > 0\,, \\ &a^2 \in \left[0, \frac{21 - 12\sqrt{3}}{\Lambda}\right]\,, \\ &q^2 \in \left[0, \frac{9 - 42a^2\Lambda + a^4\Lambda^2}{36\Lambda}\right]\,, \\ &m = \frac{\Lambda\alpha_+^2\beta_-}{3}\,. \end{aligned} \tag{1.82}$$

Setting both $a = q = 0$ leads to the non-extremal de Sitter space-time.

Scenario $(-\mathbf{1} \oplus \mathbf{1} - \mathbf{2}-)$ (naked)

Horizon positions:

$$\begin{aligned} R_{1-} &= -\alpha_- - \beta_+\,, \\ R_{1+} &= +\alpha_- - \beta_+\,, \\ R_2 &= \beta_+\,. \end{aligned} \tag{1.83}$$

Corresponding space-time parameters:

$$\begin{aligned} &\Lambda > 0\,, \\ &a^2 \in \left[0, \frac{21 - 12\sqrt{3}}{\Lambda}\right]\,, \\ &q^2 \in \left[0, \frac{9 - 42a^2\Lambda + a^4\Lambda^2}{36\Lambda}\right]\,, \\ &m = \frac{\Lambda\alpha_-^2\beta_+}{3}\,. \end{aligned} \tag{1.84}$$

Scenario $(\oplus\mathbf{2}+)$

Horizon position:

$$R_2 = \beta_-\,. \tag{1.85}$$

Corresponding space-time parameters:

$$\begin{aligned} &\Lambda < 0\,, \\ &a^2 \in \left[0, \frac{3}{|\Lambda|}\right)\,, \\ &q^2 \in [0, \infty)\,, \\ &m = \frac{\Lambda\alpha_+^2\beta_-}{3}\,. \end{aligned} \tag{1.86}$$

Setting both $a = q = 0$ leads to the non-extremal anti-de Sitter space-time.

1.2.7 Perturbing the parameters

With a vanishing Λ extremal space-times from the Kerr(–Newman) or Reissner–Nordström families form the boundary between the two-horizon scenarios and naked singularities with no horizons. It is logical to assume that extremal scenarios play a similar role for a non-vanishing Λ as well, even though the broader palette of parameters makes the situation more difficult to analyse here.

We shall tackle the problem by computing the derivatives of Δ_r with respect to the space-time parameters. If we know how Δ_r changes in the vicinity of the extremal horizon after performing a perturbation in a given parameter, we can easily deduce the horizon configuration of the perturbed extremal scenario, as the multiple root of Δ_r either continuously separates into individual ones, or disappears altogether[15]. Three of the four derivatives can be analysed effortlessly:

$$\frac{\partial \Delta_r}{\partial q} = 2q\,, \tag{1.87}$$

meaning that Δ_r increases when the absolute value of q increases,

$$\frac{\partial \Delta_r}{\partial \Lambda} = -\frac{1}{3}\left(a^2 + r^2\right) r^2\,, \tag{1.88}$$

meaning that Δ_r decreases when Λ increases, and

$$\frac{\partial \Delta_r}{\partial m} = -2r\,, \tag{1.89}$$

which means that Δ_r decreases with increasing m in the region with $r > 0$, where extremal horizons are invariably located. The sign of the remaining derivative

$$\frac{\partial \Delta_r}{\partial a} = 2a\left(1 - \frac{1}{3}\Lambda r^2\right) \tag{1.90}$$

is not immediately evident.

For scenario $(\oplus 2+)$ with $\Lambda < 0$ the derivative is manifestly positive everywhere. For the remaining extremal scenarios we shall insert the radius of the extremal horizon. For $(-1 \oplus 3-)$, we obtain

$$\left.\frac{\partial \Delta_r}{\partial a}\right|_{(-1\oplus 3-)} = 1 - \left(\frac{\Lambda m^2}{48}\right)^{1/3}\,, \tag{1.91}$$

which means that if $\Lambda m^2 < 48$, the derivative is strictly greater than 0 at the extremal horizon (and, therefore, at least in its immediate vicinity as well). This requirement is weaker then the one already imposed on Λm^2 in the extremal scenario, see (1.77). Hence, the derivative is indeed positive. For the last two extremal cases, the derivative becomes

$$\left.\frac{\partial \Delta_r}{\partial a}\right|_{\substack{(-1\oplus 2+1-)\\(-1\oplus 1-2-)}} = \frac{1}{18}\left(15 + \Lambda a^2 \pm \sqrt{9 - 42\Lambda a^2 + \Lambda^2 a^4 - 36\Lambda q^2}\right)\,. \tag{1.92}$$

For the plus sign the derivative is manifestly positive (recall that $\Lambda > 0$ in these scenarios). Further, it holds that

$$15 + \Lambda a^2 > \sqrt{9 - 42\Lambda a^2 + \Lambda^2 a^4 - 36\Lambda q^2}\,, \tag{1.93}$$

[15] In any of the extremal scenarios, we need not worry about some other complex roots suddenly becoming real when perturbing the parameters, because there either are none, or, in scenario $(\oplus 2+)$, the two complex roots result from the (negative) sign of Λ. Changing the sign of Λ is a dramatic change in the space-time and cannot be considered a perturbation.

as can be confirmed by taking the square and transferring all terms to one side. After dividing by 36, we obtain the clearly true inequality

$$6 + 2\Lambda a^2 + \Lambda q^2 > 0\,. \tag{1.94}$$

Thus, the derivative is positive for the minus case as well. All things considered, despite initial uncertainty it holds that

$$\frac{\partial \Delta_r}{\partial a} > 0 \tag{1.95}$$

at the extremal horizon in each extremal scenario.

To sum up, in the neighbourhood of the extremal horizon the value of Δ_r increases with increasing a and $|q|$ and decreases with increasing Λ and m for all extremal scenarios.

In table 1.2 one can see how the extremal scenarios change with parameter perturbations. Determining the perturbed scenario is only a matter of imagination when looking at the chart of the corresponding extremal case.

Extremal	Increased Δ_r	Decreased Δ_r
$(-1 \oplus 3-)$	$(-1 \oplus 1-)$	$(-1 \oplus 1-)$
$(-1 \oplus 2 + 1-)$	$(-1 \oplus 1-)$	$(-1 \oplus 1 - 1 + 1-)$
$(-1 \oplus 1 - 2-)$	$(-1 \oplus 1 - 1 + 1-)$	$(-1 \oplus 1-)$
$(\oplus 2+)$	$(\oplus)$	$(\oplus 1 - 1+)$

Table 1.2: Perturbations of the extremal scenarios with respect to a change in Δ_r at the radius of the extremal horizon. Δ_r increases with increasing a and $|q|$ and with decreasing Λ and m.

1.2.8 On conformal diagrams

As folk wisdom has it, "A picture is worth a thousand words". Indeed, a visual representation may facilitate understanding of a space-time and allow us to compare different solutions at a glance. An especially convenient way of visualising space-times is provided by Penrose conformal diagrams, which capture the causal structure. Their common feature is that light rays are slanted at a 45° angle, time-like world lines form acute angles with the vertical axis and space-like world lines with the horizontal axis. Therefore, conformal diagrams are a natural general-relativistic extension of a Minkowski space-time diagram from the special theory of relativity.

Conformal diagrams can be constructed after performing a series of coordinate transformations of the metric, followed by a final, conformal transformation. While coordinates of the initial metric may generally take on arbitrarily high values, coordinates of the final metric always have finite bounds. This allows us to draw originally infinite lines of what was $r \in (-\infty, \infty)$ before the transformations as finite line segments on a single sheet of paper. However, armed with the knowledge gained through our previous examination of the space-time, we can draw the diagrams immediately without actually performing any of the mentioned transformations. The key is as follows:

Conformal diagrams are composed of squares or triangles, edges of which are comprised of horizons, singularities or original coordinate infinities. In our notation of extremal space-times, each of these shapes corresponds to one of the $\pm$ signs in the space-time designation, and each of its edges corresponds to one of the neighbouring two symbols, which may be a number representing a horizon of the given multiplicity, a parenthesis representing a radial infinity, or (for "$\oplus$" and for $\theta = \pi/2$) the singularity. The singularity is always time-like (that is, drawn vertically), as it is located in a stationary area of every investigated extremal space-time. The character of both radial infinities (positive and negative) is determined by the sign of the cosmological constant Λ: a positive $\Lambda > 0$ implies a space-like boundary, a negative $\Lambda < 0$ implies a time-like boundary, and a vanishing $\Lambda = 0$ (now irrelevant to us) implies a null boundary [8].

The perhaps easiest approach to drawing the diagram is to start with a "piece" containing a radial infinity and imagine a particle emanating from it. A time-like particle goes predominantly upwards[16] in the diagram, its world line forms an angle of less than 45° with the vertical axis. While we know which piece follows after crossing a horizon, one might be unsure of its relative rotation with respect to the previously placed pieces of the diagram – and that is the moment when the imagined particle comes in handy. In stationary areas of the space-times, the particle is allowed to turn back (not necessarily geodesically) and cross the same horizon once again – which means that the square or triangle being placed must have the other edge with the same horizon positioned directly above the first instance of the given horizon. On the other hand, non-stationary areas do not allow the particle to return, which means that there cannot be the same horizons in both the lower and the upper halves of the piece.

Another thing to keep in mind is that the examined space-times contain a ring singularity in the equatorial plane only. Therefore, we have to draw two diagrams, one for $\theta = \pi/2$, where nothing can cross singularities at $r = 0$, and another for $\theta \neq \pi/2$, where lines of $r = 0$ can hypothetically be crossed and observers may find themselves in "the other half" of the space-time with $r < 0$. In the diagrams, these areas (which invariantly have a simpler structure than the areas with $r > 0$) are greyed out[17]. For a given θ, every point in the diagrams actually corresponds to a circle with $\phi \in [0, 2\pi)$.

When drawing the diagrams, it is clear that one may often extend the diagram infinitely in one or more directions, which would lead to a so-called maximal analytical extension of the diagram. The extension is performed so that there would be no endpoints of geodesics outside the singularity or coordinate infinities[18]. The overlying idea is that, theoretically, as observers pass through horizons, they might actually end up in another iteration of the space-time. An observer relentlessly passing through the black hole horizons while avoiding the singularity or the cosmological horizons (when applicable) may therefore visit an unlimited number

[16] Alternatively, one may also imagine a particle that travels backwards in time (moves downwards in the diagram) and follow the same instructions. The causal structure of every examined space-time is symmetric with respect to the particle's proper time. The metric, however, is not – reversing the flow of time would change the sign of a.

[17] Take note that even though for $\Lambda > 0$ these areas are represented as squares with two $r = 0$ lines, it is not possible to connect both of these with a time-like world line.

[18] Without the maximal analytical extension geodesics could also end at the horizons in the diagrams, whereas they are known to traverse them in finite proper time.

of iterations of the space-time. The following figures represent a "unit cell" of the extremal Kerr–Newman–(anti-)de Sitter space-times. The maximal analytical extension can be performed by simply copying and subsequently joining the cells at the appropriate loci:

- For $(\oplus 2+)$ (figure 1.4) along the R_2 horizons (vertically).
- For $(-1 \oplus 3-)$ (figure 1.5) along the $r = 0$ lines in chart (b) (horizontally).
- For $(-1 \oplus 2 + 1-)$ (figure 1.6) along the R_2 horizons in both charts (vertically) and along the $r = 0$ lines in chart (b) (horizontally).
- For $(-1 \oplus 1 - 2-)$ (figure 1.7), the situation is more complicated. Copies of diagrams (a) and (b) are to be joined along the R_2 horizons (horizontally). If the same $r = 0$ line is approached from two different neighbouring copies of the respective diagram, one must consider each side of the line to belong to the respective iteration of the space-time – the lines are not shared, despite their ambiguous position in the charts. A particle cannot pass through these lines to another copy of the space-time. Instead, for $\theta = \pi/2$, it falls into the singularity, or, for $\theta \neq \pi/2$, it moves into a copy of diagram (c), which are to be joined with (b) at $r = 0$ in planes different from the plane of the (b) diagrams. Equally, a particle passing through an $r = 0$ line in a (c) diagram must appear in a (b) diagram, i.e. passing through an $r = 0$ line for $\theta \neq \pi/2$ means going from (b) to (c) or vice versa. Perhaps the most compact way to construct the maximal extension is by establishing a plane of diagrams (b) with "rolls" of a single diagram (c) glued to every $r = 0$ line, see figure 1.8.

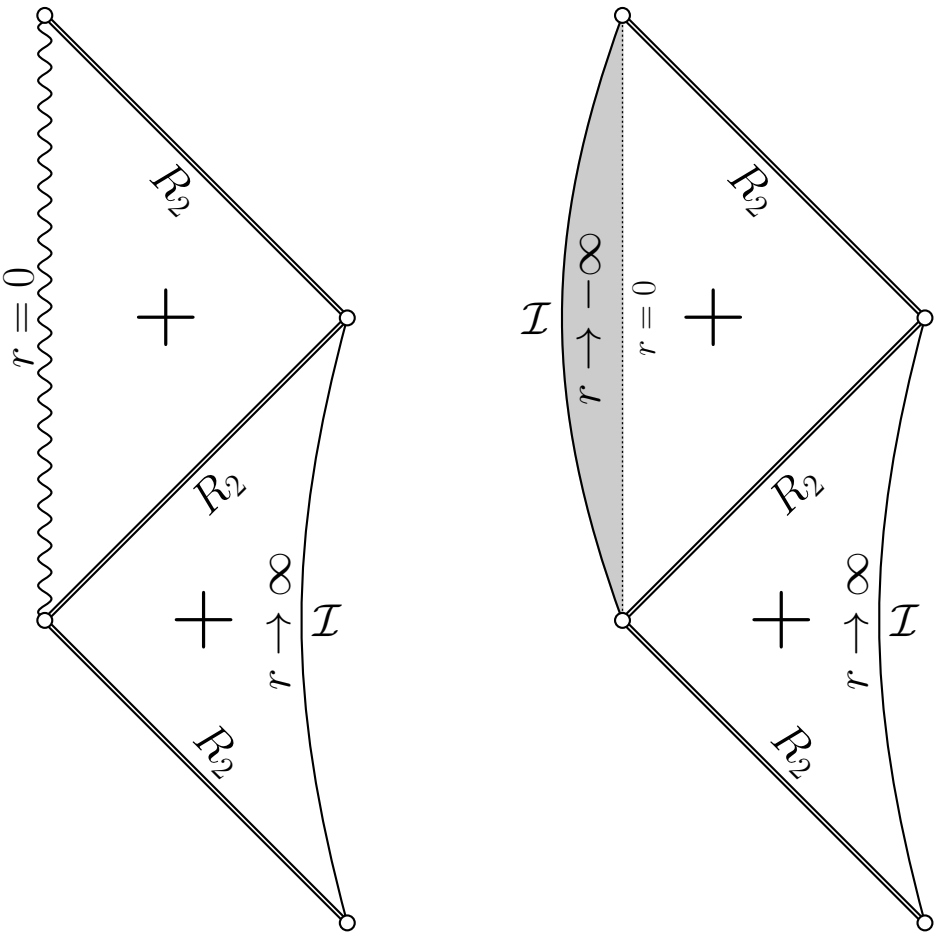

(a) $\theta = \pi/2$ (b) $\theta \neq \pi/2$

Figure 1.4: Conformal diagrams of a scenario ($\oplus 2+$) black hole ($\Lambda < 0$) for a given θ.

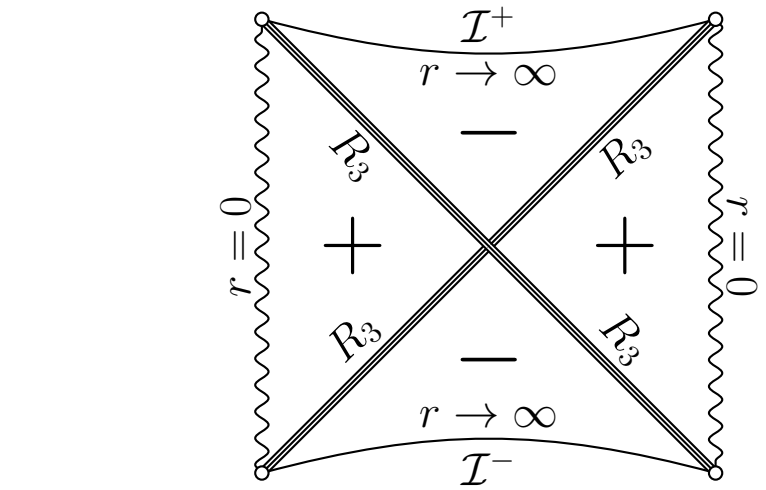

(a) $\theta = \pi/2$

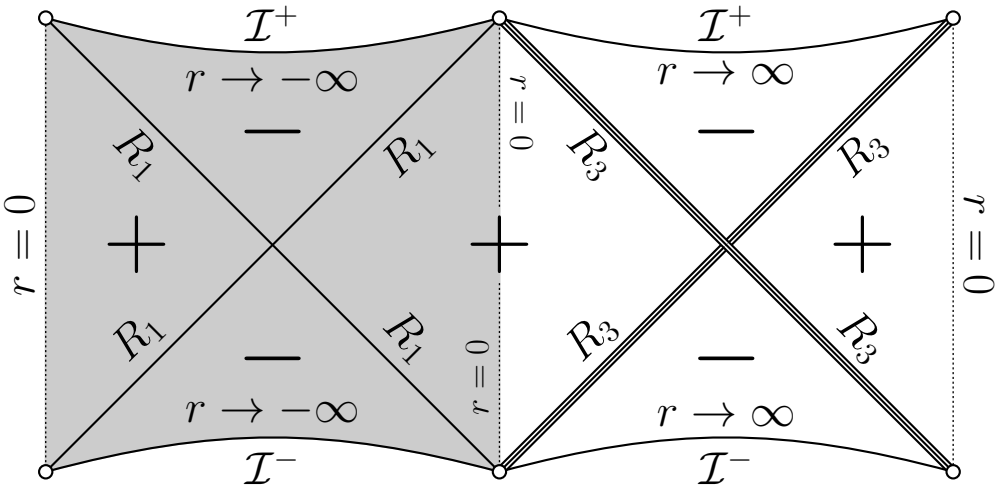

(b) $\theta \neq \pi/2$

Figure 1.5: Conformal diagrams of a scenario $(-1 \oplus 3-)$ black hole ($\Lambda > 0$) for a given θ.

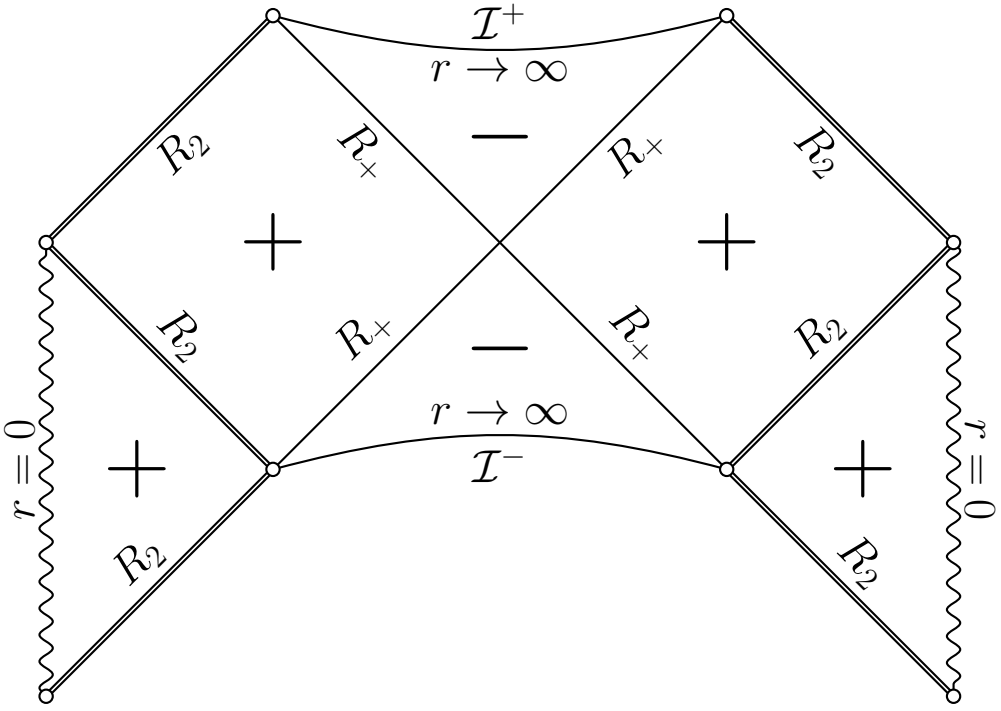

(a) $\theta = \pi/2$

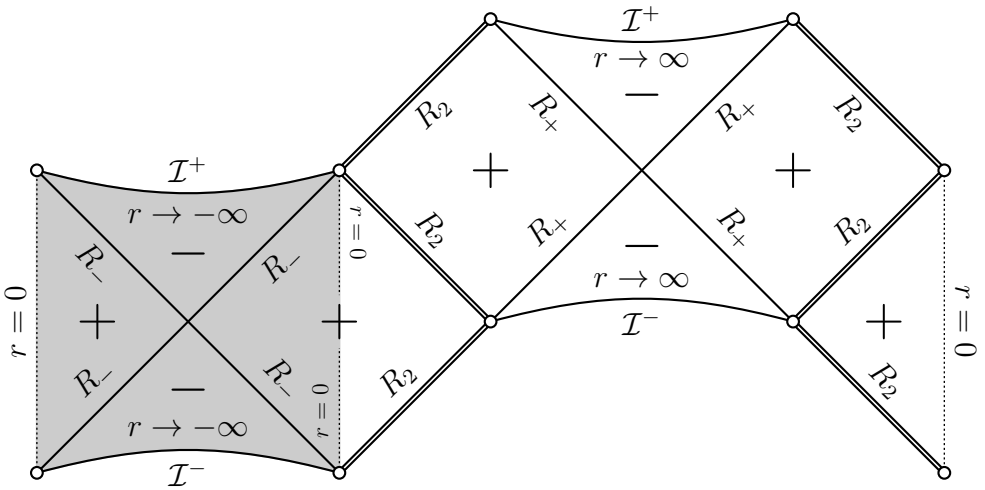

(b) $\theta \neq \pi/2$

Figure 1.6: Conformal diagrams of a scenario $(-1 \oplus 2 + 1-)$ black hole ($\Lambda > 0$) for a given θ.

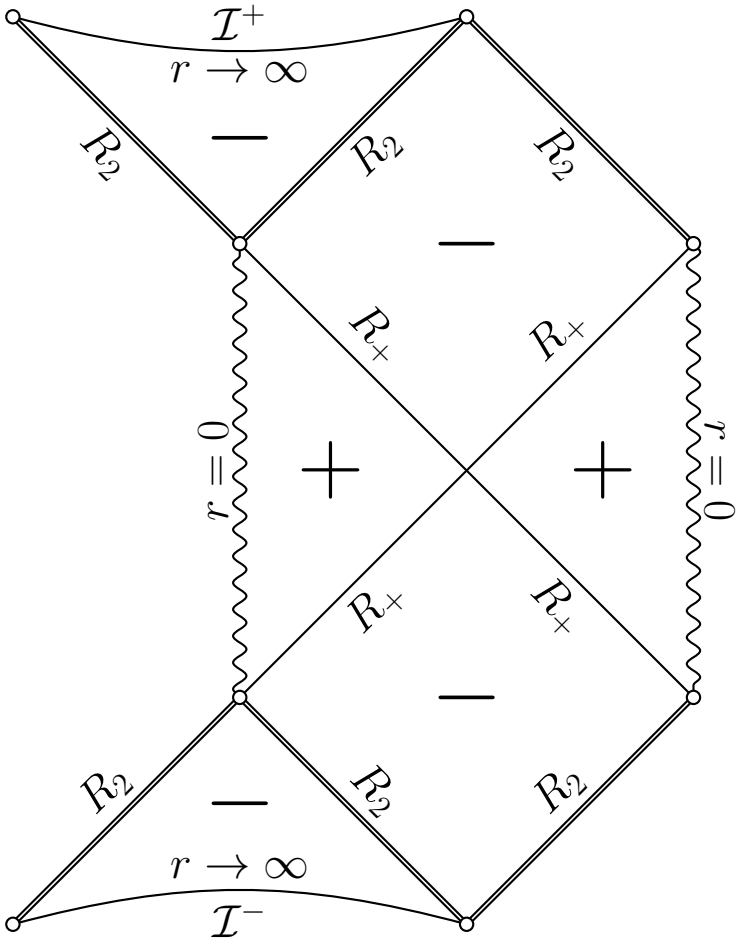

(a) $\theta = \pi/2$

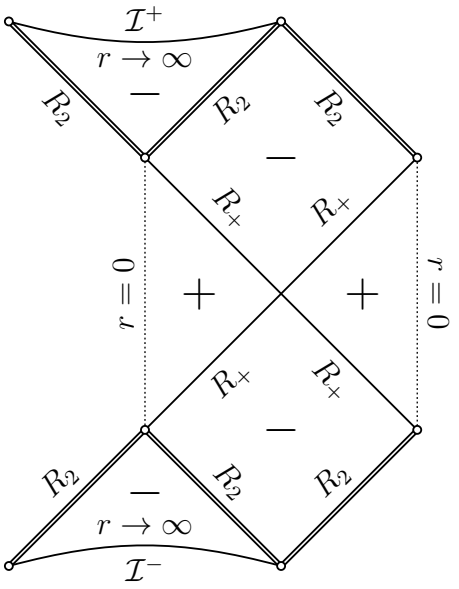

(b) $\theta \neq \pi/2$, $r > 0$

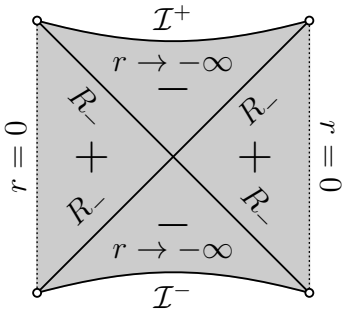

(c) $\theta \neq \pi/2$, $r < 0$

Figure 1.7: Conformal diagrams of a scenario $(-1 \oplus 1 - 2-)$ black hole ($\Lambda > 0$) for a given θ. For $\theta \neq \pi/2$, copies of diagrams (b) and (c) must lie in different planes.

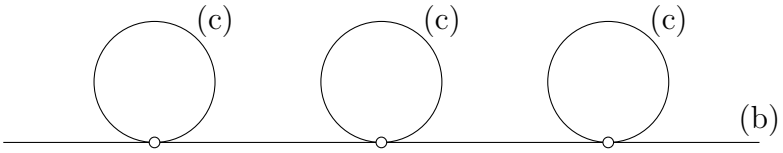

Figure 1.8: Scheme of the maximal analytical extension of the conformal diagram for scenario $(-1 \oplus 1 - 2-)$ for $\theta \neq \pi/2$. White dots represent the $r = 0$ lines in the (b) and (c) diagrams. Particles trying to move through the $r = 0$ lines "bounce off" the dots and move from diagram (b) to (c) or vice versa. (The particles are, of course, unaware of the bending of the (c) diagrams, they are only concerned with their position on the flat two-dimensional chart.)

1.2.9 Comparison with extremal Kerr–Newman scenarios

It may be of astrophysical relevance to compare our results for the Kerr–Newman–(anti-)de Sitter extremal black holes with the simpler Kerr–Newman case. For $\Lambda = 0$, horizon locations are given by

$$\Delta_r\Big|_{\Lambda=0} = r^2 - 2mr + a^2 + q^2 = 0\,. \tag{1.96}$$

Unlike the considerably more difficult case with a general Λ, the roots of a quadratic polynomial are easy to find,

$$r_\pm = m \pm \sqrt{m^2 - a^2 - q^2}\,. \tag{1.97}$$

Extremal Kerr–Newman black holes with $r_+ = r_-$ then obviously satisfy

$$m^2 = a^2 + q^2\,. \tag{1.98}$$

One can ask whether the inclusion of a non-zero cosmological constant may allow an extremal black hole to become "over-rotating" and/or "over-charged" in comparison with an extremal Kerr–Newman black hole of the same mass m, i.e. whether it is possible to have

$$m^2 < a^2 + q^2 \tag{1.99}$$

for an extremal black hole. A Kerr–Newman space-time satisfying this inequality would be that of a naked singularity.

The electric charge of astrophysical black holes is usually considered negligible compared to their mass. However, for angular momentum this is not true as observations [11, 12, 13] suggest the existence of black holes nearing extremality[19] with $a \approx m$. Not considering the cosmological term, the cosmic censorship hypothesis demands that astrophysical black holes satisfy $a \leq m$. Does a non-zero cosmological constant allow for a non-naked black hole with $a > m$?

The Kerr–Newman–(anti-)de Sitter extremal scenarios corresponding to the Kerr–Newman case are $(-1 \oplus 2 + 1-)$ and $(\oplus 2+)$, as the other ones are naked. Astrophysically relevant is the former scenario, as it includes a positive Λ in

[19] This is especially true for the black hole in Cygnus X-1 with $m \approx 15 M_\odot$ and a to m ratio thought to be up to 0.99.

accordance with current observations, while the latter includes a negative Λ. Conveniently, the expression for mass $m(\Lambda, a, q)$ is the same in both cases, as shown previously. Considering the form of the allowed intervals of a and q in both cases, it may be advantageous to introduce a new parametrisation with $x \equiv \Lambda a^2$ and $y \equiv \Lambda q^2$. With this reparametrisation, we do not need to analyse a three-dimensional problem but rather a two-dimensional one, as the expression we are going to study is

$$\frac{a^2+q^2}{m^2} = \frac{486(x+y)}{\left(6-2x+\sqrt{9-42x+x^2-36y}\right)^2\left(3-x-\sqrt{9-42x+x^2-36y}\right)}\,, \tag{1.100}$$

where for $(-1\oplus 2+1-)$, x and y must satisfy

$$\begin{aligned} x &\in \left[0, 21-12\sqrt{3}\right]\,, \\ y &\in \left[0, \tfrac{9-42x+x^2}{36}\right]\,, \end{aligned} \tag{1.101}$$

while for $(\oplus 2+)$,

$$\begin{aligned} x &\in (-3, 0]\,, \\ y &\in (-\infty, 0]\,. \end{aligned} \tag{1.102}$$

Considering astrophysical black holes, one usually expects $m, a \gg q$ as macroscopic objects tend to be electrically neutral. We thus have $|x| \gg |y|$ and as such we can ignore the terms with y in (1.100) from now on:

$$\frac{a^2+q^2}{m^2} \approx \frac{a^2}{m^2} = \frac{486x}{\left(6-2x+\sqrt{9-42x+x^2}\right)^2\left(3-x-\sqrt{9-42x+x^2}\right)}\,. \tag{1.103}$$

Now, we need to compare this function with 1 to find out whether the black hole is over-rotating ($a^2 > m^2$) or not ($a^2 < m^2$). What originally seemed as a three-dimensional problem has now been reduced a single-variable one.

Essentially, we could approach the problem by searching for extremes and regions of monotony by deriving the function. However, the function is not particularly suited to be analysed in such a way, as solving $\mathrm{d}(a^2/m^2)/\mathrm{d}x = 0$ requires finding the roots of a fourth-order polynomial. Instead, let us inspect figure 1.9 on the following page showing the course of a^2/m^2 for $x \in [-3, 21-12\sqrt{3}]$:

The right part of the chart with $x > 0$ is valid for the case of $(-1\oplus 2+1-)$, while the noticeably larger left part with $x < 0$ is valid for $(\oplus 2+)$. They coincide at $x = 0 \Leftrightarrow a = 0$, with

$$\lim_{a\to 0} \frac{a^2}{m^2} = 1\,, \tag{1.104}$$

as can be seen after rationalising the denominator in (1.103) or from the Taylor series at $x \to 0$,

$$\begin{aligned} \frac{a^2}{m^2} &= \frac{3\left(27+297x-99x^2-x^3+(9-42x+x^2)^{3/2}\right)}{2(3+x)^4} \\ &= 1+\tfrac{2}{3}x+\tfrac{7}{9}x^2+\mathcal{O}(x^3)\,. \end{aligned} \tag{1.105}$$

Regarding $(-1\oplus 2+1-)$, from figure 1.9 we can see that an extremal black hole necessarily is over-rotating for any permitted value of $x > 0$. The upper limit

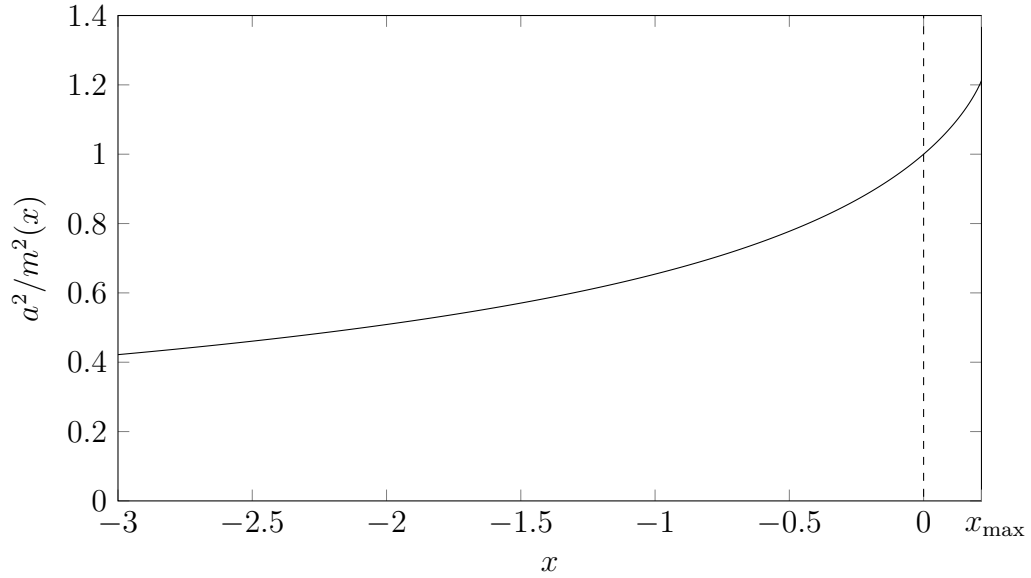

Figure 1.9: The dependence of a^2/m^2 on $x \equiv \Lambda a^2$ for the permitted values of x for the Kerr–Newman–like extremal black holes of the Kerr–Newman–(anti-)de Sitter family with $x_{\max} = 21 - 12\sqrt{3}$.

is

$$\lim_{a \to a_{\max}} \frac{a^2}{m^2} = \frac{3}{16}(3 + 2\sqrt{3}) \approx 1.21\,, \tag{1.106}$$

with $a^2_{\max} = (21 - 12\sqrt{3})/\Lambda$. Astrophysical black holes thus *can* satisfy $a > m$ without being naked singularities, but do they in reality?

Considering the cosmological constant of our universe (1.7), we can see that (omitting the considerably smaller error intervals)

$$a_{\max}\Big|_{\Lambda = 1.11 \times 10^{-52}\,\mathrm{m}^{-2}} \approx 4.4 \times 10^{25}\,\mathrm{m} \tag{1.107}$$

with corresponding mass

$$m \approx 4.0 \times 10^{25}\,\mathrm{m} \approx 2.7 \times 10^{22} M_\odot \tag{1.108}$$

given by (1.82). However, as has already been mentioned the most massive black holes ever observed have masses of the order of $10^{10} M_\odot$, (1.8), which is well below our result computed using $a_{\max}$ by 12 orders of magnitude. A looming prospect of a similarly-substantial difference between the corresponding angular momentum and $a_{\max}$ threatens the existence of measurably over-rotating black holes, as – if our anticipation proves to be true – we could effectively consider the limit $a \to 0$ and get the usual result for an extremal Kerr black hole (1.104). Indeed, by expressing a from the formula for m in (1.82) for the measured value of Λ, $q = 0$ and

$$M^{\mathrm{BH}}_{\max} \approx 1.5 \times 10^{13}\,\mathrm{m} \tag{1.109}$$

we obtain

$$a^{\mathrm{BH}}_{\max} \approx 1.5 \times 10^{13}\,\mathrm{m}\,. \tag{1.110}$$

Our numerical computations show that both values are actually equal in at least the first 15 significant digits (coinciding with machine epsilon for double precision

arithmetics), and we get almost precisely

$$\left(\frac{a_{\max}^{\mathrm{BH}}}{M_{\max}^{\mathrm{BH}}}\right)^2 = 1\,. \tag{1.111}$$

As expected, $a_{\max}^{\mathrm{BH}}$ is smaller than $a_{\max}$ by 12 orders, and we can thus effectively consider the limit $a \to 0$ for any observed black hole, which means that astrophysical black holes indeed satisfy

$$\frac{a^2}{m^2} \leq 1\,, \tag{1.112}$$

as is valid for black holes of the Kerr–Newman type as well. A theoretical deviation from this condition is negligible and would require inconceivably precise observations in order to be measured. However, even though we have not found any *yet*, one should never exclude the possibility of the existence of black holes massive enough to be actually able to satisfy $a^2/m^2 > 1$...

On the other hand, for $(\oplus 2+)$ we can see from chart 1.9 that every extremal black hole (excluding those with $x = 0$) actually satisfies $a < m$. The limit of maximal rotation is

$$\lim_{a^2 \to -3/\Lambda} \frac{a^2}{m^2} = \frac{27}{64} \approx 0.42\,, \tag{1.113}$$

which, perhaps paradoxically, represents the lowest ratio of a^2/m^2 possible for this type of extremal black holes.

As a side note, it might seem confusing that the limiting values of a^2/m^2 (1.106) and (1.113) do not depend on Λ, which means we cannot do a feasible limit of $\Lambda \to 0$ to obtain the Kerr–Newman result of $a^2/m^2 = 1$. We attribute that to the fact that the maximal permitted values of a^2 – for which these limits hold – are in both cases proportional to $1/\Lambda$. Therefore, if we consider the limit of $\Lambda \to 0$ in these maximal angular momenta, they diverge to infinity. If we want to perform the limit of $\Lambda \to 0$ while keeping a finite at the same time, the best way to do this is to do the limit of $x \to 0$ in (1.103), which we have already determined (as it is the same limit as for $a \to 0$) to be

$$\lim_{\Lambda \to 0} \frac{a^2}{m^2} = 1\,, \tag{1.114}$$

as is to be expected.

1.3 Frame-dragging

Frame-dragging is an effect common to all space-times of the Kerr family with rotating singularities, as the black hole appears to twist the space-time in the direction of its rotation. Observers then have the tendency to co-rotate with the black hole. This effect is typically more prominent in regions closer to the singularity. The mathematics in this section are not going to be fundamentally different from the "pure" Kerr solution taught in the relativistic course, but as the studied space-time is defined by a larger set of parameters, we may immerse ourselves in a plethora of different charts examining the influence of the sign of Λ on frame-dragging, or the multitude of extremal scenarios, for instance.

One of the main consequences of frame-dragging is that areas where static observers[20] can and cannot exist are not necessarily separated by horizons, unlike the Schwarzschild or Reissner–Nordström solutions, but rather by a different surface (or, a set of surfaces) called the static limit. Due to the normalisation equation

$$g_{\mu\nu}u^\mu u^\nu = -1\,, \tag{1.115}$$

which shall be discussed in greater detail in the next chapter, the static observer's four-velocity is

$$u^\mu = \left(\frac{1}{\sqrt{-g_{tt}}}, 0, 0, 0\right)\,, \tag{1.116}$$

whence one immediately sees that static observers are to be found only in areas satisfying

$$g_{tt} \equiv \frac{-\Delta_r(r) + \Delta_\theta(\theta)a^2\sin^2(\theta)}{\Xi^2\rho^2(r,\theta)} < 0\,. \tag{1.117}$$

Disregarding the manifestly non-negative denominator (which vanishes only for the singularity), the static limits are given by

$$-\Delta_r(r) + \Delta_\theta(\theta)a^2\sin^2(\theta) = 0\,. \tag{1.118}$$

The static limits and the horizons overlap only on the space-time's axis, where the second term vanishes and static particles require simply $\Delta_r(r) > 0$. In the equatorial plane at $\theta = \pi/2$ static particles are allowed in a smaller region where $\Delta_r(r) - a^2 > 0$. The part of the stationary area of the space-time not allowing for static observers bounded by the static limits and, if applicable, the horizons is called the ergosphere.

Next, focusing solely on the equatorial plane in the following, frame-dragging is also the cause of a certain asymmetry of the allowed values of the observer's angular velocity

$$\Omega \equiv \frac{\mathrm{d}\phi}{\mathrm{d}t} = \frac{\mathrm{d}\phi}{\mathrm{d}\tau}\frac{\mathrm{d}\tau}{\mathrm{d}t} = \frac{u^\phi}{u^t}\,. \tag{1.119}$$

The extremal values of Ω at a given r are attainable only by observers whose spatial motion is restricted to the ϕ-direction, their four-velocity thus being

$$u^\mu = (u^t, 0, 0, u^\phi) = u^t(1, 0, 0, \Omega)\,. \tag{1.120}$$

From the normalisation equation (1.115) we obtain

$$\left(u^t\right)^2\left(g_{tt} + 2g_{t\phi}\Omega + g_{\phi\phi}\Omega^2\right) = -1\,, \tag{1.121}$$

that is,

$$\left(u^t\right)^2 = \frac{1}{-g_{tt} - 2g_{t\phi}\Omega - g_{\phi\phi}\Omega^2}\,. \tag{1.122}$$

For this u^t to be well-defined the right-hand side must be positive, which is assured if Ω lies between the two roots of the denominator

$$\Omega^{\max}_{\min} = \frac{-g_{t\phi} \pm \sqrt{\left(g_{t\phi}\right)^2 - g_{tt}g_{\phi\phi}}}{g_{\phi\phi}} = \omega \pm \sqrt{\omega^2 - \frac{g_{tt}}{g_{\phi\phi}}}\,, \tag{1.123}$$

[20]Here, static observers are simply those who have constant spatial coordinates. However, actually defining proper staticity is somewhat more complicated. It shall be examined more thoroughly in the corresponding section of the next chapter.

where we denoted

$$\omega \equiv -\frac{g_{t\phi}}{g_{\phi\phi}} = \frac{a\Big((r^2+a^2)\Delta_\theta(\theta) - \Delta_r(r)\Big)}{(r^2+a^2)^2\Delta_\theta(\theta) - a^2\sin^2(\theta)\Delta_r(r)}\,. \tag{1.124}$$

The value of ω is constant on a given horizon R, as the θ dependence drops out due to $\Delta_r(R) = 0$, leaving

$$\omega\Big|_{\text{horizon}} \equiv \Omega_{\text{H}} = \frac{a}{R^2+a^2}\,. \tag{1.125}$$

Take note that while a time-like observer cannot achieve the extreme values of Ω, they actually represent the only two possible angular velocities of massless photons orbiting the black hole at a given radius, as can be seen from (1.121) after considering that the four-velocity of a photon is normalised to zero instead of -1.

For the equatorial plane at $\theta = \pi/2$, we have

$$\omega = \frac{a\Big(r^2+a^2-\Delta_r(r)\Big)}{(r^2+a^2)^2 - \Delta_r(r)a^2} \tag{1.126}$$

and

$$\Omega^{\text{max}}_{\text{min}} = \frac{a\Big(r^2+a^2-\Delta_r(r)\Big) \pm r^2\sqrt{\Delta_r(r)}}{(r^2+a^2)^2 - \Delta_r(r)a^2}\,. \tag{1.127}$$

Only on the horizons it holds that $\Omega_{\text{min}} = \Omega_{\text{max}} = \omega \equiv \Omega_H$. Unsurprisingly, both extremal Ω are ill-defined in the non-stationary areas of the space-time where Δ_r is negative. Furthermore, the expressions above are well-defined in areas with $g_{\phi\phi} > 0$ only, because for $g_{\phi\phi} = 0$ the values of ω and Ω_{min} diverge and for $g_{\phi\phi} < 0$ it holds that $\Omega_{\text{max}} < \Omega_{\text{min}}$ and the actual angular velocity must, in fact, lie outside of the interval defined by these values, as high absolute values of Ω now keep the observer more time-like. And, much more importantly, closed time-like curves exist in regions with $g_{\phi\phi} < 0$, which is yet another reason to be suspicious of these areas. Sometimes called "time machines", these curves allow observers following them (not necessarily on a geodesic) to travel backwards in time, possibly violating causality. Fortunately, according to the chronology protection conjecture nature seems to have its way of disarming these curves. Further, a different hypothesis called chronological censorship says that closed time-like curves (or at least parts of them) are always hidden below a horizon, which means that an observer living in the outer part of the space-time can never experience any violation of causality due to the hidden time machine. Specifically for the Kerr–Newman solution the hypothesis is known to hold, as the problematic curves can be found only below the inner black hole horizon [14, 15].

Now, let us investigate closed time-like curves with the added ingredient of a non-zero cosmological constant. In the equatorial plane, we have

$$g_{\phi\phi}\left(r, \theta = \tfrac{\pi}{2}\right) = \frac{-\Delta_r(r)a^2 + \left(r^2+a^2\right)^2}{\Xi^2 r^2} = \frac{1}{\Xi^2 r^2}\left(\Xi r^4 + \Xi a^2 r^2 + 2ma^2 r - a^2 q^2\right)\,. \tag{1.128}$$

One can immediately see that $g_{\phi\phi}$ is negative in the vicinity of the singularity, and it is not due to the cosmological constant Λ (included in Ξ), but rather due

to the singularity's charge q. Closed time-like curves in the area with $r > 0$ are thus present in the Kerr–Newman solution as well, while in the original Kerr solution the phenomenon is confined to the area with $r < 0$. Concentrating on the area with $r > 0$, it is obvious now that $g_{\phi\phi}$ has exactly one positive root, because all the terms of the polynomial in the parentheses sans the absolute one are positive[21]. Does the inclusion of Λ make it possible for the radius at which $g_{\phi\phi} = 0$ to appear in any stationary area in the space-time, further complicating the analysis of the space-time? Fortunately not:

In the equatorial plane, it holds that

$$g_{t\phi}^2 - g_{tt} g_{\phi\phi} = \frac{\Delta_r}{\Xi^4}\,, \tag{1.129}$$

which we have already used in deriving (1.127). On the horizons (where $\Delta_r = 0$) in the equatorial plane, g_{tt} reduces to

$$g_{tt} = \frac{a^2}{\Xi^2 r^2} > 0\,. \tag{1.130}$$

Inserting this result into the previous equation, we have

$$g_{t\phi}^2 - \frac{a^2}{\Xi^2 r^2} g_{\phi\phi} = 0 \tag{1.131}$$

on the horizons, which means that $g_{\phi\phi}$ must be positive. This also means that – at least in the equatorial plane – the only positive root of $g_{\phi\phi}$ must be located in the area between the singularity and the first positive horizon, if there are any for the examined combination of the space-time parameters. In fact, the entire region with negative $g_{\phi\phi}$ must be hidden below the horizons (if there are any) regardless of the choice of θ with the exception of $\theta \in \{0, \pi\}$ (the axis of the space-time), where $g_{\phi\phi} \equiv 0\ \forall r$. Again, for any $\theta \in (0, \pi)$ there is at most one positive root of $g_{\phi\phi}$, as terms containing r are once more positive,

$$\begin{aligned} g_{\phi\phi}(r,\theta) = \frac{\sin^2\theta}{\Xi^2\rho^2(r,\theta)}\Big(&\Xi r^4 + \Xi a^2(1+\cos^2\theta)r^2 + 2ma^2(1-\cos^2\theta)r + \\ &+ \Xi a^4\cos^2\theta + a^2q^2(\cos^2\theta - 1)\Big)\,. \end{aligned} \tag{1.132}$$

Take note that for a certain θ, the function may be positive in the entire $r > 0$ area, because the terms not depending on r in the parentheses may be positive for a constant $\theta \neq \pi/2$, provided that $(\Xi a^2 + q^2)\cos^2\theta > q^2$. Now, we can prove that the positive root of $g_{\phi\phi}$ (if there is any for a given θ) is confined between $r = 0$ and the first horizon (if applicable) for any θ by computing the value of $g_{\phi\phi}(\bar{r}, \theta)$ for $\bar{r}$ satisfying $g_{\phi\phi}(\bar{r}, \theta = \pi/2) = 0$ and showing it is positive. The only positive root for a general $\theta \in (0, \pi)$ cannot therefore lie farther away from $r = 0$ than the root of $g_{\phi\phi}(r, \theta = \pi/2)$ in the equatorial plane, where it is indeed located between the singularity and the first horizon (if applicable) as shown above. As the horizons are spherical in our coordinates, the surface $g_{\phi\phi}(r, \theta) = 0$ and the horizons then cannot cross. From (1.128) it follows that the root of $g_{\phi\phi}(r, \pi/2)$ satisfies the relation

$$\Xi\bar{r}^4 + \Xi a^2\bar{r}^2 + 2ma^2\bar{r} - a^2q^2 = 0\,. \tag{1.133}$$

[21] Recall that from condition (1.4) we have $\Xi > 0$.

Now, after rearranging (1.132) to

$$g_{\phi\phi}(r,\theta) = \frac{\sin^2\theta}{\Xi^2\rho^2(r,\theta)}\Big(\left(\Xi a^2 r^2 - 2ma^2 r + \Xi a^4 + a^2 q^2\right)\cos^2\theta + \\ + \Xi r^4 + \Xi a^2 r^2 + 2ma^2 r - a^2 q^2\Big)\,, \tag{1.134}$$

we can see that terms not proportional to $\cos^2\theta$ vanish for $\bar{r}$ due to equation (1.133). To see that the rest of the expression is positive for $\bar{r}$ as promised, we shall once again take advantage of the relation above and substitute for the only negative term in the polynomial multiplying the cosine, $-2ma^2 r$. We obtain a remarkably simple result

$$g_{\phi\phi}(\bar{r},\theta) = \frac{\sin^2\theta\cos^2\theta}{\Xi\rho^2(\bar{r},\theta)}\left(a^2+\bar{r}^2\right)^2\,, \tag{1.135}$$

which is indeed positive. The chronological censorship is observed.

Thus, the dubious volume with $g_{\phi\phi} \leq 0$ is yet another nuisance plaguing the area containing the singularity, the other being that all observers in this area would be exposed to a naked singularity. Even though it is invariantly a stationary part of the space-time, as $\Delta_r(r=0) = a^2 + q^2 > 0$ unless $a = q = 0$, it is hardly an ideal place for a physical observer to live in.

We may take one step further and prove that closed time-like curves must lie at smaller r than the ergosphere with $g_{tt} > 0$, as has already been proved for the Kerr–Newman space-time [16]. To our knowledge, this property has not been shown previously for the space-time at hand. Take note that the ergosphere may be comprised of not only the area around the horizons, but it may also consist of one additional region with toroidal topology for scenarios with disappearing black hole horizons. The root of $g_{\phi\phi}$, however, would lie below that "island" as well: the full expression for g_{tt} is

$$g_{tt}(r,\theta) = \frac{1}{3\Xi^2\rho^2(r,\theta)}\Big(\Lambda a^4(1-\cos^2\theta)\cos^2\theta - 3a^2\cos^2\theta + \\ + \Lambda r^4 + (\Lambda a^2 - 3)r^2 + 6mr - 3q^2\Big)\,. \tag{1.136}$$

In the following, we shall see that for any given $\theta \notin \{0,\pi\}$ (i.e. not on the space-time's axis, where $g_{\phi\phi} \equiv 0$) it holds that $g_{\phi\phi}(\tilde{r},\theta) > 0$ with $\tilde{r}(\theta)$ satisfying $g_{tt}(\tilde{r},\theta) = 0$. Expressing m from this equation and inserting into $g_{\phi\phi}(\tilde{r},\theta)$ (1.132), we obtain

$$g_{\phi\phi}(\tilde{r},\theta) = \frac{\sin^2\theta}{3\Xi^2}\Big((6-3\cos^2\theta)a^2 + (2-\cos^2\theta)\Lambda a^4\cos^2\theta + 3\Delta_\theta(\theta)\tilde{r}^2\Big)\,. \tag{1.137}$$

Returning once more to (1.4), we can see that

$$3\Xi = \Lambda a^2 + 3 > 0\,. \tag{1.138}$$

After multiplying the first term by $\cos^2\theta$ the inequality still stands, as we are reducing the absolute value of the only term that may be negative. We thus have

$$3\Delta_\theta = \Lambda a^2\cos^2\theta + 3 > 0\,. \tag{1.139}$$

The term with $\tilde{r}^2$ in (1.137) is therefore manifestly positive even for a negative cosmological constant[22]. Further, after multiplying the inequality by $a^2 > 0$, we can substitute in the second term in (1.137) and obtain

$$g_{\phi\phi}(\tilde{r},\theta) > \frac{\sin^2\theta}{3\Xi^2}\Big((6-3\cos^2\theta)a^2 + (2-\cos^2\theta)(-3a^2) + 3\Delta_\theta(\theta)\tilde{r}^2\Big) = \\ = \frac{\sin^2\theta}{\Xi^2}\Delta_\theta(\theta)\tilde{r}^2 > 0 \tag{1.140}$$

as promised. Hence, the only positive root of $g_{\phi\phi}$ (if there is such a root in the first place for the given θ) must be located closer to $r = 0$ than all positive roots of g_{tt}. Since $g_{tt}(r = 0, \theta) < 0$, the regions with $g_{\phi\phi} < 0$ and $g_{tt} > 0$ do not intersect. Closed time-like curves must indeed lie below the innermost ergosphere.

Take note that there are no closed time-like curves in the θ-direction only, as

$$g_{\theta\theta} = \frac{\rho^2}{\Delta_\theta} > 0 \ \forall\theta, r\,. \tag{1.141}$$

Returning to the equatorial plane, one may also be interested in the limits of the above-mentioned angular velocities for extreme r. For $r \to 0^+$ one has

$$\lim_{r\to 0}\Omega_{\min} = \lim_{r\to 0}\Omega_{\max} = \lim_{r\to 0}\omega = \frac{1}{a} \tag{1.142}$$

regardless of the choice of Λ. For $r \to \infty$ one has

$$\lim_{r\to\infty}\omega = \frac{\Lambda a}{3\Xi} \tag{1.143}$$

and

$$\lim_{r\to\infty}\Omega^{\max}_{\min} = \frac{\Lambda a \pm \sqrt{-3\Lambda}}{3\Xi}\,, \tag{1.144}$$

where the latter limit requires a non-positive Λ, which is consistent with (1.127) after considering that $\Delta_r(r) \to -\infty$ for $\Lambda > 0$. Take note that Λ is important for the asymptotic behaviour of these functions, but m and q are irrelevant. For $\Lambda = 0$ the latter limits vanish. Somewhat counterintuitively, for $\Lambda < 0$ it holds that $\lim_{r\to\infty}\omega < 0$. The limit of $\Omega_{\max}$ is, however, always positive for negative Λ, as can be easily seen from (1.123) considering that – as we now know – the second term in the square root is negative for sufficiently large r and negative Λ.

Let us end the chapter with some figures illustrating our results. In figure 1.10 we can see constant t and ϕ slices of Kerr–Newman–anti-de Sitter space-times ($\Lambda < 0$) of all three horizon configurations. The figures depict the horizons and the static limits of the space-time with the non-stationary areas, the ergosphere and the area containing closed time-like curves highlighted. Take note that the size of the ergosphere varies with the space-time parameters and it may disappear altogether for a naked singularity even for a non-vanishing a. Next, figure 1.11 contains slices of two Kerr–Newman–de Sitter space-times. The two solutions are both of the most general family containing four non-degenerate horizons, but their ergospheres are different: for one space-time the ergospheres by the cosmological and the outer black hole horizons are disjoint, for the other they

[22]Ensuring $\Delta_\theta > 0$ was, in fact, the main motivation for introducing the condition (1.4).

are interconnected, which has implications for the possibility of the existence of static observers in the equatorial plane. The remaining horizon combinations are omitted, as the inner part of the pictures would look similarly to 1.10. The last two figures are charts of the allowed angular momenta along with ω for the equatorial plane of the space-times portrayed in the previous figures[23]. Notice that the space-time with the interconnected ergosphere does not permit static observers in the equatorial plane, while the other solution does.

[23]Contrary to our usual practice, the axes are scaled to multiples of a instead of m to better display the limits for $r \to 0$.

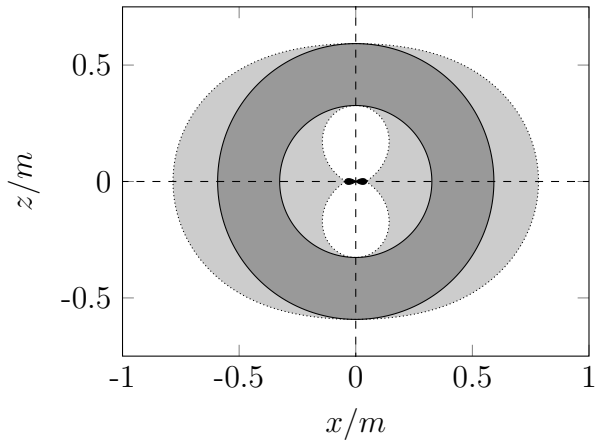

(a) Scenario $(\oplus 1-1+)$, $\{\Lambda, m, a, q\} = \{-10^{-3}\,\mathrm{u}^{-2}, 65\,\mathrm{u}, 40\,\mathrm{u}, 20\,\mathrm{u}\}$.

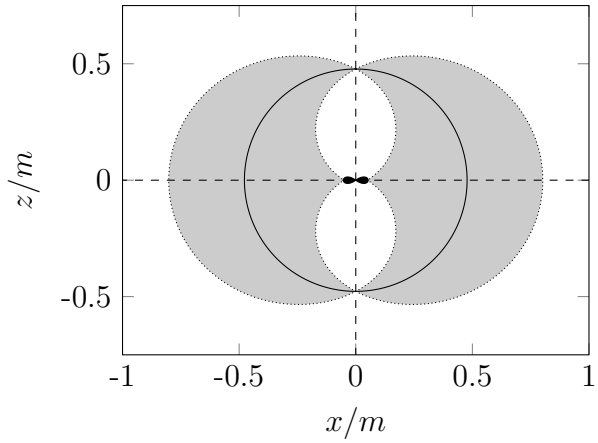

(b) Scenario $(\oplus 2+)$, $\{\Lambda, m, a, q\} = \{-10^{-3}\,\mathrm{u}^{-2}, 60.78\,\mathrm{u}, 40\,\mathrm{u}, 20\,\mathrm{u}\}$. The value of m is rounded to two decimal places.

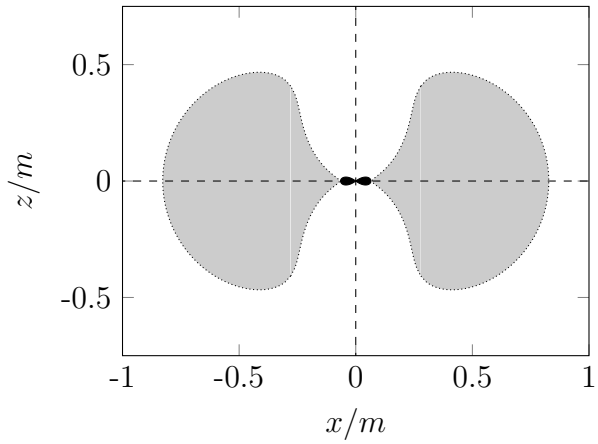

(c) Scenario $(\oplus)$, $\{\Lambda, m, a, q\} = \{-10^{-3}\,\mathrm{u}^{-2}, 55\,\mathrm{u}, 40\,\mathrm{u}, 20\,\mathrm{u}\}$.

Figure 1.10: Examples of structure of the space-time for all three possible horizon configurations with $\Lambda < 0$, sections with constant t and ϕ. Black circles represent the horizons, dotted curves the static limits. Light gray colour represents the ergosphere, dark gray the area with $\Delta_r < 0$ and black the area with closed time-like curves. Coordinates x and z are given by (1.12).

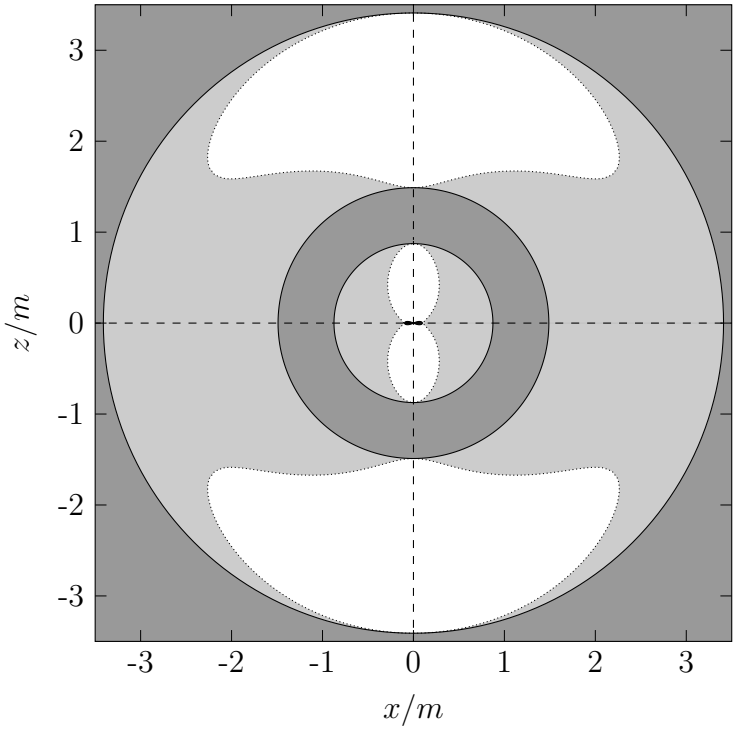

(a) Interconnected ergosphere, $\{\Lambda, m, a, q\} = \{10^{-3}\,\mathrm{u}^{-2}, 11\,\mathrm{u}, 10\,\mathrm{u}, 5\,\mathrm{u}\}$.

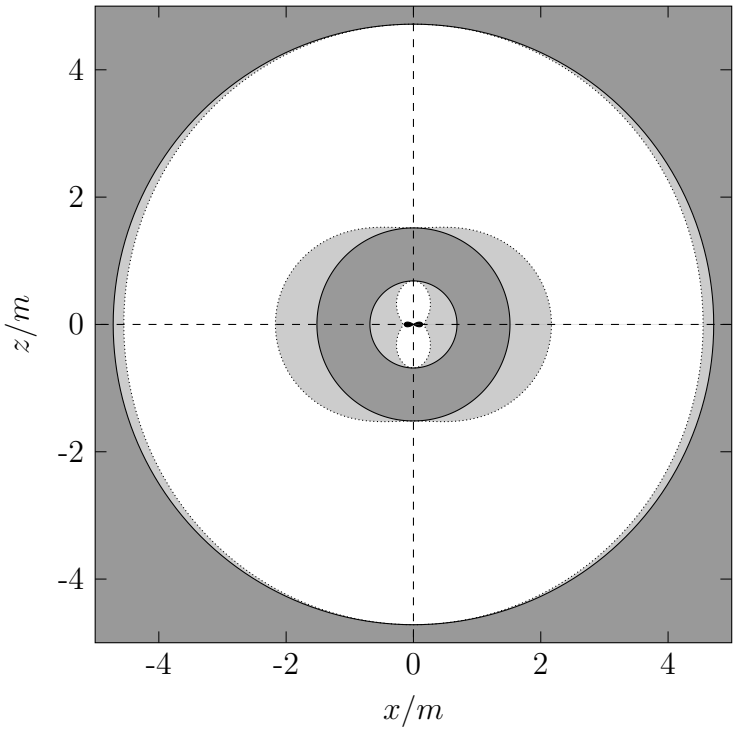

(b) Disjoint ergosphere, $\{\Lambda, m, a, q\} = \{10^{-3}\,\mathrm{u}^{-2}, 9\,\mathrm{u}, 7\,\mathrm{u}, 5\,\mathrm{u}\}$.

Figure 1.11: Examples of structure of the space-time for horizon configuration $(-1 \oplus 1 - 1 + 1-)$ with $\Lambda > 0$, sections with constant t and ϕ. Black circles represent the horizons, dotted curves the static limits. Light gray colour represents the ergosphere, dark gray the area with $\Delta_r < 0$ and black the area with closed time-like curves. Coordinates x and z are given by (1.12).

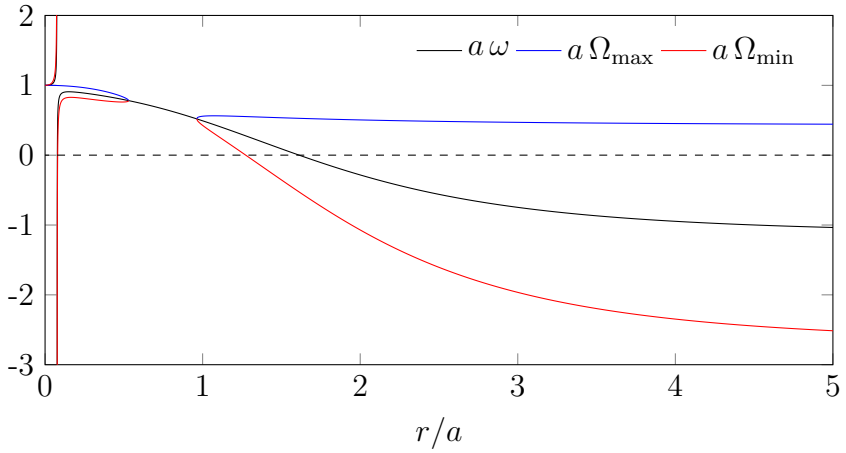

(a) Scenario $(\oplus 1-1+)$, $\{\Lambda, m, a, q\} = \{-10^{-3}\,\mathrm{u}^{-2}, 65\,\mathrm{u}, 40\,\mathrm{u}, 20\,\mathrm{u}\}$.

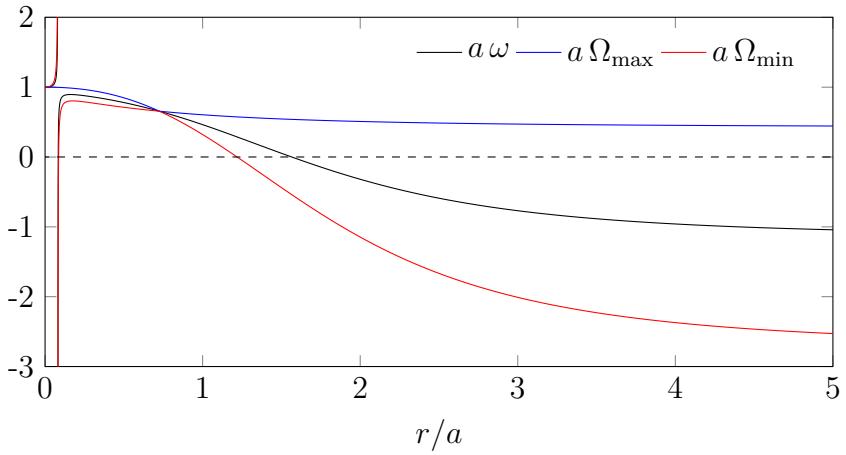

(b) Scenario $(\oplus 2+)$, $\{\Lambda, m, a, q\} = \{-10^{-3}\,\mathrm{u}^{-2}, 60.78\,\mathrm{u}, 40\,\mathrm{u}, 20\,\mathrm{u}\}$. The value of m is rounded to two decimal places.

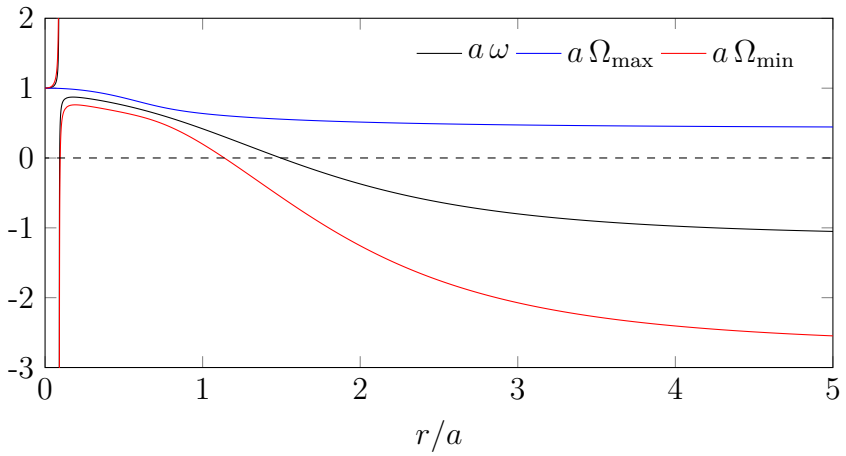

(c) Scenario $(\oplus)$, $\{\Lambda, m, a, q\} = \{-10^{-3}\,\mathrm{u}^{-2}, 55\,\mathrm{u}, 40\,\mathrm{u}, 20\,\mathrm{u}\}$.

Figure 1.12: Examples of boundaries of the allowed angular velocities for observers in the equatorial plane for all three possible horizon configurations with $\Lambda < 0$.

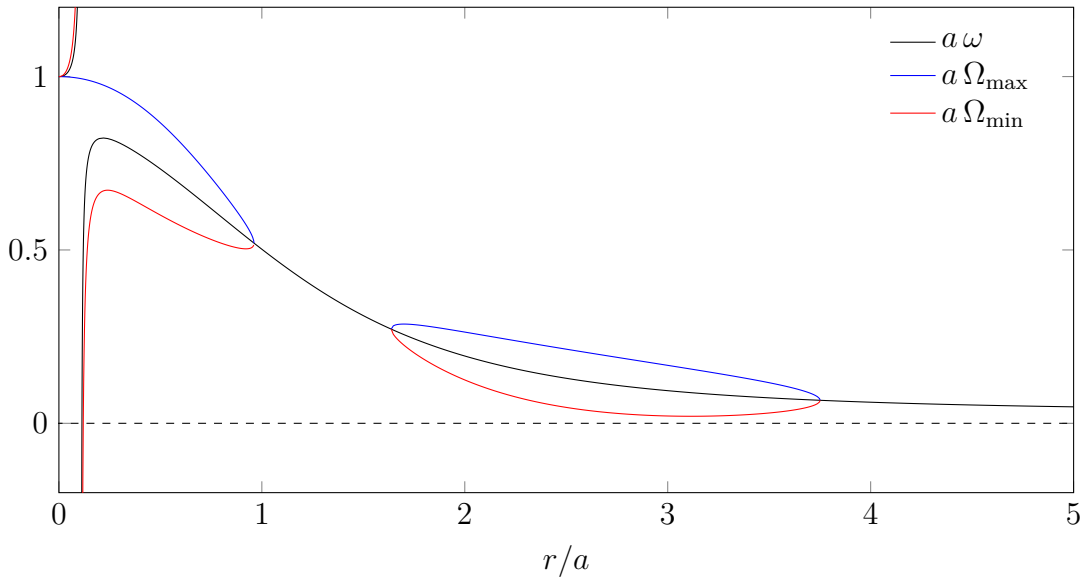

(a) Interconnected ergosphere, $\{\Lambda, m, a, q\} = \{10^{-3}\,\mathrm{u}^{-2}, 11\,\mathrm{u}, 10\,\mathrm{u}, 5\,\mathrm{u}\}$.

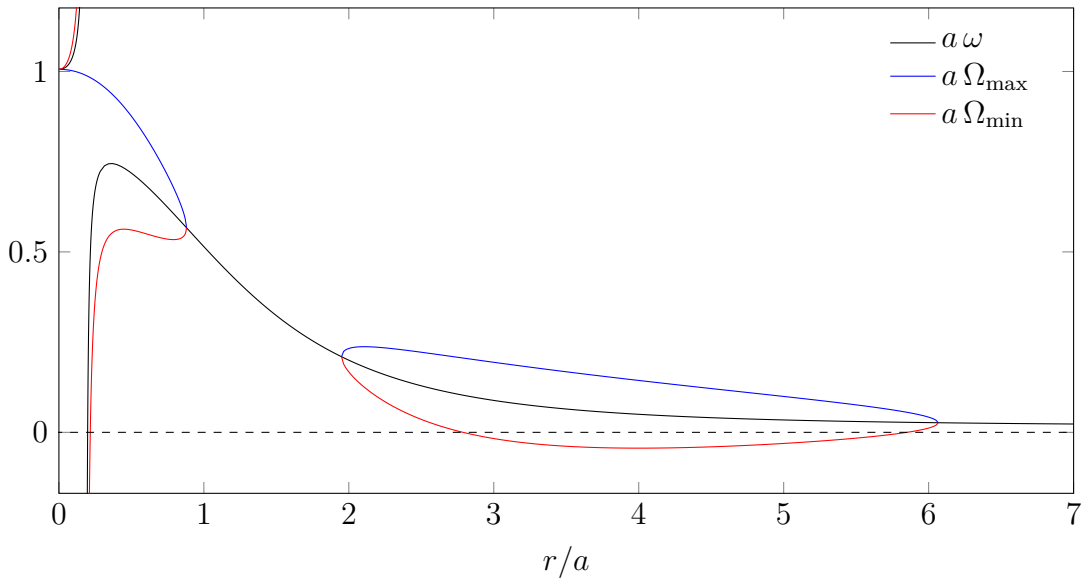

(b) Disjoint ergosphere, $\{\Lambda, m, a, q\} = \{10^{-3}\,\mathrm{u}^{-2}, 9\,\mathrm{u}, 7\,\mathrm{u}, 5\,\mathrm{u}\}$.

Figure 1.13: Examples of boundaries of the allowed angular velocities for observers in the equatorial plane for horizon configuration $(-1 \oplus 1 - 1 + 1-)$ with $\Lambda > 0$.

2. Electrogeodesics

One of the main goals of the thesis is to investigate motion of test particles in the Kerr–Newman–(anti-)de Sitter space-time, focusing especially on charged ones. As only the electromagnetic force can affect particles in this space-time[1], motion is electrogeodesical for charged particles or geodesical for uncharged ones.

In our investigation, we shall make use of the formalism of Lagrangian mechanics. In it, the dynamics of a system is described by an appropriate Lagrangian $\mathcal{L}$, a scalar function of the particle's coordinates and velocity. For us, one of the possible Lagrangian densities (see Appendix A) reads

$$\mathcal{L} = \frac{1}{2} g_{\mu\nu} \dot{x}^\mu \dot{x}^\nu + \kappa \dot{x}^\mu A_\mu \,, \tag{2.1}$$

where κ is the particle's charge-to-mass ratio and x^μ is its four-position. $\dot{x}^\mu$ is the total derivative of x^μ with respect to a variable (denoted p in the general case) we shall use to parametrise motion, $\dot{x}^\mu = \mathrm{d}x^\mu/\mathrm{d}p$. The most natural choice of the parameter in question is the particle's proper time τ, which measures proper distance along the trajectory and is invariant under coordinate transformations. $\dot{x}^\mu$ then becomes the particle's four-velocity u^μ and it can be expected that considering this parametrisation would lead to the simplest possible form of the equations of motion, since the first term in the Lagrangian (2.1) measures essentially the invariant distance along the path. However, not always can τ be used: perhaps most notably it is true for photons, whose proper time is constant. One can easily derive a relation between $\mathrm{d}p$ and $\mathrm{d}\tau$,

$$\sqrt{-g_{\mu\nu}\dot{x}^\mu \dot{x}^\nu} = \sqrt{-g_{\mu\nu} \frac{\mathrm{d}x^\mu}{\mathrm{d}p} \frac{\mathrm{d}x^\nu}{\mathrm{d}p}} = \frac{\mathrm{d}\tau}{\mathrm{d}p} \,. \tag{2.2}$$

In the case of $p = \tau$, we obtain the standard formula for the normalisation of the four-velocity for a time-like particle (that is, a particle moving slower than light) we have already used in the previous chapter,

$$g_{\mu\nu} u^\mu u^\nu = -1 \,. \tag{2.3}$$

The equations of motion are Lagrange's equations of the second kind,

$$\frac{\mathrm{d}}{\mathrm{d}p} \left(\frac{\partial \mathcal{L}}{\partial \dot{x}^\alpha} \right) - \frac{\partial \mathcal{L}}{\partial x^\alpha} = 0 \,. \tag{2.4}$$

For our Lagrangian and for a general parameter p, the partial derivatives are

$$\begin{aligned} \frac{\partial \mathcal{L}}{\partial x^\alpha} &= \frac{1}{2} g_{\rho\sigma,\alpha} \dot{x}^\rho \dot{x}^\sigma + \kappa \dot{x}^\beta A_{\beta,\alpha} \,, \\ \frac{\partial \mathcal{L}}{\partial \dot{x}^\alpha} &= g_{\alpha\beta} \dot{x}^\beta + \kappa A_\alpha \,. \end{aligned} \tag{2.5}$$

The Lagrange equations further contain

$$\frac{\mathrm{d}}{\mathrm{d}p} \left(\frac{\partial \mathcal{L}}{\partial \dot{x}^\alpha} \right) = g_{\alpha\beta} \ddot{x}^\beta + g_{\alpha\beta,\gamma} \dot{x}^\beta \dot{x}^\gamma + \kappa A_{\alpha,\beta} \dot{x}^\beta \,, \tag{2.6}$$

[1] It goes without saying that gravitation influences particle motion as well, but it is not considered *a force* per se in general relativity.

the second term of which can be recast as

$$g_{\alpha\beta,\gamma}\dot{x}^\beta\dot{x}^\gamma = \frac{1}{2}\left(g_{\alpha\beta,\gamma} + g_{\alpha\gamma,\beta}\right)\dot{x}^\beta\dot{x}^\gamma \tag{2.7}$$

due to the symmetry of $\dot{x}^\beta\dot{x}^\gamma$ in the two indices. After rearranging the terms and indices, the Lagrange equations become

$$\begin{aligned} g_{\alpha\beta}\ddot{x}^\beta + \frac{1}{2}\left(g_{\alpha\beta,\gamma} + g_{\alpha\gamma,\beta} - g_{\beta\gamma,\alpha}\right)\dot{x}^\beta\dot{x}^\gamma + \kappa\left(A_{\alpha,\beta} - A_{\beta,\alpha}\right)\dot{x}^\beta = \\ = g_{\alpha\beta}\ddot{x}^\beta + \Gamma_{\alpha\beta\gamma}\dot{x}^\beta\dot{x}^\gamma + \kappa F_{\beta\alpha}\,u^\beta = 0\,, \end{aligned} \tag{2.8}$$

where $\Gamma_{\alpha\rho\sigma}$ are the Christoffel symbols of the first kind,

$$\Gamma_{\alpha\rho\sigma} = \frac{1}{2}\left(g_{\alpha\rho,\sigma} + g_{\sigma\alpha,\rho} - g_{\rho\sigma,\alpha}\right)\,. \tag{2.9}$$

Finally, after multiplying the result by $g^{\alpha\mu}$, using the antisymmetry of $F_\beta{}^\mu$ and renaming the indices for aesthetic reasons, we obtain the preferred form of the equations of motion,

$$\frac{\mathrm{D}\dot{x}^\mu}{\mathrm{d}p} \equiv \ddot{x}^\mu + \Gamma^\mu{}_{\rho\sigma}\dot{x}^\rho\dot{x}^\sigma = \kappa F^\mu{}_\nu\,\dot{x}^\nu\,. \tag{2.10}$$

In this formula the astute reader recognises the geodesic equation with an added force term $\kappa F^\mu{}_\nu\,\dot{x}^\nu$ corresponding to the electromagnetic interaction [17]. The parameter p is an affine parameter, as the equation is in its purest, simplest form. For massive particles the equations can be written using the proper time τ as

$$\frac{\mathrm{D}u^\mu}{\mathrm{d}\tau} \equiv \frac{\mathrm{d}u^\mu}{\mathrm{d}\tau} + \Gamma^\mu{}_{\rho\sigma}u^\rho u^\sigma = \kappa F^\mu{}_\nu\,u^\nu\,. \tag{2.11}$$

While the electrogeodetic equation usually operates with τ as its parameter, is it really necessary to use exclusively τ as the parameter for massive particles? No, as it turns out, we do not *need* to use τ – but it makes our life considerably easier. Let us try to go from equation (2.11) back to (2.10) by considering a different parameter (not necessarily affine) as a function of the proper time, $p(\tau)$. Subsequently, the conditions $p(\tau)$ must fulfil for it to be an affine parameter as well shall manifest themselves. It holds that

$$\frac{\mathrm{d}}{\mathrm{d}\tau} = \frac{\mathrm{d}p}{\mathrm{d}\tau}\frac{\mathrm{d}}{\mathrm{d}p}\,. \tag{2.12}$$

Substituting $\tau \to p(\tau)$ in (2.11), we obtain

$$\frac{\mathrm{d}^2x^\mu}{\mathrm{d}p^2}\left(\frac{\mathrm{d}p}{\mathrm{d}\tau}\right)^2 + \frac{\mathrm{d}x^\mu}{\mathrm{d}p}\frac{\mathrm{d}^2p}{\mathrm{d}\tau^2} + \Gamma^\mu{}_{\rho\sigma}\frac{\mathrm{d}x^\rho}{\mathrm{d}p}\frac{\mathrm{d}x^\sigma}{\mathrm{d}p}\left(\frac{\mathrm{d}p}{\mathrm{d}\tau}\right)^2 = \kappa F^\mu{}_\nu\frac{\mathrm{d}x^\nu}{\mathrm{d}p}\frac{\mathrm{d}p}{\mathrm{d}\tau}\,. \tag{2.13}$$

We now aim to find such a parameter $p(\tau)$ for which the last equation would be a multiple of (2.10). The equations of motion would then be the same and $p(\tau)$ would be, alongside τ itself, an affine parameter. Our new $p(\tau)$ must eliminate the additional second term on the left side of the equation and change all the original terms by the same coefficient. After considering that the term with κ is

multiplied by a different power of $\mathrm{d}p/\mathrm{d}\tau$ than the other terms, we find out that the only possible affine reparametrisation is

$$p(\tau) = \tau + \tau_0 \,, \tag{2.14}$$

an addition of a constant. On the other hand, a standard geodesic equation for an uncharged particle with $\kappa = 0$ allows for a linear rescaling of τ, $p(\tau) = a\tau + b$ with a and b constant[2]. Therefore, disregarding the trivial additive constant, the only affine parameter for massive particles is τ and the normalisation of the four-velocity (2.3), of course, holds. If we wanted to use another parameter, we would need to resort to using the more complex equation (2.13), which would further convolute an already difficult mathematical problem.

For photons, the affine parameter shall be denoted λ in the following. It has no relation to photon proper time, because the proper time is constant and no function of it can be used to parametrise photon motion. The normalisation of the analogue of the four-velocity for photons is

$$g_{\mu\nu}\frac{\mathrm{d}x^\mu}{\mathrm{d}\lambda}\frac{\mathrm{d}x^\nu}{\mathrm{d}\lambda} \equiv g_{\mu\nu}\dot{x}^\mu\dot{x}^\nu = 0 \,. \tag{2.15}$$

2.1 Integrals of motion

Seeing that the metric $g_{\mu\nu}$ (1.1) and the four-potential A_μ (1.3) do not depend on coordinate time t and angle ϕ, neither is $\mathcal{L}$ a function of these variables. These two coordinates are therefore cyclic and are associated with conservation of certain quantities, constants of motion: energy E and angular momentum L parallel to the axis of rotation of the black hole. For a general parametrisation

$$\begin{aligned} -E \equiv \frac{\partial\mathcal{L}}{\partial\dot{t}} &= g_{tt}\dot{t} + g_{t\phi}\dot{\phi} + \kappa A_t \,, \\ L \equiv \frac{\partial\mathcal{L}}{\partial\dot{\phi}} &= g_{t\phi}\dot{t} + g_{\phi\phi}\dot{\phi} + \kappa A_\phi \,. \end{aligned} \tag{2.16}$$

Specifically, for a parametrisation using proper time τ,

$$\begin{aligned} -E &= g_{tt}u^t + g_{t\phi}u^\phi + \kappa A_t \,, \\ L &= g_{t\phi}u^t + g_{\phi\phi}u^\phi + \kappa A_\phi \,. \end{aligned} \tag{2.17}$$

Take note that while we use the standard sign convention, the signs of these constants may be chosen arbitrarily. Selecting the opposite sign of a constant would require changing the sign before odd powers of the redefined constant in formulae containing it. Further, notice that these constants actually are the t and ϕ components of the generalised four-momentum of the particle $p_\alpha \equiv \partial\mathcal{L}/\partial\dot{x}^\alpha$.

We called the constants of motion the energy E and the angular momentum L purely out of analogy with asymptotically flat space-times. In such cases interpreting the integrals of motion is done by projecting the four-momentum of the particle on the four-velocity of a privileged observer: a static observer in flat

[2]If we used this particular transformation for our electrogeodesics, we would obtain the standard electrogeodesic equation but for a different particle with $\kappa' = \kappa/a$.

spatial infinity[3]. However, with a non-zero Λ, our space-time is not endowed with such observers and interpreting the integrals of motion cannot be done in such a way. Nonetheless, when referring to them by name, we shall use the above terms out of lack of a more proper nomenclature.

Another famous integral of motion is the Carter constant. It is, however, difficult to obtain the constant from the Lagrangian formalism and one resorts to the Hamilton–Jacobi equation. Even though we focus on relativistic Lagrangian mechanics, for the sake of completeness we chose to dedicate Appendix B to the Hamilton–Jacobi equation and the Carter constant.

Last but not least, since the Lagrangian does not depend explicitly on τ, the value of the Hamiltonian is a constant of motion too. Also calculated in Appendix B, it turns out that the value is a multiple of the normalisation of $\dot{x}^\alpha$.

2.2 On the normalisation equation

Before moving on to solving the electrogeodesic equations, it may prove useful to examine the normalisation equation

$$g_{\mu\nu}u^\mu u^\nu = -1\,. \tag{2.3}$$

It is a non-linear first-order differential equation that provides a condition on the particle's four-velocity.

Eventually, when we begin solving the equations numerically, we will need to choose the initial four-velocity in such a way that fulfils the normalisation. Is the normalisation then preserved after an integration step or does the four-velocity need to be normalised after every step again and again? Let us find out:

$$\begin{aligned}\frac{\mathrm{d}}{\mathrm{d}\tau}\left(g_{\mu\nu}u^\mu u^\nu\right) = \frac{\mathrm{D}}{\mathrm{d}\tau}\left(g_{\mu\nu}u^\mu u^\nu\right) = g_{\mu\nu}\left(\frac{\mathrm{D}u^\mu}{\mathrm{d}\tau}u^\nu + u^\mu\frac{\mathrm{D}u^\nu}{\mathrm{d}\tau}\right) = \\ = 2g_{\mu\nu}u^\mu\frac{\mathrm{D}u^\nu}{\mathrm{d}\tau} = 2\kappa g_{\mu\nu}u^\mu F^\nu{}_\iota\, u^\iota = 2\kappa F_{\mu\iota}u^\mu u^\iota = 0\,.\end{aligned} \tag{2.18}$$

First, we used that the total and absolute derivative are interchangeable upon acting on a scalar. In the next two steps, we remembered that every metric is covariantly constant, $g_{\mu\nu;\alpha} = 0$, and symmetric, $g_{\mu\nu} = g_{\nu\mu}$. After that, we inserted the equations of motion (2.11) and noticed that we are left with a product of $F_{\mu\iota}$, antisymmetric in μ and ι, and $u^\mu u^\iota$, which are symmetric in their indices. Therefore, the sought derivative is equal to zero, and we should never need to reapply the normalisation equation at any point after setting the initial four-velocity. However, as numerical computations are always affected by rounding errors, it is definitely worthwhile to check the normalisation occasionally and adjust the four-velocity accordingly, if needed.

Another related question is whether we cannot replace one of the four electrogeodesic equations with the normalisation when solving the system. The electrogeodesic equations are second order, and replacing one of them with the normalisation would not only possibly simplify the system (for numerical and analytical computations alike), but also lower the number of the needed initial conditions by

[3]Knowing the physical interpretation, the signs of the constants can no longer be chosen arbitrarily.

one component of the starting four-velocity. Our lives would then become easier by not having to worry about the normalisation of the initial four-velocity in numerical simulations. The procedure of proving interchangeability of one of the electrogeodesic equations and the normalisation equation is similar to the previous calculation, but with a twist. The fixed index of the equation to be swapped out shall be $\aleph$[4], the remaining three indices shall be represented by Latin script. The other three electrogeodesic equations are assumed to hold.

$$\begin{aligned} 0 = \frac{1}{2}\frac{\mathrm{D}}{\mathrm{d}\tau}\left(g_{\mu\nu}u^\mu u^\nu\right) = g_{\mu\nu}u^\mu\frac{\mathrm{D}u^\nu}{\mathrm{d}\tau} = g_{\mu\aleph}u^\mu\frac{\mathrm{D}u^\aleph}{\mathrm{d}\tau} + g_{\mu a}u^\mu\frac{\mathrm{D}u^a}{\mathrm{d}\tau} = \\ = g_{\mu\aleph}u^\mu\frac{\mathrm{D}u^\aleph}{\mathrm{d}\tau} + \kappa g_{\mu a}u^\mu F^a{}_\iota\, u^\iota = g_{\mu\aleph}u^\mu\frac{\mathrm{D}u^\aleph}{\mathrm{d}\tau} + \kappa F_{a\iota}u^a u^\iota = \\ = g_{\mu\aleph}u^\mu\frac{\mathrm{D}u^\aleph}{\mathrm{d}\tau} + \kappa F_{a\aleph}u^a u^\aleph + \cancel{\kappa F_{ab}u^a u^b} = u_\aleph\left(\frac{\mathrm{D}u^\aleph}{\mathrm{d}\tau} + \kappa F_a{}^\aleph u^a\right) = \\ = u_\aleph\left(\frac{\mathrm{D}u^\aleph}{\mathrm{d}\tau} - \kappa F^\aleph{}_a\, u^a\right) = u_\aleph\left(\frac{\mathrm{D}u^\aleph}{\mathrm{d}\tau} - \kappa F^\aleph{}_\mu\, u^\mu\right), \end{aligned} \tag{2.19}$$

where in the last two steps we exclusively used the antisymmetry of the electromagnetic tensor. From this result follows that for a non-zero $u_\aleph$ its corresponding electrogeodesic equation (2.11) is satisfied automatically if the remaining three equations and the (derivative of the) normalisation equation hold. This also means that we cannot swap out equations corresponding to vanishing components of the covariant four-velocity. For example, for motion restricted to the equatorial plane at $\theta = \pi/2$ we have $u^\theta = 0$, and (as $g_{\theta t} = g_{\theta r} = g_{\theta\phi} \equiv 0$) also $u_\theta = 0$. The corresponding equation of motion for θ must, therefore, be preserved. Actually, this may be in our best interests, as for these initial conditions the equation simplifies into $\mathrm{d}^2\theta/\mathrm{d}\tau^2 = 0$, a trivial equation ensuring (and assuring us) that the particle stays in the equatorial plane.

Take note that the zeroes in the last two numbered equations have slightly different origins: In the first one, we computed the time derivative of the left-hand side of the normalisation equation to find out whether we would need to renormalise the four-velocity after each step in numerical computations. We found out that the normalisation is preserved even without our intervention. In the second equation, we assumed the normalisation equation to hold at any time (with or without our help in the simulations), and we simply performed the time derivative of both sides of the equation, whence came the initial zero.

The above conclusions hold for photons as well, because we are dealing only with the derivatives of the normalisation, its actual value is irrelevant as long as it is constant. Assuming $\kappa = 0$ only makes the proofs shorter.

Now, let us begin investigating specific types of motion. As we aim to provide analytical results, we shall focus on the equatorial plane and on the space-time's axis only. These special values of θ simplify the equations enough for us to be able to make some interesting discoveries, which we will often demonstrate using numerical methods. Greater emphasis shall be put on the area with positive r. First, we shall deal with static particles.

[4]We use the Hebrew letter *aleph* to emphasise that there is never any summation to be performed over this index.

2.3 The static case

To say the first thing that comes to mind, a static particle is a particle that does not move through space. However, as early as in elementary school pupils are taught that motion is relative: we need to specify an object regarding to which our examined particle is at rest. In classical physics, the situation is quite simple: we define a Cartesian coordinate system with the other object at its origin, and say that the particle is at rest with respect to the object when its Cartesian coordinates are constant. In general relativity, defining a static particle is a somewhat trickier matter. One can examine particles that would be static in a certain set of coordinates, but general relativity allows for unlimited transformations of coordinate systems, and a static particle in one set of coordinates may not be static in another one. For rotating black holes, however, one can look at the particle's angular momentum to characterise staticity with an invariant property. Thus the concept of a *zero angular momentum observer*, or simply ZAMO, is introduced: It is an observer who orbits[5] the black hole in such a way his angular momentum vanishes. A particle coinciding with this observer could be considered to be somewhat more invariantly static with respect to the rotating black hole in question. As has already been discussed, L cannot be easily interpreted as the angular momentum of the particle due to the space-time's non-zero cosmological constant. However, in the limit of $\Lambda = 0$ the interpretation holds and it is natural to extend the definition of ZAMOs to the case of $L = 0$ in our space-time as well.

In this section, we shall approach the problem of static particles from both points of view. First, we shall investigate particles static in our coordinate system, as it could be considered an extension of the classical spherical coordinate system (at least in the stationary areas of the space-time) and it is, therefore, not entirely unreasonable to say that this is the system in which a "truly" static particle ought to have constant spatial coordinates, that is, its world line should be $x^\mu = (t, r_0, \theta_0, \phi_0)$ with constant r_0, θ_0 and ϕ_0. The spatial components of the particle's four-velocity vanish, $u^i = 0$. From the normalisation of the four-velocity (2.3), we get $u^t = 1/\sqrt{-g_{tt}(r_0, \theta_0)}$. We thus have a constant four-velocity

$$u^\mu = \left(\frac{1}{\sqrt{-g_{tt}(r_0, \theta_0)}}, 0, 0, 0 \right) \tag{2.20}$$

and, as such, the total derivatives of its components with respect to τ are equal to zero[6]. This ansatz is applicable only in the stationary areas of the space-time where $g_{tt} < 0$. At the static limit, defined previously as the surface satisfying $g_{tt} = 0$, u^t would diverge. In the dynamic areas this u^μ does not describe a time-like particle.

Inserting the above four-velocity into the equations of motion, we see that two of the four are reduced into the identity $0 = 0$, namely those corresponding to

[5] In our coordinates, by "orbiting" we mean a time-like circular motion in the ϕ coordinate with constant r and θ.

[6] This is not equivalent to saying that the particle's four-acceleration $\mathrm{D}u^\mu/\mathrm{d}\tau$ vanishes. For an electrogeodesic, the four-acceleration is equal to the force term $\kappa F^\mu{}_\nu \, u^\nu$.

the t and ϕ components of the four-acceleration. The remaining two equations,

$$\begin{aligned} -\Gamma^{r}{}_{tt}u^t + \kappa F^{r}{}_{t} &= 0\,, \\ -\Gamma^{\theta}{}_{tt}u^t + \kappa F^{\theta}{}_{t} &= 0\,, \end{aligned} \tag{2.21}$$

impose conditions on the position of static particles[7].

The problem of solving the four non-linear second-order differential equations of motion to find four functions of proper time describing the particle's position $x^\mu(\tau)$ is hereby reduced to solving a set of two algebraic equations for two constants r_0 and θ_0 (due to the axial symmetry of the space-time, ϕ_0 would then be arbitrary). Even though the situation becomes considerably simpler, finding a general solution still remains nontrivial.

A further simplification of the problem – which may be our best hope for deriving any analytical results – consists in selecting a particular θ_0 for which we shall try to find a corresponding r_0. The two values of θ_0 we are going to look into are $0 \Leftrightarrow \pi$ (equivalent due to the reflection symmetry of the space-time) and $\pi/2$. The former represents particles on the black hole's axis of rotation, the latter particles in the equatorial plane. As it turns out, when substituted into (2.21), both of these values reduce the second equation to an identity. Therefore, we need to solve one equation to find a single constant, r_0. The subscript "0" shall be omitted in the following.

2.3.1 The axis

For $\theta \in \{0, \pi\}$, the remaining equation of motion is

$$\begin{aligned} \Big[& \Lambda s r^7 - \kappa q \Lambda r^6 + 3\Lambda a^2 s r^5 - 3(ms - \kappa q) r^4 + \\ & + 3\left((a^4\Lambda + q^2)s - 2\kappa q m\right) r^3 + \kappa q (a^4\Lambda + 3q^2) r^2 + \\ & + a^2\left((a^4\Lambda + 3q^2)s + 6\kappa q m\right) r + \\ & + 3a^2\left(a^2 m s - \kappa q (a^2 + q^2)\right) \Big] \Big[(a^2 + r^2)^3 s \Big]^{-1} = 0 \end{aligned} \tag{2.22}$$

with

$$s = \sqrt{\frac{\Delta_r(r)}{\rho^2(r, \theta = 0)}}\,. \tag{2.23}$$

If we didn't insist on preserving the Lorentzian signature of the metric by fulfilling (1.4), s would need to be multiplied by $\mathrm{sgn}(\Xi)$. The left-hand side of the equation is well-defined only in the stationary areas of the space-time where $\Delta_r > 0$, which corresponds to our original ansatz for u^μ.

Even with all the simplifications we have made, finding an analytical solution for r for a general space-time is still very difficult. However, we may choose a

[7] Perhaps more precisely, considering the four-velocity of the static particle as an initial condition, the two vanishing equations of motion say that two components of u^μ are constant at the beginning of the observed motion. The remaining two equations must be met in order to ensure that all four components of u^μ are not changing at the initial time. Since the space-time is stationary, a four-velocity constant at the initial time then remains constant indefinitely. The same is also true for stationary circular orbits in the next chapter.

different approach to this problem and look for a "properly-charged" particle that would remain still at a given r in a given space-time. While (2.22) is a complicated irrational equation in r, it is linear in κ and easy to solve:

$$\kappa = -\frac{\Lambda r^5 + 2a^2\Lambda r^3 - 3mr^2 + (a^4\Lambda + 3q^2)r + 3a^2 m}{3q(r+a)(r-a)s}\,. \tag{2.24}$$

If $q \neq 0$, this expression is well-defined in the stationary areas of the space-time with the possible exception of $r = \pm a$, which may or may not be in the stationary area[8]. A problem with $q = 0$ is to be expected, as for an uncharged black hole the charge of the particle is irrelevant. Fine-tuning of κ then cannot help in any way to make the particle static. The case of $r = \pm a$ is more interesting:

For $r = \pm a$, the terms with κ in (2.22) vanish, and the rest of the equation is remarkably reduced into

$$\frac{4a^4\Lambda + 3q^2}{a^3} = 0\,. \tag{2.25}$$

If the space-time's parameters fulfil this condition, any particle can remain at rest at $r = \pm a$ regardless of its charge[9]. The problem with $a = 0$ in the condition is of no relevance, as that would mean our desired static particles are in the singularity[10] at $r = \pm a = 0$. Assuming $a \neq 0$, we may recast requirement (2.25) as

$$\Lambda = -\frac{3}{4}\frac{q^2}{a^4}\,, \tag{2.26}$$

whence it is obvious that Λ has to be non-positive. That unfortunately prohibits astrophysical black holes from having any particles at rest at $r = \pm a$ as the universe is thought to have a positive Λ, cf. (1.7). Comparing with (1.4), we can easily find a condition on the ratio of a^2 and q^2,

$$q^2 < 4a^2\,. \tag{2.27}$$

Whether $r = \pm a$ is in the stationary area of the space-time, as required by our ansatz, is given by the sign of $\Delta_r(r = \pm a)$. In particular, if we inquire about static particles, we have

$$\Delta_r(r = \pm a)\Big|_{\Lambda = -\frac{3}{4}\frac{q^2}{a^4}} = 2a^2 + \frac{3}{2}q^2 \mp 2ma\,. \tag{2.28}$$

The negative solution is thus always in the stationary area, while the positive one further requires

$$m < \frac{4a^2 + 3q^2}{4a}\,. \tag{2.29}$$

[8] In order to avoid confusion, let us point out that positive values of r are not "above" and negative "below" the black hole on its axis – that is determined by θ. As has already been mentioned before, due to the reflection symmetry of the space-time we now concurrently examine both $\theta = 0$ and π, i.e. both "above" and "below". Negative r represent the analytically extended part of the space-time.

[9] Take note that the particle may even be uncharged.

[10] The Kerr–type rotating black holes have a ring singularity located in the equatorial plane at $\theta = \pi/2$, not on their axis. However, for $a = 0$ one has a non-rotating black hole with a point singularity at $r = 0$ regardless of θ.

Take note that while these static positions may exist in the Kerr and the KNadS solutions, not only are they nowhere to be found in the KNdS space-time, as we have already commented, but they also do not exist in the asymptotically flat Kerr–Newman solution, as can be seen from (2.26): non-zero a and q manifestly require a non-zero Λ as well. Likewise, the same can also be said of the Kerr–(anti-)de Sitter solutions, because having a non-zero Λ and vanishing q violates (2.26) as well.

Now that we have established the possibility of the existence of static uncharged particles, we are left with the question what holds them in place, because it is neither electromagnetism (as the particles stay in place regardless of their charge) nor a repulsive cosmological constant (as the required negative Λ is actually attractive, to make the situation even more puzzling) in a kind of an equilibrium with gravity. It turns out [18, 19] that *repulsive gravity* is a common occurrence in naked-singularity space-times (among them e.g. a Kerr naked singularity). If the above conditions on the parameters result in a naked singularity, it is natural to assume that we have just discovered yet another manifestation of this phenomenon. In order to prove that, we need to return to Δ_r one more time:

$$\Delta_r(r)\Big|_{\Lambda=-\frac{3}{4}\frac{q^2}{a^4}} = (r^2+a^2)\left(1+\frac{q^2}{4a^4}r^2\right) - 2mr + q^2\,. \tag{2.30}$$

Inserting inequality (2.29) into Δ_r (keeping in mind that for $-m$ we have to change the inequality sign), we obtain

$$\begin{aligned}\Delta_r(r)\Big|_{\text{repulsion}} &> (r^2+a^2)\left(1+\frac{q^2}{4a^4}r^2\right) - \frac{4a^2+3q^2}{2a}r + q^2 = \\ &= \frac{(r-a)^2(q^2r^2+2aq^2r+4a^4+4a^2q^2)}{4a^4}\,.\end{aligned} \tag{2.31}$$

The resulting polynomial acting as a lower bound has a double root at $r=a$ and the remaining roots are not real[11]. Since the polynomial is positive at $r=0$ and $r\to\pm\infty$, it is obvious that it is positive almost everywhere, with the sole exception of $r=a$, where it is equal to zero. Due to the presence of the strict inequality in (2.31), we have

$$\Delta_r(r)\Big|_{\text{repulsion}} > 0 \quad \forall\, r\,, \tag{2.32}$$

which means that the polynomial has no real roots. A space-time allowing for static uncharged particles at positive r thus has no horizons and therefore indeed contains a naked singularity[12]. A sample course of $\Delta_r(r)$ near the function's minimum for parameters satisfying the aforementioned conditions is shown in figure 2.1 on the following page. Take note that inequality (2.29), instrumental in proving that the space-time is that of a naked singularity, is not required by static particles at $r=-a$. However, for $r<0$ the only stationary area invariantly contains the singularity, meaning these particles experience a naked singularity as well.

[11] The quadratic polynomial $q^2r^2 + 2aq^2r + 4a^4 + 4a^2q^2$ has a negative discriminant $-4(4a^4q^2+3a^2q^4)$.

[12] For the Kerr solution this observation can be done directly from (2.29), which for $q=0$ reduces into $m<a$, the known condition for the singularity's nakedness.

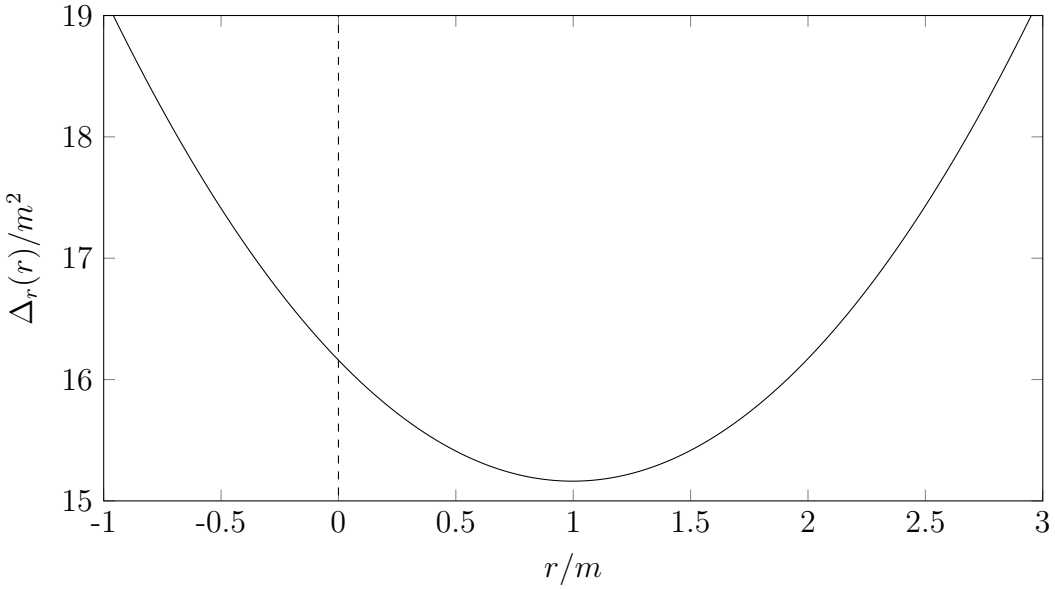

Figure 2.1: The course of $\Delta_r(r)$ corresponding to the scenario of repulsive gravity with parameters $\{\Lambda, \underline{m}, \underline{a}, \underline{q}\} = \{-7.5 \times 10^{-7}\,\mathrm{u}^{-2}, 25\,\mathrm{u}, 100\,\mathrm{u}, 10\,\mathrm{u}\}$. The values of all parameters are precise, the free parameters are underlined.

Before moving on to the equatorial plane, let us have a quick look at the integrals of motion (2.17). For $\theta \in \{0, \pi\}$, we obtain

$$\begin{aligned} E &= \frac{\Delta_r(r)u^t + \Xi q r \kappa}{\Xi^2 \rho^2(r, \theta = 0)}\,, \\ L &= 0 \end{aligned} \tag{2.33}$$

regardless of the particle's u^ϕ, as the ϕ coordinate is degenerate on the axis, $g_{\phi\mu} = 0\ \forall\mu$. To evaluate E for static particles, u^t is to be substituted from (2.20) and for $r \neq \pm a$, κ is given by (2.24). This fortunate result means that particles static on the space-time's axis in our coordinate system also fulfil the other staticity condition and are ZAMOs[13].

2.3.2 The equatorial plane

For $\theta = \pi/2$ we need to solve a seemingly simpler equation than in the previous case,

$$\begin{aligned} \frac{\Delta_r(r)}{\Delta_r(r) - a^2}\Big[\Lambda\tilde{s}r^5 - q\kappa\Lambda r^4 - \Big(3m\tilde{s} + q\kappa(a^2\Lambda - 3)\Big)\, r^2 + \\ + 3q(q\tilde{s} - 2\kappa m)r + 3q^3\kappa\Big]\Big[r^4\tilde{s}\Big]^{-1} = 0 \end{aligned} \tag{2.34}$$

with

$$\tilde{s} = \sqrt{\frac{\Delta_r(r) - a^2}{\rho^2(r, \theta = \pi/2)}}\,. \tag{2.35}$$

[13]Even though their angular momentum vanishes as well, radially-moving particles are not ZAMOs, as ZAMOs are by definition allowed to move in the t and ϕ directions only.

This time, the left-hand side of the equation is not well-defined everywhere in the stationary area of the space-time, but rather only in a smaller area satisfying

$$\Delta_r > a^2 \Leftrightarrow g_{tt}\Big|_{\theta=\pi/2} < 0\,. \tag{2.36}$$

It is to be expected that for a general θ, static particles would not persist in the whole stationary area due to frame-dragging. The axis is spared from this effect, which is the reason we did not need to restrict ourselves to a smaller part of the stationary area in the previous case. As was already discussed near the end of the previous chapter, the condition $g_{tt} = 0$ gives the static surface, which separates areas where static observers in our coordinates can ($g_{tt} < 0$) and cannot ($g_{tt} > 0$) exist.

Once again, finding the static particle's κ is considerably easier than solving the equation of (no) motion for r,

$$\kappa = -\frac{\Lambda r^4 - 3mr + 3q^2}{3qr\tilde{s}}\,. \tag{2.37}$$

A divergence for $q = 0$ is to be expected. There are no other problems with this expression outside the singularity and the area where $g_{tt} > 0$.

Unlike the preceding case, there is no particular r in the allowed area for which the term with κ in equation (2.34) vanishes. This can also be seen from (2.37), where this particular r would cause a division by zero as in the previous case.

For $\theta = \pi/2$ and $u^\phi = 0$, the integrals of motion (2.17) are

$$\begin{aligned} E &= \frac{(\Delta_r(r) - a^2)u^t + \Xi qr\kappa}{\Xi^2\rho^2(r, \theta = \pi/2)}\,, \\ L &= \frac{a\Big((\Delta_r(r) - r^2 - a^2)u^t + \Xi qr\kappa\Big)}{\Xi^2\rho^2(r, \theta = \pi/2)}\,, \end{aligned} \tag{2.38}$$

with u^t given by (2.20) and κ by (2.37). This time, angular momentum L is generally non-vanishing (unless we consider the limit of $a = 0$) and, therefore, not all static particles in our coordinates are ZAMOs. To determine which static particles indeed are ZAMOs, we can set $L = 0$ and obtain an additional condition on the position of the static particles. Solving the equation directly is once again quite troublesome, but with a little trick we can acquire a less complicated condition on r rather effortlessly: We shall solve the equation for κ instead of r and by subsequently comparing the obtained value to the original one (2.37) we procure the sought condition. From $L = 0$ we get

$$\kappa = \frac{\Lambda r^4 + \Lambda a^2 r^2 + 6mr - 3q^2}{3qr\tilde{s}} \tag{2.39}$$

and by comparing the two, we immediately see that r needs to satisfy

$$2\Lambda r^3 + \Lambda a^2 r + 3m = 0\,, \tag{2.40}$$

which means that there may be up to three different radii at which we can find static ZAMOs fulfilling the electrogeodesic equations. Unfortunately, for $\Lambda > 0$ (and thus also for our universe) this condition manifestly forbids the existence of

such particles in the area with $r > 0$. On the other hand, for $\Lambda < 0$ the polynomial always has exactly one positive root, as can be shown using either Descartes' rule of signs or the more intricate theorem of Sturm. Both theorems are presented and (2.40) is thoroughly analysed in Appendix C. However, one must bear in mind that condition (2.40) does not mean that the positive root satisfies $\Delta_r(r) - a^2 > 0$ as required by $\tilde{s}$. This inequality is to be viewed as an additional constraint on the space-time if it were to contain static electrogeodesic ZAMOs in the equatorial plane. Indeed, this condition is not necessarily satisfied for every space-time for the positive root of (2.40): e.g. for $\{\Lambda, m, a, q\} = \{-10^{-3}\,\mathrm{u}^{-2}, 10\,\mathrm{u}, 1\,\mathrm{u}, 1\,\mathrm{u}\}$ the positive root is $r/m \approx 2.47$, where $(\Delta_r - a^2)/m^2 \approx 2.39$. However, after considering a new mass $m = 25\,\mathrm{u}$ the positive root $r/m \approx 1.34$ is below the static limit with $(\Delta_r - a^2)/m^2 \approx -0.21$.

A method allowing us to investigate orbiting ZAMOs shall be introduced in section 2.4.3 dealing with the effective potential in the equatorial plane. Unfortunately, due to the complexity of the equations it seems it can be applied in numerical computations only...

2.4 Motion in the equatorial plane

2.4.1 Stationary circular orbits

In astronomy, perhaps the most interesting kind of motion is the orbital motion around a celestial object. From the rings of Saturn to the rotation of the galactic spiral arms, these orbits are amongst the most common types of motion to be observed.

First, let us focus on stationary circular orbits. They are characterised by constant non-zero u^t and u^ϕ with vanishing u^r and u^θ. Then, $\mathrm{d}u^\alpha/\mathrm{d}\tau$ in the equations of motion (2.11) must be equal to zero. World lines of these particles are $x^\mu = (t, r_0, \theta = \pi/2, \phi)$ with constant r_0 and $\theta = \pi/2$. We choose to study particles in the equatorial plane as it is the plane of the reflection symmetry of the space-time. We thus expect that if there is a plane where stationary circular orbits exist, it is this one, as the particle cannot be forced to leave the plane electrogeodesically due to the aforementioned symmetry. Furthermore, note that there is no such thing as non-stationary circular electrogeodetic orbit in the equatorial plane in our space-time due to its rotational symmetry.

Inserting these conditions into the equations of motion, three of them turn into an identity. The last one,

$$-\Gamma^r{}_{\rho\sigma} u^\rho u^\sigma + \kappa F^r{}_\nu u^\nu = 0\,, \tag{2.41}$$

can be viewed as a differential equation for $t(\tau)$ and $\phi(\tau)$, or, equivalently, as a simpler algebraic equation for constant u^t and u^ϕ. The equation ensures that $\mathrm{d}u^r/\mathrm{d}\tau$ vanishes throughout the motion, forcing the particle to remain at a circular orbit. So far, we have one equation for two unknowns. In order to get a unique solution, we need to complete the system by adding another equation: the

normalisation of four-velocity[14] (2.3),

$$g_{\mu\nu}u^\mu u^\nu = -1\,. \tag{2.3}$$

The two equations are quadratic in both u^t and u^ϕ, which means they can have up to four unique solutions for a given space-time at a given r. The real solutions may represent physical orbits. Trying to solve the equations for u^t and u^ϕ directly by expressing one quantity (as a function of the other one) from one equation and inserting into the other could, however, lead to some misleading results, as expressing the other quantity would require taking the square of the remaining equation in order to eliminate a square root brought in by solving the previous quadratic equation for the inserted quantity. Taking the square of an equation has the unfortunate possible consequence of doubling the number of roots, half of which may not actually satisfy the original equation. How to recognise these superfluous results?

As a matter of fact, with a convenient substitution

$$\Omega \equiv \frac{\mathrm{d}\phi}{\mathrm{d}t} = \frac{\mathrm{d}\phi}{\mathrm{d}\tau}\frac{\mathrm{d}\tau}{\mathrm{d}t} = \frac{u^\phi}{u^t}\,, \tag{2.42}$$

which we have already worked with in the last section of the previous chapter, we can avoid taking the questionable square of an equation entirely. **For $q\kappa \neq 0$** one power of u^t can be easily factored out in equation (2.41) for motion with four-velocity $u^\mu = u^t(1,0,0,\Omega)$. We are then left with a linear equation yielding

$$u^t = \frac{3\Xi q\kappa r(a\Omega - 1)}{(\Lambda r^4 - 3mr + 3q^2)(a\Omega - 1)^2 + 3r^4\Omega^2}\,. \tag{2.43}$$

After inserting u^t into the normalisation we obtain a rather lengthy fourth-order polynomial equation for Ω,

$$\begin{aligned}
&\Big[9a^2q^2\left(a^4 + 2a^2r^2 + r^4 - a^2\Delta_r\right)\kappa^2 + \\
&\qquad + \left(3(2\Lambda a^2 + 3)r^8 - 18ma^2r^5 + 18a^2q^2r^4 + a^4A\right)\Big]\Omega^4 - \\
&- \Big[18aq^2\left(2a^4 + 3a^2r^2 + r^4 - 2a^2\Delta_r\right)\kappa^2 + \\
&\qquad + 4a\left(3\Lambda r^8 - 9mr^5 + 9q^2r^4 + a^2A\right)\Big]\Omega^3 + \\
&+ \Big[9q^2\left(6a^4 + 6a^2r^2 + r^4 - 6a^2\Delta_r\right)\kappa^2 + \\
&\qquad + 6\left(\Lambda r^8 - 3mr^5 + 3q^2r^4 + a^2A\right)\Big]\Omega^2 - \\
&- \Big[18aq^2\left(2a^2 + r^2 - 2\Delta_r\right)\kappa^2 + 4aA\Big]\Omega + \\
&+ \Big[9q^2\left(a^2 - \Delta_r\right)\kappa^2 + A\Big] \;=\; 0\,,
\end{aligned} \tag{2.44}$$

with

$$A = \Lambda^2 r^8 - 6\Lambda m r^5 + 6\Lambda q^2 r^4 + 9m^2r^2 - 18mq^2 r + 9q^4\,. \tag{2.45}$$

[14] In context with what has been said in section 2.2, we are effectively exchanging one of the equations of motion-turned-identities corresponding to a non-zero component of u_α (that is, u_t or u_ϕ) for the normalisation equation.

Needless to say, we shall not write down a general solution of this equation for Ω due to its immense length, as usual for quartic equations. However, the solutions become considerably shorter for the Reissner–Nordström–(anti-)de Sitter spacetime,

$$\Omega\Big|_{a=0} = \pm\frac{\sqrt{6}}{6r^2}\sqrt{-2\Lambda r^4 - 3q^2\kappa^2 + 6mr - 6q^2 \pm 3|q\kappa|\sqrt{4r^2 - 12mr + (8+\kappa^2)\,q^2}}\,, \tag{2.46}$$

where all four sign combinations may represent physical orbits. Take note that Ω does not depend on the sign of the particle's charge κ, as there are no odd powers of κ present in the polynomial above. On the other hand, u^t and, by extension, $u^\phi \equiv u^t\Omega$ are affected by the sign.

Another thing to keep in mind is that while we can have four real different admissible values of Ω, their corresponding u^t may not necessarily be positive, which further reduces the number of physical solutions. Particles with $u^t < 0$ are thought to move backwards in time and, therefore, shall be considered unphysical. The problem is illustrated in figure 2.2 on the following page.

For $q\kappa = 0$ one must be more careful. A naive limit in the previous result cannot be used here, as *both* powers of u^t can be eliminated from equation (2.41). We are left with a *quadratic* equation for Ω, meaning that the extra two angular velocities arise from the electromagnetic interaction of the particle and the black hole. It is then possible to obtain u^t from the normalisation of the four-velocity after inserting Ω. In the following, we shall consider only $\kappa = 0$, as κ is always paired with q in the equations of motion, while the opposite is not true. If $q = 0$, κ disappears from the equations as well and the limit may be, therefore, performed in the result for a vanishing κ regardless of its actual value.

Expressing Ω from (2.41) with $\kappa = 0$ gives us[15]

$$\Omega\Big|_{\kappa=0} = \frac{a(\Lambda r^4 - 3mr + 3q^2) \pm r^2\sqrt{-3\Lambda r^4 + 9mr - 9q^2}}{3\left(\Xi r^4 - ma^2 r + a^2q^2\right)}\,. \tag{2.47}$$

The normalisation equation yields

$$u^t\Big|_{\kappa=0} = \pm\frac{\Xi r}{\sqrt{\Big(a^2\Delta_r(r) - (a^2+r^2)^2\Big)\Omega^2 + 2a\Big(a^2 + r^2 - \Delta_r(r)\Big)\Omega + \Big(\Delta_r(r) - a^2\Big)}}\,, \tag{2.48}$$

whence one can see that if there are real u^t for a given set of parameters, we can always choose the positive one regardless of the sign of r.

The Schwarzschild limit of the angular velocity yields the simplest relativistic analogue of the Kepler's third law [20]

$$\Omega\Big|_{\Lambda=a=q=0} = \pm\sqrt{\frac{m}{r^3}}\,. \tag{2.49}$$

2.4.2 Photon orbits

The equations are somewhat simpler for photons. Motion of photons (i.e. massless and uncharged particles) is governed by the geodesic equations (photon κ

[15] Interestingly, this *can* be obtained by setting $\kappa = 0$ in 2.44. However, using (2.43) to get u^t would incorrectly lead to $u^t = 0$.

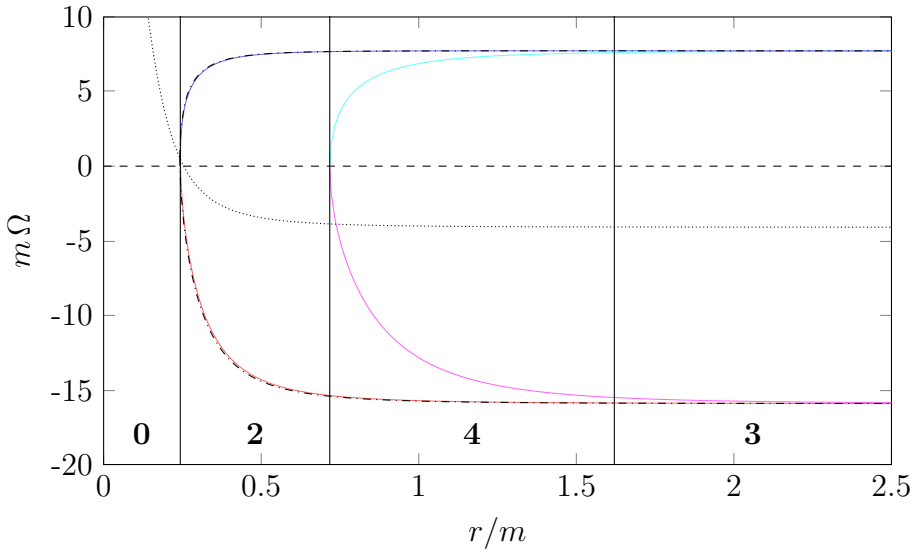

(a) The dependence of Ω on r for the four coloured solutions to the equations of motion. The solutions tend to the extreme angular velocities Ω_{min} or Ω_{max}, represented by the black dash-dotted curves. The dotted curve is that of $\omega \equiv -g_{t\phi}/g_{\phi\phi}$. The r/m axis is shorter than in the second figure, as the rest of the chart would be uneventful: all four coloured Ω remain real and very close to the corresponding extreme value. Notice how inconspicuously the boundary between 4 and 3 physical solutions looks. We would not be able to draw the line solely from our knowledge of the four values of Ω without also knowing their corresponding u^t.

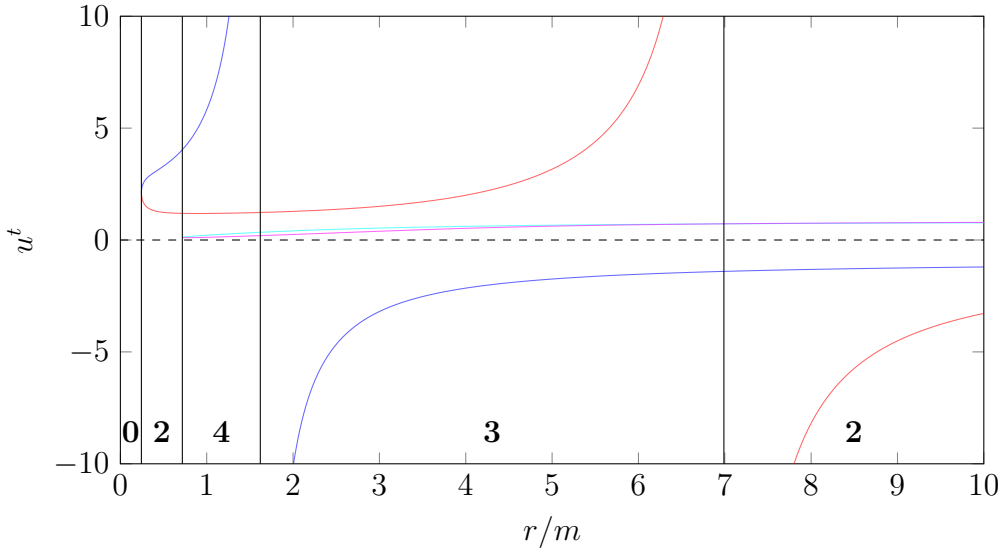

(b) The dependence of u^t on r for the four solutions. One can clearly see that real Ω permit negative u^t.

Figure 2.2: The dependence of the allowed angular velocities Ω and their corresponding u^t on r for space-time $\{\Lambda, m, a, q\} = \{-0.04\,\text{u}^{-2}, 90\,\text{u}, 3\,\text{u}, 20\,\text{u}\}$ and particle $\kappa = 25$. Pairs of corresponding Ω and u^t are drawn with matching colours in the two charts. The black vertical lines divide areas with a different number of permitted physical (i.e. $u^t > 0$) angular velocities for the given particle at a given r, the numbers themselves are written in boldface at the bottom of the charts.

vanishes). For stationary orbits in the equatorial plane we have

$$-\Gamma^{r}{}_{\rho\sigma}\frac{\mathrm{d}x^{\rho}}{\mathrm{d}\lambda}\frac{\mathrm{d}x^{\sigma}}{\mathrm{d}\lambda}=0\,, \tag{2.50}$$

where λ is some affine parameter, and their normalisation equation is

$$g_{\mu\nu}\frac{\mathrm{d}x^{\mu}}{\mathrm{d}\lambda}\frac{\mathrm{d}x^{\nu}}{\mathrm{d}\lambda}=0 \tag{2.51}$$

instead of -1. Considering

$$\Omega\equiv\frac{\mathrm{d}\phi}{\mathrm{d}t}=\frac{\mathrm{d}\phi}{\mathrm{d}\lambda}\left(\frac{\mathrm{d}t}{\mathrm{d}\lambda}\right)^{-1}\,, \tag{2.52}$$

$\mathrm{d}t/\mathrm{d}\lambda$ can actually be eliminated from both of these equations, and we are left with a set of two equations for the angular velocity of an orbiting photon Ω and the corresponding radius of the orbit r. There are two angular velocities solving the equations,

$$\Omega_{\pm}=\frac{a\left(r^2+a^2-\Delta_r(r)\right)\pm r^2\sqrt{\Delta_r(r)}}{(r^2+a^2)^2-\Delta_r(r)a^2}\,, \tag{2.53}$$

which are equal to $\Omega_{\mathrm{max/min}}$ (1.127), the two extreme values of the permitted angular velocities for a given r, with r satisfying

$$\begin{aligned}3\Xi^2r^4+6m\left(\Lambda a^2-3\right)r^3+\left(27m^2-4\Lambda a^2q^2+12q^2\right)r^2-\\-12m\left(a^2+3q^2\right)r+12q^2\left(a^2+q^2\right)=0\,.\end{aligned} \tag{2.54}$$

As r are the roots of a fourth-degree polynomial, there are at most four different stationary photon orbits in the space-time.

For the Schwarzschild solution the only (double) non-zero root of the polynomial above is the well-known [20]

$$r\Big|_{\Lambda=a=q=0}=3m\,, \tag{2.55}$$

which always lies in the stationary area of the space-time, with the corresponding velocities[16]

$$\Omega_{\pm}\Big|_{\Lambda=a=q=0}=\pm\frac{1}{3\sqrt{3}m}\,. \tag{2.56}$$

Furthermore, since Λ is always paired with a^2 in (2.54), the radii do not depend on Λ in the Reissner–Nordström–(anti-)de Sitter space-time. For $a=0$ there are two double roots of (2.54),

$$r_{\pm}\Big|_{a=0}=\frac{3}{2}m\pm\frac{1}{2}\sqrt{9m^2-8q^2}\,, \tag{2.57}$$

as long as $9m^2>8q^2$. However, one must keep in mind that these radii must further satisfy $\Delta_r|_{a=0}(r_{\pm})>0$ in order to represent a permitted photon orbit, as $\Omega_{\pm}$ (2.53) would otherwise contain a non-zero imaginary part[17]. For $9m^2=8q^2$ the

[16] These are also the limit of $r\to 3m$ in (2.49).

[17] In the non-stationary areas of the space-time the ansatz for the photon four-velocity satisfies the normalisation equation if and only if $u^t=\Omega=0$, which does not represent a physically reasonable particle.

photon orbit is located at $r = 3m/2$, coinciding with the position of the the triple horizon of an extremal Reissner–Nordström–de Sitter solution. However, apart from the condition $9m^2 = 8q^2$, the extremal scenario also requires a particular $\Lambda = 2/(9m^2)$. Finally, there are no photon orbits if $9m^2 < 8q^2$. Moreover, take note that even though $r_\pm$ do not depend on Λ for a non-rotating black hole[18], the angular velocities, given by

$$\Omega_\pm\Big|_{a=0} = \pm\frac{\sqrt{-\Lambda r^4 + 3mr - 3q^2}}{\sqrt{3}r^2}\,, \tag{2.58}$$

do. One can also see that for a vanishing a, we have

$$\Omega_-\Big|_{a=0} = -\Omega_+\Big|_{a=0} \tag{2.59}$$

for massless and massive particles alike, because for $a = 0$ there is no frame-dragging present to tip the balance towards one direction or the other.

2.4.3 Effective potential

Perfectly circular orbits, as interesting as they may be, represent only one type of particle motion in the equatorial plane. Real particles, however, tend to move in the radial direction as well. One way of dealing with this motion is to establish an effective potential. We shall do so by means of the integrals of motion (2.17).

Using them, one can easily find

$$u^t = \frac{\Xi}{r^2\Delta_r}\Big(-\Xi\left(a^2\Delta_r - (a^2+r^2)^2\right)E + a\Xi\left(\Delta_r - (a^2+r^2)\right)L - (a^2+r^2)rq\kappa\Big) \tag{2.60}$$

and

$$u^\phi = \frac{\Xi}{r^2\Delta_r}\Big(-a\Xi\left(\Delta_r - (a^2+r^2)\right)E + \Xi\left(\Delta_r - a^2\right)L - arq\kappa\Big)\,. \tag{2.61}$$

Take note that even though we now have u^t and u^ϕ as functions of r, E, L and κ, so far we know nothing about u^r. Therefore, although one may be tempted to say that the integrals of motion give us a simple way of finding the four-velocities corresponding to circular orbits, particles with these u^t and u^ϕ actually may not be orbiting the black hole at all, depending on the initial conditions. To find u^r, we shall insert the other components of the four-velocity into the normalisation equation (2.3), keeping in mind that we are interested in particles with $u^\theta = 0$, to obtain

$$\frac{1}{2}\left(u^r\right)^2 = -V(r; E, L, \kappa)\,, \tag{2.62}$$

where V is the sought effective potential,

$$V(r; E, L, \kappa) = \frac{\Xi^2}{2r^4}\Big(\left(\Delta_r(r) - (a^2+r^2)\right)(aE - L)^2 - \left(a^2+r^2\right)r^2E^2 + r^2L^2\Big) + \\ + \frac{q\kappa}{2r^3}\Big(2\Xi\left(a^2+r^2\right)E - 2\Xi aL - q\kappa r\Big) + \frac{\Delta_r(r)}{2r^2}\,. \tag{2.63}$$

[18]Whether $r_\pm$ lie in the stationary area or not, however, does depend on Λ.

If a particle of given E, L and κ is to be allowed to exist at a given r, its u^r must be real, or, equivalently, its corresponding effective potential must be negative.

Ideally, one would now separate the characteristics of the particle and the dependence on r and recast (2.62) as

$$\frac{1}{2}\left(u^r\right)^2 + \mathcal{V}(r) = f(E, L, \kappa)\,, \tag{2.64}$$

because that would allow us to draw a chart of $\mathcal{V}$ for a given space-time and compare it with $f(E, L, \kappa)$ (which may also depend on the space-time's parameters) for different particles to find turning points for a given particle or stationary circular orbits at a glance. Actually, we would be content even if f did not contain every information about the particle uniquely, however convenient that would be. The more parameters that can be moved over to f there are, the less often we need to redraw the potential when we change the particle. E.g., even if we could not separate E and L from the dependence on r, we would still be able to draw the potential for a class of particles characterised by their E and L and easily find the effect of κ by comparing the curve with f. Unfortunately, not even that is possible here. We thus need to replot V every time we change the space-time (as expected) or the particle (very inconvenient). The value of such graphs is, therefore, severely diminished. Nonetheless, interesting analytical results can be obtained even without such separation.

For a given particle the turning points, where u^r vanishes, are located at

$$V(r; E, L, \kappa) = 0\,. \tag{2.65}$$

After multiplying V by r^4 it is clear that we are looking for the roots of a sixth-degree polynomial. The leading term of the polynomial, proportional to Λr^6, clearly comes from the last term in (2.63). Setting $\Lambda = 0$ would simplify the polynomial dramatically to a fourth-order one, although its general solution would still be overly long to be included here.

To obtain circular orbits, one further needs to set

$$\frac{\mathrm{d}}{\mathrm{d}r}V(r; E, L, \kappa) = 0\,. \tag{2.66}$$

We are thus presented with a set of two equations, both of which must be satisfied for a given particle to orbit at some r. We may understand these equations as conditions on E and L for a particle with a given κ to orbit at a given r. One can then find u^t and u^ϕ from (2.60) and (2.61). Obtaining E and L from the potential for a general space-time, unfortunately, once again needs to be performed numerically, as the equations are quadratic in both unknowns.

Furthermore, we can use the potential to determine the stability of said orbits. As the sign in the definition of V is the same as in classical mechanics, stable orbits are located in the minima of the potential (i.e. $\mathrm{d}^2V/\mathrm{d}r^2 > 0$) and unstable in the maxima ($\mathrm{d}^2V/\mathrm{d}r^2 < 0$). Examples of V for a stable and an unstable orbit are shown in figure 2.3 on the next page. In subfigure 2.3a one can also see that $V < 0$ may be satisfied even for unphysical particles travelling backwards in time, which need to be numerically eliminated by computing u^t from E, L and κ in a given interval of r.

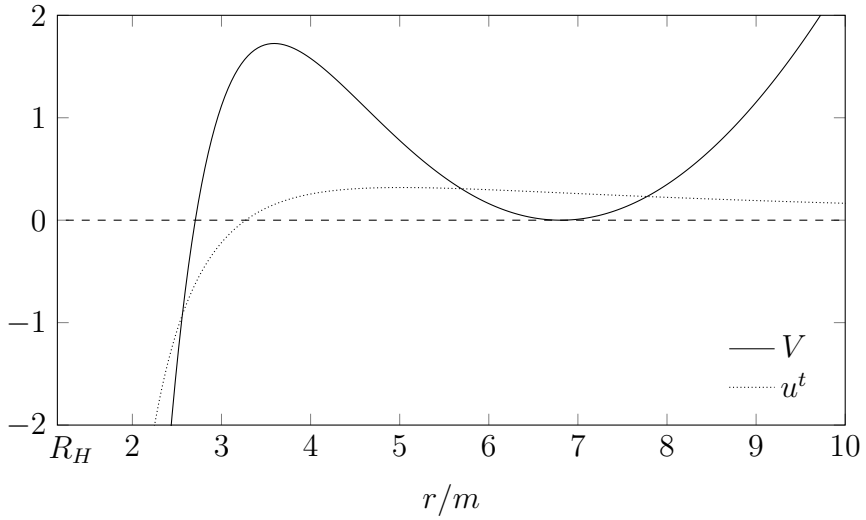

(a) Stable orbit at $r_{\mathrm{O}} \approx 6.8m$ for space-time $\{\Lambda, m, a, q\} = \{-10^{-3}\,\mathrm{u}^{-2}, 27\,\mathrm{u}, 17\,\mathrm{u}, 3\,\mathrm{u}\}$ and particle with $\kappa = 200$ and $u^\phi = 4\times10^{-4}$ corresponding to $E \approx 7.469$ and $L \approx 138.1$. R_H is the position of the outer black hole horizon. The dotted curve of u^t shows that a negative V is not enough to guarantee the possibility of the existence of a particle with given $\{E, L, \kappa\}$ at a particular r, as physical particles further require $u^t > 0$.

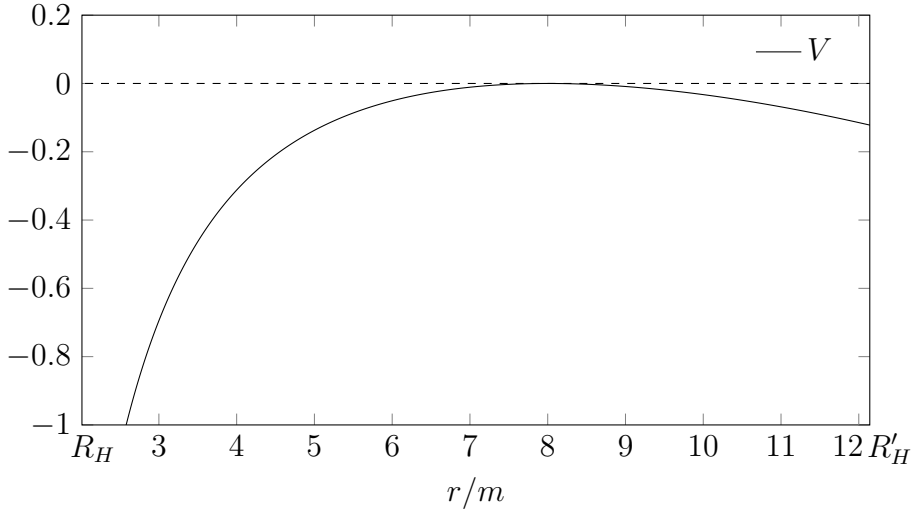

(b) Unstable orbit at $r_{\mathrm{O}} = 8m$ for $\{\Lambda, m, a, q\} = \{1.7 \times 10^{-6}\,\mathrm{u}^{-2}, 100\,\mathrm{u}, 27\,\mathrm{u}, 0.24\,\mathrm{u}\}$ and particle with $\kappa \approx -1520$ and $u^\phi = 4 \times 10^{-4}$ corresponding to $E \approx 0.1969$ and $L \approx 216.3$. R_H is the position of the outer black hole horizon and R'_H of the cosmological horizon. u^t, not present in the chart, is positive everywhere in the selected range of r.

Figure 2.3: Examples of the effective potential V corresponding to a stable and an unstable circular orbit.

The stable case was perturbed in figure 2.4 and the unstable in figure 2.5 on the following two pages. In these simulations, the perturbations were performed by changing the initial position of the particles whilst keeping the initial spatial components of their four-velocities the same (their integrals of motion, however, changed nonetheless). Alternatively, one could perturb their initial four-velocity, or a combination thereof. Regardless of which method is used, if it leads to a change in the particle's E or L, it results in a change of the curve of V. If the perturbed particle finds itself in a place where the perturbed potential is positive, an unphysical perturbation has been made. An example of an unphysical perturbation would be slightly changing the radial position of a particle that is originally located on a stable orbit without changing the integrals of motion, as $V > 0$ in the vicinity of stable orbits.

As in the classical case, when a particle moves towards an unstable orbit in a potential permitting it, it starts to wind on the orbit while never quite matching it[19]. For a particle nearing the unstable orbit at r_{O}, the Taylor series of the effective potential

$$V(r \to r_{\mathrm{O}}) = \frac{1}{2} V''(r_{\mathrm{O}}) \, (r - r_{\mathrm{O}})^2 + \mathcal{O}\left((r - r_{\mathrm{O}})^3\right) \tag{2.67}$$

loses its absolute and linear terms, as circular orbits satisfy $V = V' = 0$. The leading term's coefficient $V''(r_{\mathrm{O}})/2$ is negative, because we are dealing with an unstable orbit located in the maximum of the potential. Inserting the series into (2.62), we obtain

$$u^r \equiv \frac{\mathrm{d}r}{\mathrm{d}\tau} \approx -\sqrt{|V''(r_{\mathrm{O}})|} \, (r - r_{\mathrm{O}}) \,, \tag{2.68}$$

where we have chosen the minus sign after taking the square root, as it corresponds to particles moving towards the orbit. The differential equation can be solved easily by performing separation of variables, yielding

$$r(\tau) \approx r_{\mathrm{O}} + K \mathrm{e}^{-\sqrt{|V''(r_{\mathrm{O}})|} \, \tau} \tag{2.69}$$

as the leading terms in the vicinity of the unstable orbit[20]. Here, K is the constant of integration depending on the initial conditions (recall that r_{O} is the position of the circular orbit, not the initial position of the particle). As expected, the approaching particle reaches the orbit in $\tau \to \infty$, although it gets arbitrarily close in finite time[21]. The situation is shown in figure 2.6 on page 68 where the initially equidistantly positioned particles with the same κ and integrals of motion eventually follow the circular orbit almost perfectly. The figure also shows the correspondence of a numerical trajectory to the analytical result (2.69).

[19] For stable orbits no radial motion of the given particle may occur in the vicinity of the orbit.

[20] In the same way one can see that if $V'(r_{\mathrm{O}})$ did not vanish and $V'(r_{\mathrm{O}}) \, (r - r_{\mathrm{O}})$ was the leading term in the series of $V(r \to r_{\mathrm{O}})$, then the particle would begin moving into the allowed area with $r(\tau) \approx r_{\mathrm{O}} - V'(r_{\mathrm{O}}) \, \tau^2/2$ in the vicinity of r_{O} (constant of integration vanishes after setting $r(\tau = 0) = r_{\mathrm{O}}$), confirming that circular orbits indeed require $V'(r_{\mathrm{O}}) = 0$.

[21] When performing numerical simulations examining this type of motion, the physical instability makes the model prone to misleading results stemming from rounding errors, as sometimes the particle may "bounce off" or "trespass through" the minimum of the potential in spite of what has been said above.

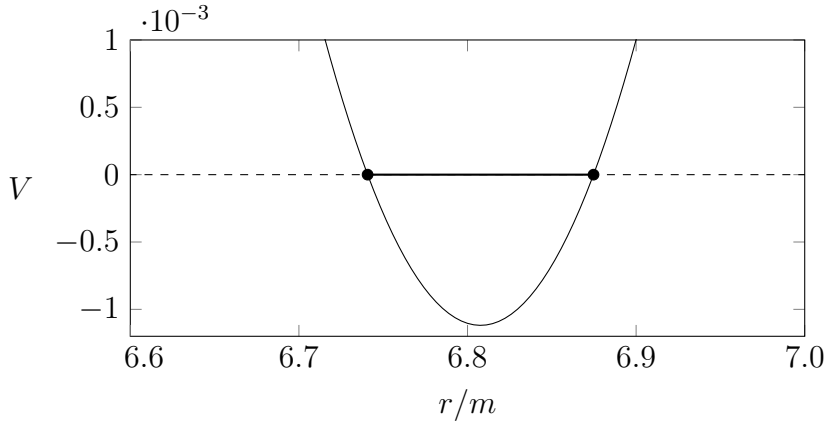

(a) The course of the effective potential V in the vicinity of the perturbed particle's position. In the r direction the particle oscillates between the two points corresponding to $V = 0$ on the highlighted line segment.

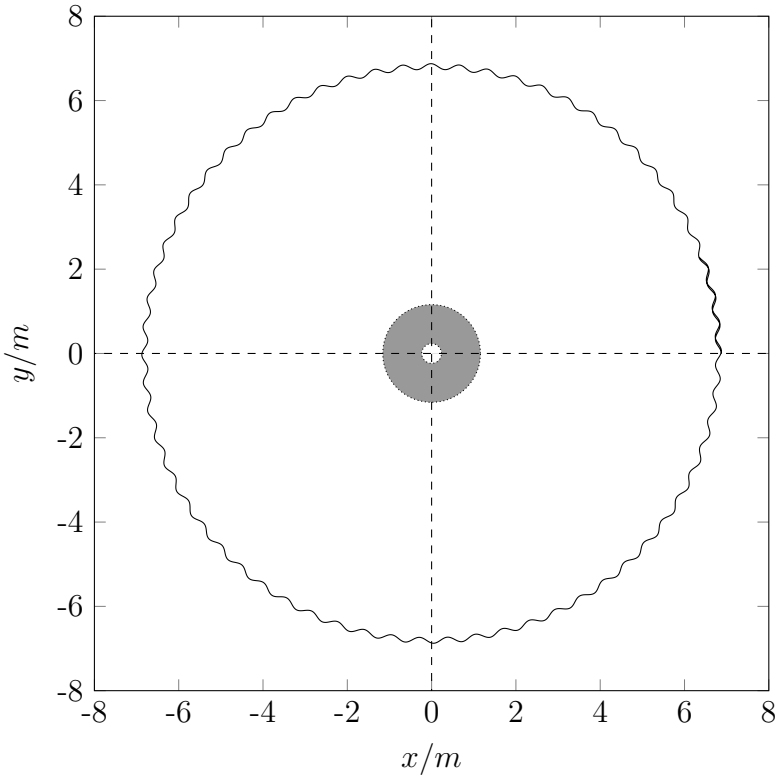

(b) The perturbed particle's trajectory in the equatorial plane for $\phi_{\text{init}} = 0$ integrated for $\Delta\tau = 600m$ so that over one full circle around the central mass would be complete. The trajectory does not close after one circle as evidenced by the subtle broadening of the curve in the right part of the chart. Gray colour represents the non-stationary area of the space-time with $\Delta_r < 0$. Coordinates x and y are given by (1.11).

Figure 2.4: A perturbation to the stable circular orbit from 2.3a for space-time $\{\Lambda, m, a, q\} = \{-10^{-3}\,\mathrm{u}^{-2}, 27\,\mathrm{u}, 17\,\mathrm{u}, 3\,\mathrm{u}\}$. The particle's initial radial position is now $r_{\text{init}} = 1.01 r_{\text{O}}$ and the spatial components of its initial four-velocity remain the same, resulting in slightly different $E \approx 7.470$ and $L \approx 138.5$.

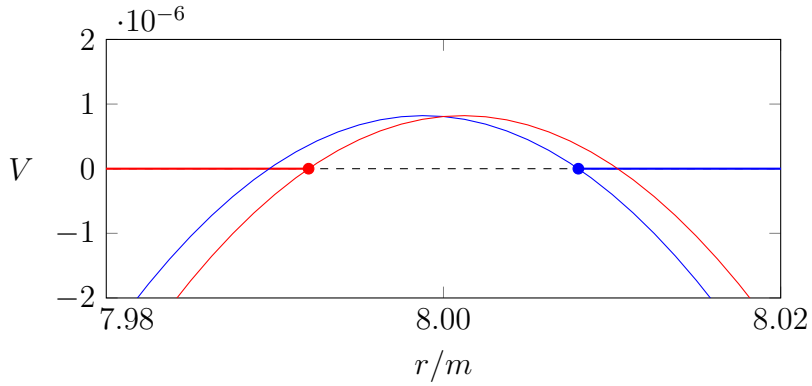

(a) The course of the effective potential V in the vicinity of the perturbed particle's position for $k = 3$. In the r direction the particles move away from the starting point at $V = 0$ on the highlighted line. The constants of motion are $E \approx 0.1970$ and $L \approx 216.8$ for the blue particle and $E \approx 0.1968$ and $L \approx 215.8$ for the red one.

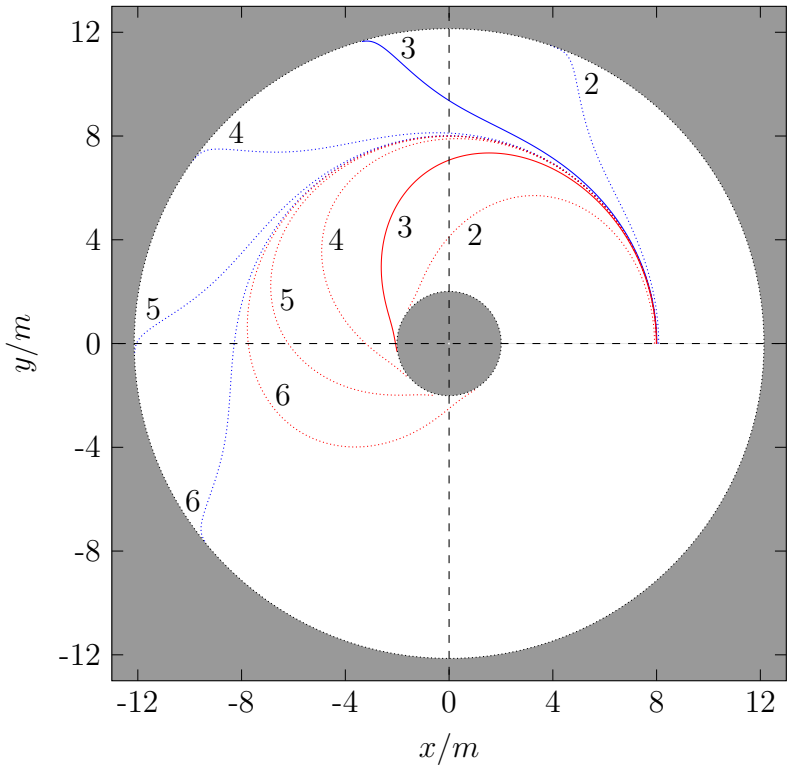

(b) The trajectories of multiple perturbed particles in the equatorial plane for $\phi_{\text{init}} = 0$ integrated until they reach a horizon. The curves are numbered by k characterizing their initial perturbation, the full lines for $k = 3$ correspond to the chart above. Gray colour represents the non-stationary area of the space-time with $\Delta_r < 0$. The inner black hole horizon is not visible unless zoomed in. Coordinates x and y are given by (1.11).

Figure 2.5: A perturbation to the unstable circular orbit from 2.3b for space-time $\{\Lambda, m, a, q\} = \{1.7 \times 10^{-6}\,\text{u}^{-2}, 100\,\text{u}, 27\,\text{u}, 0.24\,\text{u}\}$. The particle's initial radial position is now $r_{\text{init}} = r_{\text{O}} \pm \delta r$ with $\delta r = 10^{-k} r_{\text{O}}$. The blue curves correspond to the plus sign, the red ones to the minus sign. In all cases the spatial components of the initial four-velocity remain the same as in the unperturbed model, resulting in slightly different E and L (varies for each case).

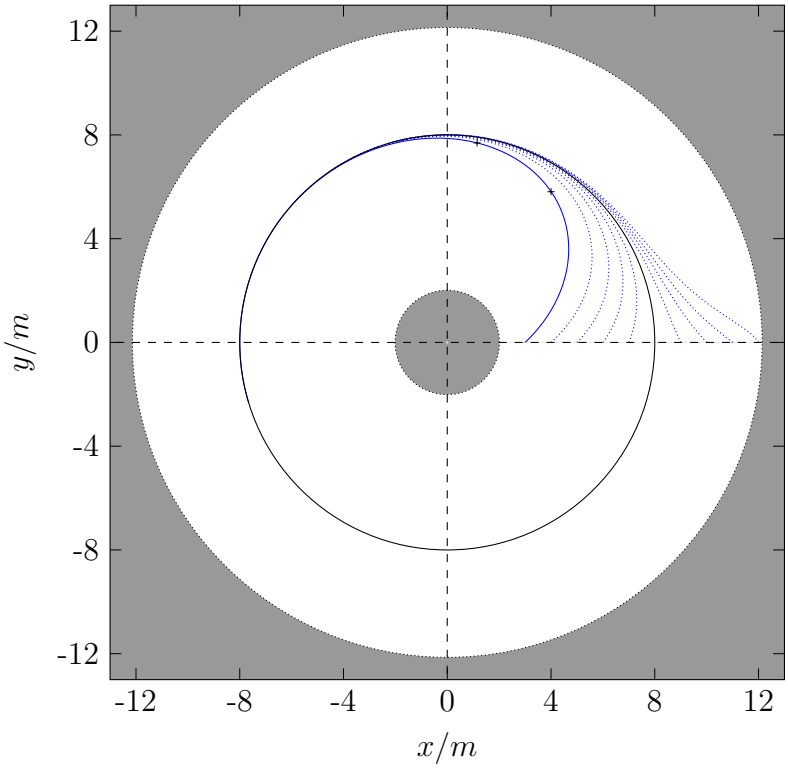

(a) The winding of particles (blue) around the unstable orbit (black) at $r_O = 8m$ in the equatorial plane of space-time $\{\Lambda, m, a, q\} = \{1.7 \times 10^{-6}\,\mathrm{u}^{-2}, 100\,\mathrm{u}, 27\,\mathrm{u}, 0.24\,\mathrm{u}\}$. Each particle satisfies $\kappa \approx -1520$, $E \approx 0.1969$ and $L \approx 216.3$, corresponding to the potential shown in 2.3b. The initial radii of the particles are whole number multiples of m in the area between the outer black hole horizon and the cosmological horizon, starting at $3m$ and ending at $12m$. The full line corresponds to the chart below, the marks on it represent the particle's position at $\tau = 10m$ and $\tau = 20m$. Gray colour represents the non-stationary area of the space-time with $\Delta_r < 0$. The inner black hole horizon is not visible unless zoomed in. Coordinates x and y are given by (1.11).

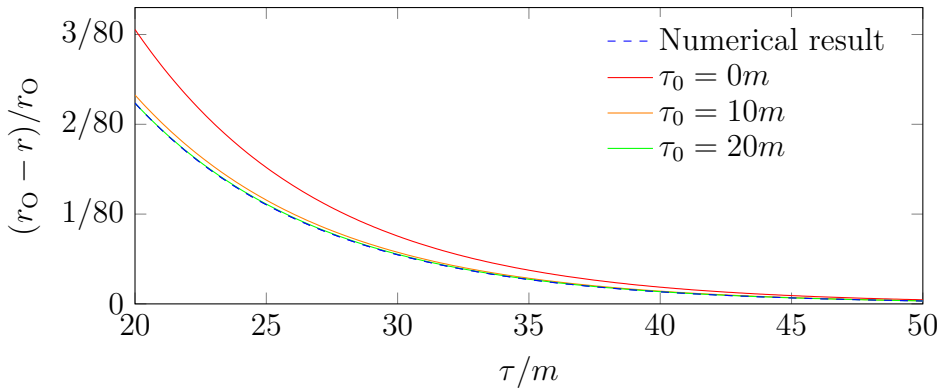

(b) The correspondence of $r_O - r$ for the innermost particle from the previous chart (the blue curve) to (2.69) with K evaluated at three different τ_0 corresponding to the starting point of the trajectory and the two marks. As expected, the closer to r_O we choose the initial condition in (2.69), the closer the analytical result follows the numerical trajectory. The green and blue curves almost precisely overlap.

Figure 2.6: Winding of particles around an unstable orbit in the equatorial plane.

As a side note, κ seems to have a considerable effect on the stability of orbits, see figure 2.7 below, where we consider two particles with the same integrals of motion but with different charge-to-mass ratios in the same space-time. One particle may enjoy the security of a stable orbit, while the orbit the other particle is allowed to follow is an unstable one.

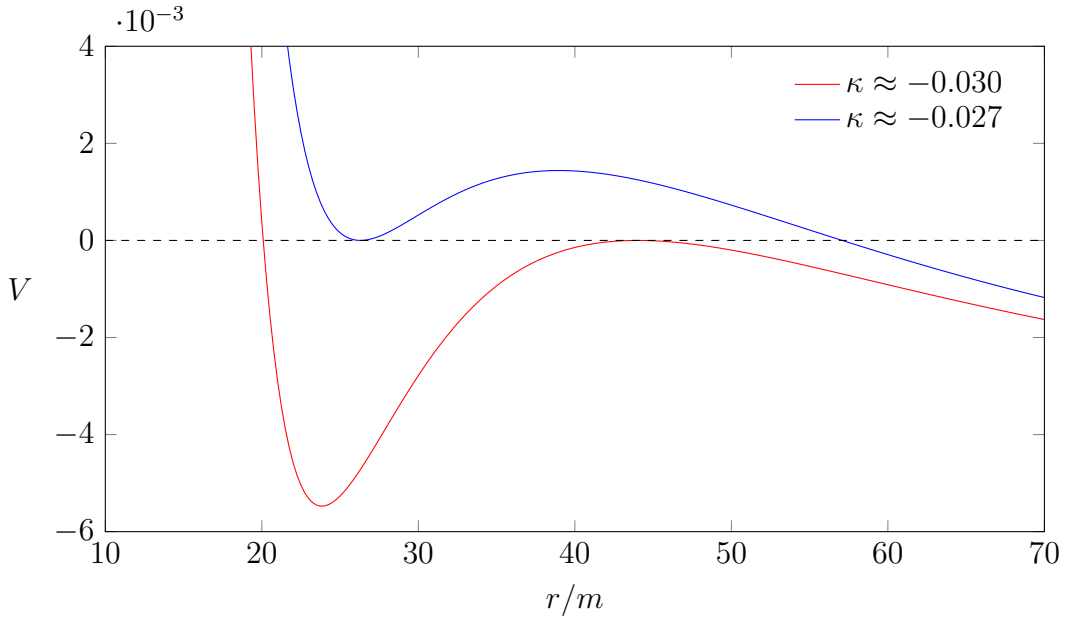

Figure 2.7: A comparison of two effective potentials in a space-time with parameters $\{\Lambda, m, a, q\} = \{10^{-8}\,\mathrm{u}^{-2}, 1\,\mathrm{u}, 75\,\mathrm{u}, 5\,\mathrm{u}\}$ for two particles with the same $E = 1$ and $L = 15$ but different κ. The blue particle can be in a stable orbit at $r/m \approx 26$, the red one in an unstable one at $r/m \approx 44$.

The limits of the effective potential are

$$\lim_{r\to\pm\infty} V = -\mathrm{sgn}(\Lambda)\infty \tag{2.70}$$

and

$$\lim_{r\to 0} V = \infty\,, \tag{2.71}$$

which means that the singularity can be viewed as an infinite potential barrier (recall that radial particle motion requires $V < 0$). This seems to be yet another manifestation of the already-discussed repulsive gravity.

Similarly, one can also derive an effective potential for photons satisfying

$$\frac{1}{2}\left(\dot{r}\right)^2 = -V_\gamma(r; E, L)\,. \tag{2.72}$$

After inserting $\kappa = 0$ and assuming $g_{\mu\nu}\dot{x}^\mu\dot{x}^\nu = 0$ in the derivation, we obtain

$$V_\gamma(r; E, L) = \frac{\Xi^2}{2r^4}\Big(\left(\Delta_r(r) - (a^2 + r^2)\right)(aE - L)^2 - \left(a^2 + r^2\right)r^2E^2 + r^2L^2\Big)\,, \tag{2.73}$$

a result already known and thoroughly analysed in previous literature [21, 22]. As for massive particles, we can use the potential to determine the radii of photon

orbits. After expressing E from $V_\gamma = 0$ and inserting it into $\mathrm{d}V_\gamma/\mathrm{d}r = 0$, we correctly obtain (2.54), provided that both E and L are non-vanishing. Vanishing integrals of motion for photons,

$$\begin{aligned} g_{tt}\dot{t} + g_{t\phi}\dot{\phi} &= 0\,, \\ g_{t\phi}\dot{t} + g_{\phi\phi}\dot{\phi} &= 0\,, \end{aligned} \tag{2.74}$$

mean that $\dot{t}$ and $\dot{\phi}$ are equal to zero, because the determinant of the system is generally non-zero,

$$\det \begin{pmatrix} g_{tt} & g_{t\phi} \\ g_{t\phi} & g_{\phi\phi} \end{pmatrix} = -\frac{\Delta_r(r)}{\Xi^4}\,. \tag{2.75}$$

The determinant vanishes only on the horizons, which are not suited to be analysed in the used coordinates. We would, therefore, be dealing with an unphysical photon frozen in time. The second derivative of V_γ, after inserting E obtained from $\mathrm{d}V_\gamma/\mathrm{d}r = 0$, reduces into

$$\left.\frac{\mathrm{d}^2 V_\gamma}{\mathrm{d}r^2}\right|_{\text{orbit}} = -\frac{4\Xi^2 L^2(3mr - 4q^2)}{r^2\left(\Xi r^2 + 3mr - 2q^2\right)^2}\,, \tag{2.76}$$

which means that stable orbits ($\mathrm{d}^2V_\gamma/\mathrm{d}r > 0$) are those satisfying

$$r < \frac{4}{3}\frac{q^2}{m} \tag{2.77}$$

if there are any in the given space-time, while unstable orbits satisfy the opposite inequality.

The $r \to 0$ limit of V_γ is the same as for V,

$$\lim_{r\to 0} V_\gamma = \infty\,, \tag{2.78}$$

but the limits for radial infinities are finite for photons,

$$\lim_{r\to\pm\infty} V_\gamma = -\frac{\Xi^2}{3}\left(\Lambda(aE - L)^2 + 3E^2\right)\,. \tag{2.79}$$

Nevertheless, finiteness of the potential is irrelevant when determining if a particle can escape into infinity or not, as only the sign of the potential matters.

Additionally, one may use the effective potential to find ZAMOs, i.e. particles on stationary circular orbits with $L = 0$. Once again, we have two equations at our disposal, $V = 0$ and $\mathrm{d}V/\mathrm{d}r = 0$, this time somewhat simplified due to the vanishing L. Recall that when we analysed static particles, we found out what the particle's charge-to-mass ratio κ must be for the particle to remain static at a given r both at the axis and in the equatorial plane. Naturally, one would try to use the equations to obtain E and κ, the two non-vanishing characteristics of the particle, similarly to the static case. Unfortunately, that would again require us to deal with equations that are quadratic in both unknowns, leaving us unable to analytically decide which solutions are physical and which are not. Once more the task is to be solved numerically only[22].

[22] One could solve the equations analytically for κ and m, but expressing one property of the particle and one property of the space-time does not seem to be beneficial in any way.

Last but not least, inserting the four-velocity of a static particle into E and L, the resulting potential expectedly vanishes. Expressing κ from $\mathrm{d}V/\mathrm{d}r = 0$, we obtain the known result from the previous chapter (2.37). Unfortunately, finding the static particle's stability from the second derivative of V requires us to deal with a polynomial of order eight in r, necessitating numerical computations for every given scenario.

2.5 Radial motion along the axis of rotation

Another type of motion of interest is the purely-radial one. As the examined space-time is not spherically symmetric, the direction of particle's motion matters. Due to frame-dragging, the rotation of the black hole pushes nearby particles in its direction. Consequently, we shall focus on radial motion along the black hole's rotation axis for now, as it is the only particle direction never affected by dragging.

The axis position is $\theta \in \{0, \pi\}$, which of course shall also be the θ component of our particle's four-position x^μ. Due to the space-time's symmetries, both values of θ are equivalent and interchangeable in any of the results. Apart from the initial θ, the only other condition we impose on our particle is that $u^\theta = 0$ at an arbitrary initial time. The remaining components of the four-velocity are not expected to be constant.

In the following, we denote

$$\rho_0^2(r) \equiv \rho^2(r, \theta = 0) = r^2 + a^2 \,. \tag{2.80}$$

After inserting the appropriate value of θ into the equations, the θ equation reduces significantly into

$$\frac{\mathrm{d}u^\theta}{\mathrm{d}\tau} + \frac{2r}{\rho_0^2(r)} u^r u^\theta = 0 \,. \tag{2.81}$$

Consequently, a particle that does not move in the θ direction at a given initial time remains forever bound to the axis, as expected from the symmetry of the problem. Thus, we can safely disregard this equation.

As it turns out, we can also disregard the equation for ϕ. Of course, the ϕ coordinate is degenerate at the axis, nonetheless the corresponding electrogeodesic equation is *not*, perhaps surprisingly, an identity of the type $0 = 0$. However, seeing that the metric tensor does not depend on ϕ and

$$g_{\phi\mu}\Big|_{\theta\in\{0,\pi\}} = 0 \;\forall\mu \,, \tag{2.82}$$

the value of u^ϕ is utterly irrelevant in the remaining equations and, as such, shall not be of our concern.

This time, the remaining two equations,

$$\begin{aligned} \frac{\mathrm{d}^2 t}{\mathrm{d}\tau^2} &= -\Gamma^t{}_{\rho\sigma}(r) \frac{\mathrm{d}x^\rho}{\mathrm{d}\tau} \frac{\mathrm{d}x^\sigma}{\mathrm{d}\tau} + \kappa F^t{}_\nu(r) \frac{\mathrm{d}x^\nu}{\mathrm{d}\tau} \,, \\ \frac{\mathrm{d}^2 r}{\mathrm{d}\tau^2} &= -\Gamma^r{}_{\rho\sigma}(r) \frac{\mathrm{d}x^\rho}{\mathrm{d}\tau} \frac{\mathrm{d}x^\sigma}{\mathrm{d}\tau} + \kappa F^r{}_\nu(r) \frac{\mathrm{d}x^\nu}{\mathrm{d}\tau} \,, \end{aligned} \tag{2.83}$$

must inevitably be viewed as a set of differential equations for the t and r components of x^μ, because we have to contend with varying r on the right-hand sides

of the equations. In the general case, solving the equations seems impossible, instead a more useful variant of the effective potential has been developed and shall be discussed later on in the chapter. But first, a brief detour on the subject of photons...

2.5.1 Null geodesics & near-horizon approximation

The equation for $\mathrm{d}r/\mathrm{d}t$ can be obtained directly from the normalisation

$$g_{\mu\nu}\frac{\mathrm{d}x^\mu}{\mathrm{d}\lambda}\frac{\mathrm{d}x^\nu}{\mathrm{d}\lambda} = 0 \tag{2.84}$$

after considering

$$\frac{\mathrm{d}r}{\mathrm{d}\lambda} = \frac{\mathrm{d}r}{\mathrm{d}t}\frac{\mathrm{d}t}{\mathrm{d}\lambda}\,, \tag{2.85}$$

which allows us to eliminate $\mathrm{d}t/\mathrm{d}\lambda$ from the equation.

The result is remarkably simple,

$$\frac{\mathrm{d}r}{\mathrm{d}t} = \pm\frac{\Delta_r(r)}{\Xi\rho_0^2(r)} \tag{2.86}$$

and it represents the speed of light in our coordinates (generally not equal to one) for photons on the axis.

After setting $a = q = 0$ we obtain the known result for the Schwarzschild–anti-de Sitter geometry [23]

$$\left.\frac{\mathrm{d}r}{\mathrm{d}t}\right|_{a=q=0} = \pm\left(1 - \frac{2m}{r} - \frac{1}{3}\Lambda r^2\right)\,. \tag{2.87}$$

Also considering $\Lambda = 0$, the Schwarzschild limit is [24]

$$\left.\frac{\mathrm{d}r}{\mathrm{d}t}\right|_{\Lambda=a=q=0} = \pm\frac{r-2m}{r}\,. \tag{2.88}$$

To transfer to the Minkowski space-time of special relativity, we further set $m = 0$ and obtain

$$\left.\frac{\mathrm{d}r}{\mathrm{d}t}\right|_{\Lambda=m=a=q=0} = \pm 1 \tag{2.89}$$

as is to be expected, because the used coordinates become the standard spherical coordinates after setting all parameters of the metric equal to zero.

Interestingly, result (2.86) holds for hypothetical charged massless particles as well, because the particle's charge does not enter the normalisation equation, which is sufficient to get $\mathrm{d}r/\mathrm{d}t$ for radial motion on the axis. While the charge has no effect on the magnitude of the three-velocity, which is invariantly given by the speed of light for massless particles, for a general θ it would influence the null particle's trajectory by bending it. Due to the symmetries of the space-time, however, no bending can occur for radially-moving particles on the axis, meaning it is indeed possible to consider $\mathrm{d}\theta = 0$ in the normalisation equation to characterise radial motion. Nevertheless, the charge does enter the electrogeodesic equation, changing $\mathrm{d}r/\mathrm{d}\lambda$ and $\mathrm{d}t/\mathrm{d}\lambda$, but, again, not $\mathrm{d}r/\mathrm{d}t$. Hence, for these

particles an outside observer cannot really say anything about the charge solely by observing the particle's trajectory.[23]

In the general case $\mathrm{d}r/\mathrm{d}t$ cannot be integrated to obtain $r = r(t)$ in terms of elementary functions. However, should we take interest in null geodesics in the neighbourhood of a given horizon, we can perform the near-horizon approximation to obtain the leading term in $r(t)$ by integrating the leading term of the Taylor series of $\mathrm{d}r/\mathrm{d}t$ at the horizon of multiplicity m located at $r = R_m$. As the leading term's power depends on the multiplicity, we shall make use of the factorisation of $\Delta_r(r)$ once more, considering

$$\Delta_r(r) = \delta_m(r)(r - R_m)^m \,, \tag{2.90}$$

where

$$\delta_m(r) = -\frac{\Lambda}{3} \prod_{i=1}^{4-m} (r - r_i) \,, \tag{2.91}$$

with $r_i \neq R_m$ being the remaining roots of $\Delta_r(r)$[24]. If there are any, multiple roots are to be counted individually in δ_m. At $r = R_m$, δ_m is also equal to

$$\delta_m(R_m) = \frac{1}{m!} \frac{\mathrm{d}^m}{\mathrm{d}r^m} \Delta_r(r) \bigg|_{r=R_m} \,. \tag{2.92}$$

In the following, it will become clear that we usually only need to know the value of δ_m at a horizon. It is then advantageous to use the latter expression for evaluating $\delta_m(R_m)$, as the former assumes and requires $\Lambda \neq 0$, because it stems from a factorisation of a fourth-order polynomial $\Delta_r(r)$. For $\Lambda = 0$ the order of the polynomial reduces to two and the factorisation becomes inaccurate, requiring a redefinition of δ_m. However, the second formula holds (only on a horizon!) even in the limit of a vanishing cosmological constant. Moreover, in the second expression we do not need to know the values of the other roots of $\Delta_m(r)$.

Further denoting

$$\zeta_m(r) \equiv \frac{\delta_m(r)}{\Xi \rho_0^2(r)} \,, \tag{2.93}$$

we obtain

$$\frac{\mathrm{d}r}{\mathrm{d}t} = \pm\zeta_m(r)\,(r - R_m)^m = \pm\zeta_m(R_m)\,(r - R_m)^m + \mathcal{O}\left((r - R_m)^{m+1}\right) \,. \tag{2.94}$$

The leading term can be then integrated trivially by separation of variables.

For the case of a horizon of multiplicity one[25] we get

$$t \approx \pm\frac{1}{\zeta_1(R_1)} \ln(r - R_1) + t_0 \,, \tag{2.95}$$

[23] Similarly, in the equatorial plane no amount of charge can deflect orbiting massless particles away from it. While the expression for the angular velocity (2.53) remains the same, as it can also be extracted from the normalisation equation, the permitted radii of charged photon orbits shift, since we needed to complete the system by including the (electro)geodesic equation to obtain the polynomial for r (2.54).

[24] These roots may be complex and, therefore, not represent physical horizons. Furthermore, there is always at least one root $r_1 \neq R_m$, because it is impossible to have a quadruple horizon in our space-time as discussed previously.

[25] The remaining horizons may or may not be of a higher multiplicity or disappearing.

where t_0 is a constant of integration determined by the initial conditions (so that the photon would be reasonably close to the horizon at t_0 for the approximation to hold), or

$$r \approx \exp\Big[\pm\,\zeta_1(R_1)\,(t-t_0)\Big] + R_1\,, \tag{2.96}$$

Unfortunately, for the most general case of four distinct roots of $\Delta_r(r)$ we are unable to write reasonable analytic expressions for R_1 and $\delta_1(r)$. For extremal scenarios, however, the positions of the horizons are known to us and we are able to express $r(t)$ completely in terms of the space-time's parameters. Nonetheless, the exponential dependence of r on t holds for both non-extremal and extremal space-times alike as long as we are studying motion near a horizon of multiplicity one.

Motion near double horizons, appearing in three of the four possible extremal scenarios, has a different functional dependence,

$$t \approx \mp\frac{1}{\zeta_2(R_2)\,(r-R_2)} + t_0\,, \tag{2.97}$$

leading to

$$r \approx \mp\frac{1}{\zeta_2(R_2)\,(t-t_0)} + R_2\,. \tag{2.98}$$

Finally, for the triple horizon we obtain

$$t \approx \mp\frac{1}{2\zeta_3(R_3)\,(r-R_3)^2} + t_0\,, \tag{2.99}$$

or

$$r \approx \pm\frac{1}{\sqrt{\mp 2\zeta_3(R_3)\,(t-t_0)}} + R_3\,. \tag{2.100}$$

The triple horizon's position is (1.76)

$$R_3 = \sqrt[3]{\frac{3}{4}\frac{m}{\Lambda}}\,, \tag{2.101}$$

and, after considering all the properties of the extremal scenario, ζ_3 becomes

$$\zeta_3(R_3) = \frac{2}{3}\frac{\Lambda^2 R_3}{(\Lambda R_3^2-1)\,(5\Lambda R_3^2-3)} < 0\,, \tag{2.102}$$

depending on only two space-time's parameters, Λ and m. The sign can be easily inferred from the manifestly negative sign of $\delta_3(R_3) = -4\Lambda R_3/3$, since it holds that $\mathrm{sgn}\big(\zeta_m(r)\big) = \mathrm{sgn}\big(\delta_m(r)\big)$. Knowing the sign of $\zeta_3(R_3)$, the interpretation of the four possible sign combinations in $r(t)$ is now clear: the upper sign in $t(r)$ describes photons nearing the triple horizon and the lower one photons moving away from it in order for the photons to move towards the coordinate future. This sign translates to the sign inside the square root in $r(t)$. The outer sign reflects whether the photon is above the horizon or not. For $r > R_3$ the sign of the first term in $r(t)$ must be positive for both incoming and outgoing particles alike so that the proper dependence of r on necessarily increasing t is achieved. For $r < R_3$ the sign must be negative.

2.5.2 Effective potential & static particles revisited

The same method for establishing an effective potential as for equatorial motion works here as well. The situation here is, however, somewhat simpler, since we have to consider only two components of the four-velocity instead of the three above. Moreover, only one constant of motion is relevant here as L vanishes. From the equation for E (2.17) we obtain

$$u^t = \frac{\Xi}{\Delta_r}\Big(\Xi\rho_0^2(r)E - rq\kappa\Big)\,. \tag{2.103}$$

Substituting into the normalisation equation, we obtain, similarly as before,

$$\frac{1}{2}\left(u^r\right)^2 = -V(r;E,\kappa)\,, \tag{2.104}$$

where the effective potential is

$$V(r;E,\kappa) = -\frac{1}{2\rho_0^4(r)}\Big(\Xi\rho_0^2(r)E - rq\kappa\Big)^2 + \frac{\Delta_r(r)}{2\rho_0^2(r)}\,. \tag{2.105}$$

As for equatorial motion, the turning points are the solutions to $V(r) = 0$, which again requires us to look for the roots a polynomial of degree six. Once more, unfortunately, the potential is also unable to differentiate between physical particles travelling forwards ($u^t > 0$) and backwards ($u^t < 0$) in time, as is shown in figure 2.10 later on in this section on page 80. This time, however, we will find a way around the problem.

Recall that for equatorial motion, if it further holds that $\mathrm{d}V/\mathrm{d}r = 0$, then there are stationary circular orbits at the corresponding r, with the sign of $\mathrm{d}^2V/\mathrm{d}r^2$ determining their stability. For motion bound to the axis, if V and $\mathrm{d}V/\mathrm{d}r$ concurrently vanish, a static particle may be located at the corresponding r, and the second derivative again tells us whether the position is stable (minimum of $V \;\Leftrightarrow\; \mathrm{d}^2V/\mathrm{d}r^2 > 0$) or not (maximum of $V \;\Leftrightarrow\; \mathrm{d}^2V/\mathrm{d}r^2 < 0$). Unlike the previous case, this time we actually can solve the first two equations analytically for E and κ. As V is quadratic in E, there are two solutions to $V(E) = 0$, one of which is

$$E = \left(\frac{\Delta_r}{s} + q\kappa r\right)\Big(\Xi\rho_0^2(r)\Big)^{-1}\,, \tag{2.106}$$

with

$$s = \sqrt{\frac{\Delta_r(r)}{\rho_0^2(r)}}\,. \tag{2.107}$$

After inserting this E into $\mathrm{d}V/\mathrm{d}r = 0$, the corresponding κ turns out to be

$$\kappa = -\frac{\Lambda r^5 + 2a^2\Lambda r^3 - 3mr^2 + (a^4\Lambda + 3q^2)r + 3a^2m}{3q(r+a)(r-a)s}\,. \tag{2.108}$$

In this expression the attentive reader certainly recognises our previous result (2.24), confirming the equivalence of the two approaches.

However, the other solution to $V(E) = 0$, differing by the sign of the term Δ_r/s, would lead to an opposite sign of κ. Not only this result was not discovered

when we first tackled the problem in the corresponding chapter, it is also not corroborated by performed numerical simulations, which confirm the original result only, see figure 2.8 below. This unphysical κ originates from taking the square of u^t (2.103), originally linear in E, in the normalisation equation. Indeed, the correct E for static particles (or the turning points, for that matter) may be obtained directly from the definition of the integral of motion (2.17) after inserting the four-velocity of a static particle (2.20)[26]. The unphysical root is invariantly lesser than the physical one as Δ_r/s is positive: s is positive by definition and Δ_r must be positive too, because no turning points may be located in non-stationary areas of the space-time (with $g_{tt} > 0$), where the ansatz for a static particle (2.20) violates the normalisation of the four-velocity. As it is a result of taking the square of u^t, the unphysical E actually corresponds to static particles travelling backwards in time with $u^t = -1/\sqrt{-g_{tt}} < 0$, which can be easily proved by inserting this u^t into (2.17).

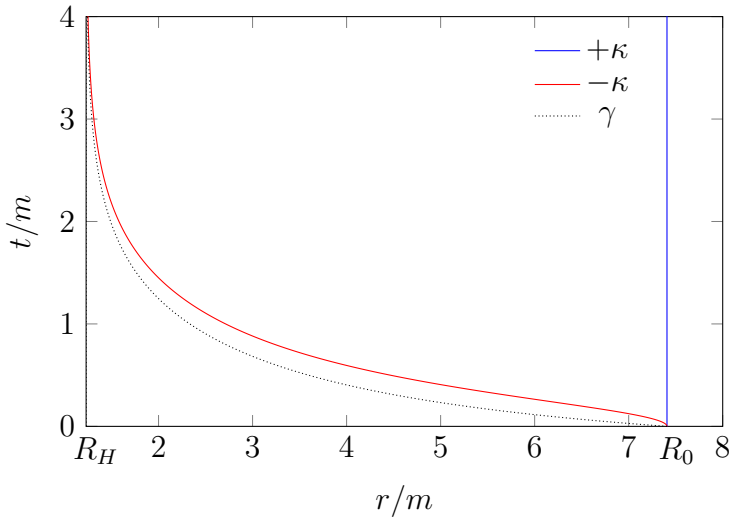

Figure 2.8: The world lines of a particle with $\kappa \approx -182$ given by (2.108) and its oppositely-charged twin for $\{\Lambda, m, a, q\} = \{-10^{-3}\,\mathrm{u}^{-2}, 27\,\mathrm{u}, 14\,\mathrm{u}, -4\,\mathrm{u}\}$. As expected, the blue particle remains static at the initial position R_0, while the red one does not, as it moves towards the outer black hole horizon at R_H. Note that even though a part of the red particle's world line satisfies $|\mathrm{d}r/\mathrm{d}t| > 1$, the particle does not move faster than light, as the speed of light in the used coordinates is generally not equal to one. The dotted curve is the world line of a photon released simultaneously obtained by integrating (2.86) to demonstrate that effect.

As a matter of fact, we can use relation (2.106) to establish a "lite" effective potential $W(r;\kappa)$ able to determine the dependence of the locations of the turning points on E for particles of a certain κ in a given space-time[27]. The turning points

[26]Take note that a similar approach is not applicable in the case of equatorial motion, as particles at the turning points are generally still moving in space in the ϕ direction.

[27]In principle, we could have similarly obtained E as a root of V in the equatorial plane, however, there were not any means of determining which root of V was the physical one analytically due to the presence of L. Nonetheless, it seems that one may do that easily in the Hamilton–Jacobi formalism and subsequently obtain a separated effective potential in the equatorial plane as well [25].

are solutions to

$$E = W(r;\kappa)\,, \tag{2.109}$$

with

$$W(r;\kappa) = \left(\frac{\Delta_r(r)}{s(r)} + q\kappa r\right)\left(\Xi\rho_0^2(r)\right)^{-1}\,. \tag{2.110}$$

Similarly, one can establish a potential of the same kind for the unphysical particles travelling backwards in time using the aforementioned second root of $V(E)$, obtaining

$$\overline{W}(r;\kappa) = \left(-\frac{\Delta_r(r)}{s(r)} + q\kappa r\right)\left(\Xi\rho_0^2(r)\right)^{-1}\,. \tag{2.111}$$

In the following, we shall focus primarily on W, but the same analysis leading to similar results can be performed for $\overline{W}$ as well.

It is not immediately clear whether the allowed areas for a given E are "above" or "below" the curve of the lite potential, i.e. whether it should hold that $E \geq W$ or $E \leq W$. For the original effective potential the allowed areas are for $V \leq 0$. Since V (2.105) is quadratic in E and the leading term's coefficient is negative, the allowed E for a given r must lie outside the open interval defined by the roots of $V(E)$. Moreover, since the lesser root is unphysical (as explained above), the allowed E are greater than or equal to the greater root of V, which is, by definition, W. Thus, for a particle with the charge-to-mass ratio κ and energy E to be located in the allowed area, it must hold that

$$E \geq W(r;\kappa) \tag{2.112}$$

as in the classical case. This result is further corroborated by numerical simulations, see figure 2.9 on the next page with an example of the two effective potentials for a particle moving on the axis along with its world line. For the stated reasons, for particles travelling backwards in time it must hold that

$$E \leq \overline{W}(r;\kappa)\,. \tag{2.113}$$

Similarly as if we used the original potential V, static particles can be found using $\mathrm{d}W/\mathrm{d}r = 0$. This time, however, we do not need another equation to eliminate E as it is already absent from the condition. Solving the equation for κ leads, once again, to the well-known result (2.24). The equivalence of using the first derivative of V and W is not difficult to prove:

Disregarding κ, a constant parameter mathematically irrelevant in the proof, there are two conditions $V(r;E)$ must satisfy for static particles,

$$V(r;E) = 0 \Leftrightarrow E = W(r) \tag{2.114}$$

and

$$\frac{\mathrm{d}}{\mathrm{d}r}V(r;E) = 0\,. \tag{2.115}$$

Considering $V_W \equiv V\Big(r, W(r)\Big) \equiv 0$ and taking its first derivative, we obtain[28]

$$\frac{\mathrm{d}V_W}{\mathrm{d}r} = \frac{\partial V_W}{\partial r} + \frac{\partial V_W}{\partial W}\frac{\mathrm{d}W}{\mathrm{d}r} = 0\,, \tag{2.116}$$

[28]Take note that $\mathrm{d}V/\mathrm{d}r = 0$ because we are assuming static particles, but $\mathrm{d}V_W/\mathrm{d}r = 0$ because V_W is by definition identically equal to zero. While higher derivatives of V are not necessarily vanishing, higher derivatives of V_W are.

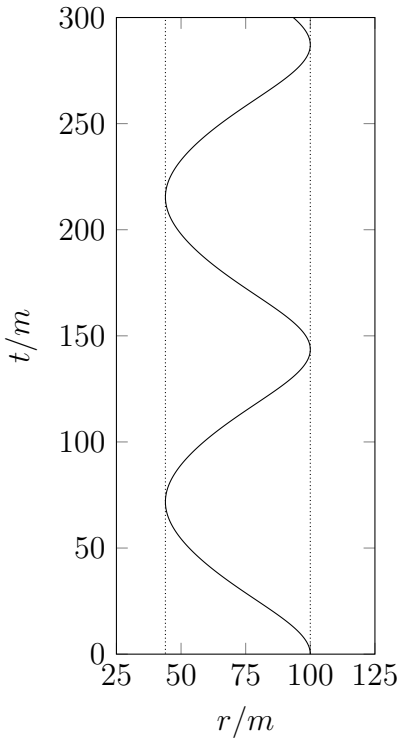

(a) The world line of the particle integrated for $\Delta\tau \approx 464m$ corresponding to $\Delta t = 300m$.

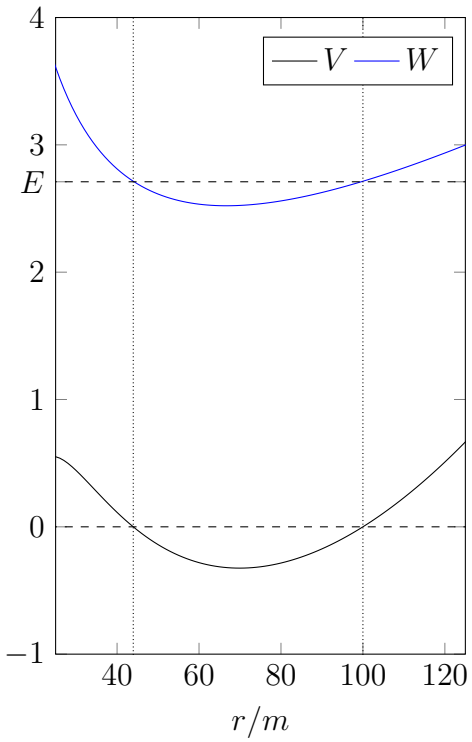

(b) The two effective potentials.

Figure 2.9: An example of particle motion on the space-time's axis for space-time $\{\Lambda, m, a, q\} = \{-10^{-3}\,\mathrm{u}^{-2}, 1\,\mathrm{u}, 0.21\,\mathrm{u}, 0.12\,\mathrm{u}\}$ and a particle with $\kappa = 531$ and $E \approx 2.71$.

which means that

$$\frac{\partial V_W}{\partial r} = -\frac{\partial V_W}{\partial W}\frac{\mathrm{d}W}{\mathrm{d}r}\,. \tag{2.117}$$

As $W(r) = E$ for the studied static particles, it holds that

$$\frac{\partial V_W}{\partial W} = \frac{\partial V}{\partial E}\,. \tag{2.118}$$

From the definition of V_W it follows that

$$\frac{\partial V_W}{\partial r} = \frac{\partial V}{\partial r} \equiv \frac{\mathrm{d}V}{\mathrm{d}r}\,. \tag{2.119}$$

We choose to write the total derivative of V with respect to r instead of the partial one, as we consider r to be the only "true" variable in $V(r; E, \kappa)$, the others being fixed parameters for the given potential. We thence obtain

$$\frac{\partial V}{\partial E}\frac{\mathrm{d}W}{\mathrm{d}r} = -\frac{\mathrm{d}V}{\mathrm{d}r} = 0\,, \tag{2.120}$$

which means that simultaneously satisfying $E = W$ and $\mathrm{d}W/\mathrm{d}r = 0$ indeed means we are dealing with a static particle. However, not all static particles necessarily need to satisfy these relations, as the latter one may seemingly be replaced by

$\partial V/\partial E = 0$ leading to the same result. Upon closer inspection, however, for $E = W$ the partial derivative remarkably reduces into

$$\left.\frac{\partial V}{\partial E}\right|_{\text{static}} = -\Xi s \tag{2.121}$$

with s defined by (2.107), which means that for the examined particles with $E = W$ the derivative is equal to zero only on the horizons.

Similarly, stability may be read off $\mathrm{d}^2W/\mathrm{d}r^2$. Considering the second derivative of $V_W \equiv 0$, we get

$$\frac{\mathrm{d}^2V_W}{\mathrm{d}r^2} = \frac{\partial^2 V_W}{\partial r^2} + \frac{\partial^2 V_W}{\partial W \partial r}\frac{\mathrm{d}W}{\mathrm{d}r} + \frac{\partial^2 V_W}{\partial r \partial W}\frac{\mathrm{d}W}{\mathrm{d}r} + \frac{\partial^2 V_W}{\partial W^2}\left(\frac{\mathrm{d}W}{\mathrm{d}r}\right)^2 + \frac{\partial V_W}{\partial W}\frac{\mathrm{d}^2W}{\mathrm{d}r^2} = 0\,. \tag{2.122}$$

The middle three terms vanish for static particles, as $\mathrm{d}W/\mathrm{d}r = 0$, and we are left with

$$\frac{\partial^2 V_W}{\partial r^2} = -\frac{\partial V_W}{\partial W}\frac{\mathrm{d}^2W}{\mathrm{d}r^2}\,, \tag{2.123}$$

which, in the same way as above, can be recast as

$$\frac{\mathrm{d}^2V}{\mathrm{d}r^2} = -\frac{\partial V}{\partial E}\frac{\mathrm{d}^2W}{\mathrm{d}r^2}\,. \tag{2.124}$$

Once again the second derivatives of V and W (assuming static particles) are directly proportional to each other with the same *positive* constant of proportionality (as for static particles $-\partial V/\partial E = \Xi s > 0$). The minima of V satisfying $V(r) = 0$ thus always translate into the minima of W satisfying $W(r) = E$ (for stable particles) and the same goes for the maxima (for unstable particles).

Unfortunately, for static particles whose staticity is guaranteed by their κ (2.108) neither of the two potentials presents us with a second derivative simple enough to determine the stability of the particles analytically. When examining a particular scenario one has to determine the stability numerically.

On the following page, figure 2.10 illustrates most of what has been said above. We can see the two effective potentials for a static particle both having the same type of extreme (a minimum corresponding to a stable position). Moreover, the examined V permits the existence of particles travelling backwards in time, which clearly correspond to the potential $\overline{W}$.

Take note that unlike V, the lite potential W may not be a continuous function[29]. Due to the presence of the square root in s, W is not defined in the non-stationary areas of the space-time where $\Delta_r < 0$.

All things considered, using the lite potential W seems advantageous over using V. The main drawback of W appears to be the absence of an analogy of the classical formula

$$v = \sqrt{2m(E - V)}\,, \tag{2.125}$$

where v represents the velocity and m the mass of the particle, to determine u^r directly from W, as the derivation of W required a vanishing u^r. The original effective potential V can, therefore, still be of use.

[29]Therefore, saying that static particles can be found at the extremes of W may be somewhat misleading, as discontinuous functions have local extremes located at the boundary of their domain, where the first derivative, in fact, typically does not vanish.

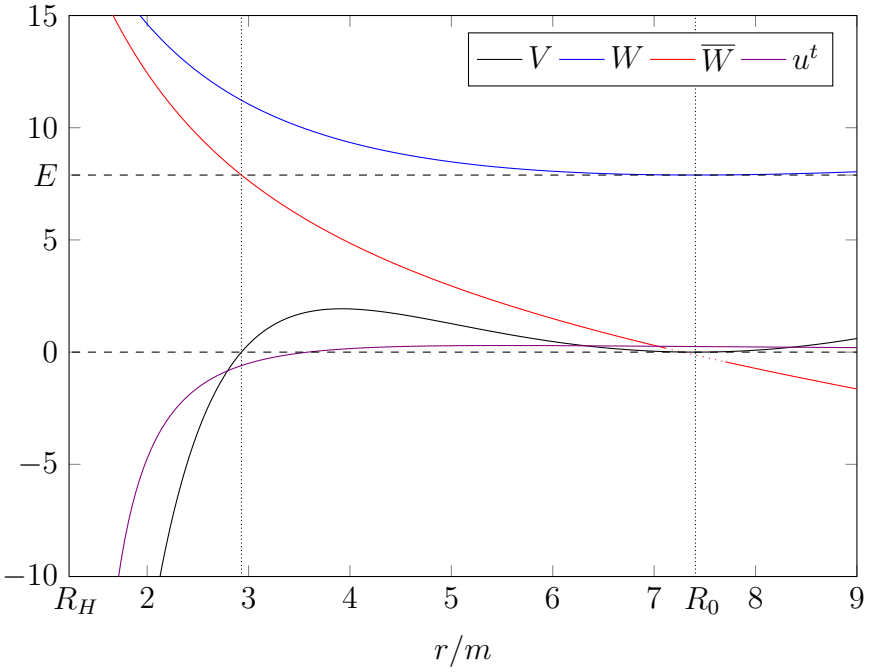

Figure 2.10: The two effective potentials for the static particle in figure 2.8 characterised by $\kappa \approx -182$ and $E \approx 7.89$ located in the space-time with parameters $\{\Lambda, m, a, q\} = \{-10^{-3}\,\mathrm{u}^{-2}, 27\,\mathrm{u}, 14\,\mathrm{u}, -4\,\mathrm{u}\}$. The particle remains static at R_0 where the potentials V and W have their minima (hence, the particle is in a stable equilibrium). The other radius at which $V = 0$ also satisfies $\overline{W} = E$. As expected, this radius is the boundary of the area where non-physical particles travelling backwards in time ($u^t < 0$) can exist. R_H is the outer black hole horizon's position. The curve of $\overline{W}$ is dotted near the static position so that one could see the minimum of V more clearly.

Returning to static particles, the other result from the corresponding section can be replicated as well: Both potentials agree on the fact that $r = \pm a$ can house static particles regardless of their κ. The first derivatives of the two potentials with respect to r for $r = \pm a$ are

$$\frac{\mathrm{d}V}{\mathrm{d}r} = \mp\frac{1}{12}\,\frac{4\Lambda a^4 + 3q^2}{a^3} \tag{2.126}$$

and

$$\frac{\mathrm{d}W}{\mathrm{d}r} = \mp\frac{\sqrt{1}}{2\sqrt{6}}\,\frac{4\Lambda a^4 + 3q^2}{\Xi a^2\sqrt{-2\Lambda a^4 + 6a^2 \mp 6am + 3q^2}}\,. \tag{2.127}$$

The derivatives vanish for

$$\Lambda = -\frac{3}{4}\frac{q^2}{a^4}\,, \tag{2.128}$$

consistent with (2.26). Provided that $V = 0 \Leftrightarrow E = W$, that is,

$$\begin{aligned} E = \frac{1}{6\Xi a}\left(\pm 3q\kappa + \sqrt{12(3 - \Lambda a^2)a^2 \mp 36am + 18q^2}\right) = \\ = \frac{2a}{4a^2 - q^2}\left(\pm q\kappa + \sqrt{4a^2 \mp 4am + 3q^2}\right)\,, \end{aligned} \tag{2.129}$$

both derivatives are indeed proportional through

$$\frac{\partial V}{\partial E} = -\frac{\Xi}{\sqrt{6}a}\sqrt{-2\Lambda a^4 + 6a^2 \mp 6am + 3q^2} = \frac{1}{8a^3}\left(q^2 - 4a^2\right)\sqrt{4a^2 \mp 4am + 3q^2}\,, \tag{2.130}$$

where the last two formulae are given both before and after inserting the required Λ. For the second expression in $\partial V/\partial E$ to be negative as required, it must hold that

$$q^2 < 4a^2\,, \tag{2.131}$$

a condition also known to us from section 2.3.1, (2.27). Furthermore, in order to be positive for $r = a$, the square root requires

$$m < \frac{4a^2 + 3q^2}{4a}\,, \tag{2.132}$$

a requirement we have already encountered as well[30], (2.29). This result was previously obtained by requiring the static particle to be in a stationary area of the space-time for $r = a$. As before, for $r = -a$ no such condition is necessary. Interestingly, E disappears from $\mathrm{d}V/\mathrm{d}r$ after setting $r = \pm a$ without any further intervention, which means that we do not have to solve $V = 0$ if we are not interested in E itself (or in $\partial V/\partial E$ as we were).

Unlike the previous case where staticity was guaranteed by κ, we are able to analyse the stability analytically here. Even though κ was irrelevant in the question of staticity, it turns out that it plays a crucial role for the stability of these particles: after substituting for Λ and, in the case of $\mathrm{d}^2V/\mathrm{d}r^2$, also E (interestingly, it does not disappear this time), the second derivatives of the potentials for $r = \pm a$ are

$$\frac{\mathrm{d}^2V}{\mathrm{d}r^2} = -\frac{1}{4a^4}\left(\mp 2am - 2q^2 \pm q\kappa\sqrt{4a^2 \mp 4am + 3q^2}\right) \tag{2.133}$$

and

$$\frac{\mathrm{d}^2W}{\mathrm{d}r^2} = -\frac{2}{a}\,\frac{\mp 2am - 2q^2 \pm q\kappa\sqrt{4a^2 \mp 4am + 3q^2}}{\left(4a^2 - q^2\right)\sqrt{4a^2 \mp 4am + 3q^2}}\,. \tag{2.134}$$

Again, the two derivatives satisfy (2.124). Therefore, the threshold κ for which the particle stability changes is

$$\kappa^{\pm}_{\mathrm{thr}} = \frac{2\left(am \pm q^2\right)}{q\sqrt{4a^2 \mp 4am + 3q^2}}\,. \tag{2.135}$$

For $r = +a$ stable positions (in the minima of the potentials) require $q\kappa < q\kappa^{+}_{\mathrm{thr}}$ and unstable $q\kappa > q\kappa^{+}_{\mathrm{thr}}$. Curiously, for $r = -a$ the inequalities are swapped and stable orbits require $q\kappa > q\kappa^{-}_{\mathrm{thr}}$, unstable $q\kappa < q\kappa^{-}_{\mathrm{thr}}$. The situation for $r = a$ is illustrated in terms of V on the following page in figure 2.11.

Further, an analogy of winding of incoming particles around an unstable orbit in the equatorial plane is present here as well, as derivation of equation (2.69) is exactly the same. Therefore, particles moving towards an unstable static position tend to reach it in infinite proper time, even though they get arbitrarily close in finite time. Figure 2.12 on page 83 illustrates both this fact and the instability itself, as the eventually incoming particles are originally perturbations of an unstable static case with the same E and κ.

[30] Recall that all the conditions combined led to a naked singularity space-time.

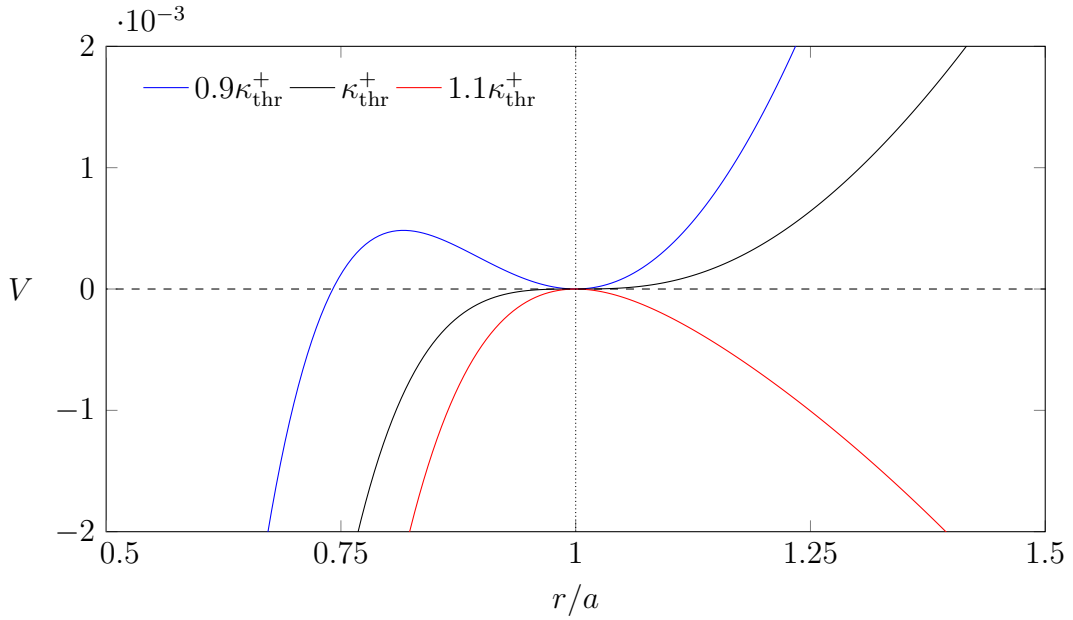

Figure 2.11: The effective potentials V in the vicinity of $r = a$ in the space-time with parameters $\{\Lambda, m, a, q\} = \{-4/7203\,\mathrm{u}^{-2}, 20\,\mathrm{u}, 21\,\mathrm{u}, 12\,\mathrm{u}\}$ allowing for static particles at $r = \pm a$ for three particles differing by their charge and E. $\kappa^+_{\text{thr}} = 47/\sqrt{129} \approx 4.14$, given by (2.135), is the charge-to-mass ratio of the black particle with $E \approx 1.88$ and it represents a marginally stable static position. The blue particle with lower $q\kappa$ and $E \approx 1.75$ is in a stable static position and the red particle with higher $q\kappa$ and $E \approx 2.01$ is in an unstable static position, in accordance with our analytical results.

The limits of V are

$$\lim_{r\to\pm\infty} V = -\mathrm{sgn}(\Lambda)\infty \tag{2.136}$$

and

$$\lim_{r\to 0} V = \frac{1}{2}\left(1 + \frac{q^2}{a^2} - \Xi^2 E^2\right) . \tag{2.137}$$

This time, unlike in the equatorial plane, there is no infinite potential barrier at $r = 0$ unless $a = 0$. Of course, the physical situation is different, as for rotating black holes of the Kerr family there is no singularity at the axis in our coordinates. If we considered a non-rotating central mass, the ring singularity would be reduced into a point one accessible from all angles and the limit of the potential would be the same as in the equatorial plane. For W, we have

$$\lim_{r\to\pm\infty} W = \sqrt{-\mathrm{sgn}(\Lambda)}\,\infty\,, \tag{2.138}$$

meaning that for $\Lambda < 0$ the limit is ∞ and for $\Lambda > 0$ the potential W is not well-defined for $r \to \pm\infty$, as is to be expected since the radial infinities are located in the non-stationary part of the space-time. For $r \to 0$, we have

$$\lim_{r\to 0} W = \frac{\sqrt{a^2 + q^2}}{\Xi a}\,, \tag{2.139}$$

which is the greater root of (2.137), in agreement with our definition of W. Again, the limit diverges to ∞ for $a = 0$ and it is finite otherwise.

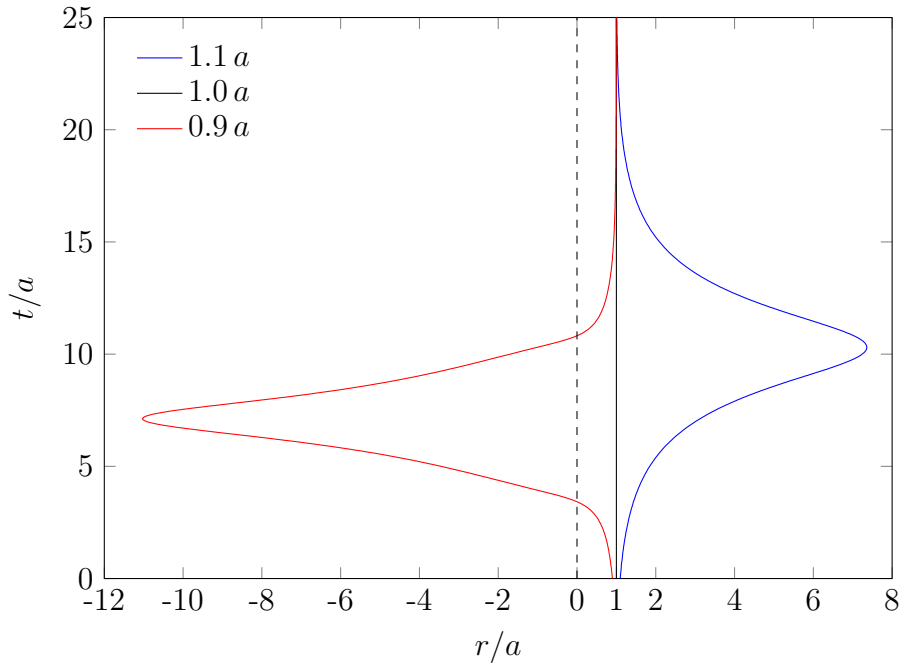

Figure 2.12: The world lines of particles with $\kappa = 2\kappa^{+}_{\text{thr}}$ given by (2.135) and $E \approx 3.16$ in space-time $\{\Lambda, m, a, q\} = \{-4/7203\,\text{u}^{-2}, 20\,\text{u}, 21\,\text{u}, 12\,\text{u}\}$ corresponding to an unstable static position at $r = a$. The black particle at a remains static, while the perturbed particles at $1.1\,a$ and $0.9\,a$ first move away from the static position considerably and then approach it in infinite proper time. As the space-time is that of a naked singularity, there are no horizons for the particles to cross. Notice that the red particle reaches $r = 0$. The ring singularity is located in the equatorial plane and not on the axis, and it cannot, therefore, obstruct particle motion in the depicted case. The particle then traverses into the area with $r < 0$ and later returns back to "our" half of the space-time.

We may establish an effective potential for photons on the axis as well, satisfying

$$\frac{1}{2}\left(\dot{r}\right)^2 = -V_\gamma(r; E)\,. \tag{2.140}$$

The potential

$$V_\gamma(r; E) = -\frac{1}{2}\Xi^2 E^2 \tag{2.141}$$

is constant and non-zero, as for photons on the axis E reduces to

$$E = -g_{tt}\dot{t} \neq 0\,. \tag{2.142}$$

Since there are no solutions to $V_\gamma = 0$, there are no turning points and, unsurprisingly, also no static positions for photons. Defining an analogue of W would, therefore, be both impossible and pointless. Take note that as the potential is constant, so is

$$\dot{r} = \pm\Xi E\,, \tag{2.143}$$

which in the limit of $a = 0$ becomes $\dot{r} = \pm E$, as known for the Schwarzschild–anti-de Sitter space-time [23]. This result does not contradict the previous non-constant $\mathrm{d}r/\mathrm{d}t \neq \dot{r}$ (2.86), as t is not an appropriate affine parameter to be used in the equations of motion for photons.

Finally, due to the relative simplicity of the problem a remark on the topic of the physicality of perturbations can be made here. Recall that for motion in the equatorial plane when we first toyed with perturbations to show the difference between stable and unstable orbits, we commented that there may be unphysical perturbations that change the potential in such a way that would not allow the perturbed particle to exist there. This time, one can easily see that accelerating the particle in the r direction is never an unphysical perturbation for static particles:

The normalisation of the four-velocity for static particles gives us

$$\left(u^t_{\text{stat}}\right)^2 = -\frac{1}{g_{tt}} = \frac{1}{|g_{tt}|}\,. \tag{2.144}$$

After adding the radial component, we have

$$\left(u^t_{\text{pert}}\right)^2 = -\frac{1}{g_{tt}} - \frac{g_{rr}}{g_{tt}}\,(u^r)^2 = \frac{1}{|g_{tt}|} + \frac{|g_{rr}|}{|g_{tt}|}\,(u^r)^2 > \left(u^t_{\text{stat}}\right)^2\,. \tag{2.145}$$

The relevant integral of motion on the axis reduces to

$$E = -g_{tt}u^t - \kappa A_t = |g_{tt}|u^t - \kappa A_t\,, \tag{2.146}$$

whence one can easily see that

$$E_{\text{pert}} > E_{\text{stat}}\,, \tag{2.147}$$

the energy of the perturbed particle increases by adding the radial component of the four-velocity. Further, for static particles we know that

$$\frac{\partial V}{\partial E} = -\Xi s < 0\,, \tag{2.148}$$

which means that if we perturb u^r of a static particle the potential V decreases as E increases. Therefore, the original static position may never become suddenly forbidden and a perturbation of this kind is, unsurprisingly, always physical.

3. Quantum tunnelling & horizon temperature

Within classical general relativity, the fate of an object that collapses to form a black hole is sealed – there is no turning back and once the horizon forms nothing can escape beyond it to the outside world. However, when studying the behaviour of quantized test fields on the fixed background of black-hole space-times, Stephen Hawking [6, 7] discovered that the virtual pairs of particles and antiparticles that flutter into their fleeting existence in the vicinity of the horizon can become separated with one of them escaping to infinity and the other – having negative energy to enable the escape of its luckier sibling – swallowed by the black hole, reducing thus the hole's energy. Although the process is extremely slow (the energy flux is inversely proportional to the square of the black hole's mass) it dramatically changes the final state of collapsing objects and the causal structure of the space-time as a whole. It has not been observed in the universe so far, but detection of an equivalent phenomenon has been reported in the so-called analogue black holes [26, 27, 28].

However, working out the details of QFT on a curved background is an uneasy task and it was thus a welcome surprise when it was discovered that the temperature of the horizon can be calculated based on the assumption that it is due to particles tunnelling through it [5]. This approach relies on the WKB approximation and enumerates the action of a particle moving through the space-time. Provided the particle stays clear of all coordinate singularities, the action is real for classically allowed trajectories and can be used to find the trajectory itself as a function of an affine parameter. Yet one can also calculate the action for paths that are forbidden in classical general relativity, such as a path crossing the black hole horizon from the inside towards the asymptotic region outside. It turns out that the action is divergent across the horizon, which calls for a regularisation eventually yielding an imaginary contribution. Proceeding then with the standard WKB approximation, we realize that the probability of the particle to tunnel out through the horizon is proportional precisely to the exponential of this imaginary part of the action, which, in turn, depends on the energy of the tunnelling particle. In the leading order, the resulting spectrum is the same as that of black-body radiation obtained by QFT calculations, as both are yielding the same temperature. However, the tunnelling method further gives corrections of higher order, unobtainable by the QFT calculations. It is due to the fact that the original Hawking's derivation was performed on a fixed background not losing energy during the black hole's evaporation, thus violating energy conservation, which, on the other hand, is one of the key ingredients of the tunnelling method. The radiation then contains correlations that may carry the information content of the black hole [5, 29, 30].

There are two equivalent main routes one can take when adopting the tunnelling approach: the null path and the Hamilton-Jacobi method, both evaluating the action for the tunnelling particle [30]. While the latter method seems to be somewhat more robust, the formalism of the former is more in line with the one used by us in the previous chapter. Therefore, in order to obtain the temperatures

of the horizons occurring in the Kerr–Newman–(anti-)de Sitter solution, we shall make use of the null geodesic method.

3.1 The null geodesic method fundamentals

The WKB approximation is a semi-classical approximation of quantum mechanics and one of the cornerstones of the tunnelling methods. It notices that without loss in generality the wave function of a system $\psi(\vec{x},t)$ can be written down as

$$\psi(\vec{x},t) = \exp\Big(\frac{i}{\hbar}S(\vec{x},t)\Big) \tag{3.1}$$

with $S(\vec{x},t)$ being a complex function. After performing an expansion in $\hbar/i$ in S,

$$S(\vec{x},t) = \sum_{n=0}^{\infty}\left(\frac{\hbar}{i}\right)^n S_n(\vec{x},t)\,, \tag{3.2}$$

and inserting the series into the Schrödinger equation, it turns out that the zeroth order S_0 – which is the most important order in the limit of negligible $\hbar$ corresponding to classical mechanics – is the classical action, also denoted I in the literature on horizon tunnelling. This is due to the fact that the resulting equation for S_0 is identical to the Hamilton–Jacobi equation for the classical action. We now apply this expansion to the problem of propagation of particles across a region where classical motion is prohibited by, for instance, energy conservation. We apply boundary conditions on both sides of the corresponding potential barrier with no ingoing modes on the outer side. If we continue the solution smoothly on both sides of the barrier we find that there is a non-zero probability for the particle to appear on the outer side of the barrier. To the lowest order in $\hbar$ and considering $\hbar = 1$ in the following, the exponential part of the emission rate is then found to be

$$\Gamma \propto e^{-2\mathrm{Im}\,S_0}\,, \tag{3.3}$$

allowing us to obtain the inverse temperature β_R of horizon R by identifying the result with the expected Boltzmann factor

$$\Gamma \propto e^{-\beta_R\omega}\,, \tag{3.4}$$

where ω is the energy of the particle.

The null geodesic method, proposed by Maulik K. Parikh and Frank Wilczek originally with the Schwarzschild solution in mind [5], consists in computing the action corresponding to a shell respecting the space-time's symmetry and crossing the horizon from the inside to the stationary area of the space-time on a (radial) null geodesic path, taking with itself a portion of the original black hole's mass m denoted ω in the form of its energy[1]. The total energy of the space-time plus the emitted particle is fixed and the shell travels on a geodesic with m replaced by $m-\omega$, the original black hole's mass minus the escaped energy. Due to the black hole's energy loss, the horizon's position changes accordingly, which is

[1]The shell's energy must by considerably smaller than the black hole's mass for the WKB approximation to hold, $\omega \ll m$ [31]. This means the last stages of the black hole's evaporation cannot be described in this way.

critical in the calculations. While the typical wavelength of the radiation is said to be of the order of the black hole's size, due to blue shift it is reasonable to use the point particle approximation near the horizons, allowing us to consider a single particle with energy ω instead of a shell. While it may seem that the method oddly ignores massive particles by considering a null path, it is actually not true, as close to the horizon massive particles asymptotically follow null geodesics as well. More often than not, due to their favourable properties (such as regularity across horizons), the preferred coordinates in which the geodesics are given are Painlevé-Gullstrand's ones. Expressing the geodesic in coordinate time, $\hat{r} \equiv \mathrm{d}r/\mathrm{d}t$, the inaugural paper [5] introduced the following procedure for evaluating the imaginary part of the action:

It holds that

$$\operatorname{Im} S_0 = \operatorname{Im} \int_{r_{\mathrm{in}}}^{r_{\mathrm{out}}} p_r \mathrm{d}r = \operatorname{Im} \int_{r_{\mathrm{in}}}^{r_{\mathrm{out}}} \int_0^{p_r} \mathrm{d}p_r' \mathrm{d}r \,, \tag{3.5}$$

as the other parts of the action except for the radial one are real (at least in the case of Schwarzschild geometry covered with regular coordinates across the horizon). To proceed with the integration, the authors invoked the Hamiltonian formalism. As explained in a previous paper [32], instead of using a Hamiltonian describing only the particle (or the shell) and containing just its degrees of freedom, to ensure the conservation of energy one needs to consider both the particle and the black hole in the Hamiltonian. Starting from the full action, an effective action containing only the non-gravitational degrees of freedom was derived. From the action's integrand (that is, the Lagrangian), one can see the particle's effective Hamiltonian is equal to the ADM mass of the black hole, given by the mass parameter of the metric for the Schwarzschild solution. Using the relevant Hamilton canonical equation

$$\hat{r} = \left.\frac{\mathrm{d}H}{\mathrm{d}p_r}\right|_{r=\mathrm{const.}} \tag{3.6}$$

the authors obtained

$$\operatorname{Im} S_0 = \operatorname{Im} \int_m^{m-\omega} \int_{r_{\mathrm{in}}}^{r_{\mathrm{out}}} \frac{\mathrm{d}r}{\hat{r}} \mathrm{d}H \,. \tag{3.7}$$

The value of the Hamiltonian H is taken as m before the emission of the particle and $m - \omega$ afterwards, as the mass parameter in the metric diminishes by the emitted particle's energy. After a simple substitution in the integral, one finally obtains

$$\operatorname{Im} S_0 = \operatorname{Im} \int_0^{+\omega} \int_{r_{\mathrm{in}}}^{r_{\mathrm{out}}} \frac{\mathrm{d}r}{\hat{r}[m-\omega']} (-\mathrm{d}\omega') \,. \tag{3.8}$$

The square bracket in $\hat{r}[m - \omega']$ is there to remind us to consider geodesics with a diminished mass parameter.

To obtain the imaginary part of the integral, one has to consider an appropriate regularisation of the otherwise divergent real integral. The original paper suggests using the so-called Feynman prescription, shifting the integrand's denominator – which vanishes on the horizon, leading to the aforementioned divergence – into the complex plane. Considering a limit to zero in the imaginary term, the

evaluation of the integral over r is done using the Sokhotski–Plemelj theorem, which in the integral form for $a < 0 < b$ reads [33]

$$\lim_{\epsilon\to 0^+}\int_a^b \frac{f(x)}{x \pm i\epsilon}\mathrm{d}x = \text{v.p.}\int_a^b \frac{f(x)}{x}\mathrm{d}x \mp i\pi f(0)\,, \tag{3.9}$$

where v.p. denotes the Cauchy principal value of the integral. Take note that in the Schwarzschild case, it holds that $r_{\text{in}} > r_{\text{out}}$, as the forbidden trajectory is thought to start just inside the initial position of the horizon (in the standard coordinates $r_{\text{in}} = 2m - \delta$ for $\delta \ll m$) and to end just outside the final position ($r_{\text{out}} = 2(m-\omega) + \delta$). Consequently, the limits of integration must be switched in order to use the formula, adding a further minus sign in the computation. For the subsequent integration over ω no similar trick is required. However, if $\hat{r}$ is complicated enough, it may not be possible to evaluate the integral in terms of elementary functions.

From (3.9) it is obvious that there are two non-equivalent ways of performing the regularisation, leading to a different sign of the imaginary part. Ignoring antiparticles for now, the correct prescription is said to be $\omega \to \omega - i\epsilon$, where $\epsilon > 0$, "so as to ensure that positive energy solutions decay in time." Apart from this cryptic message there is no other clue given to explain the choice of the sign. In subsequent papers, various authors approach the problem of the sign selection differently: some repeat the original statement without adding anything new [30, 34][2], some prefer not to talk about the sign at all [35, 36, 37, 38] and some come up with explanations seemingly unrelated to the original one [39, 40]. It may be entirely possible that some authors choose the sign in such a way that ensures the positivity of the resulting temperature, meaning a preferred result influenced the computation! We deemed the situation unsatisfactory and attempted to understand the quoted argument better.

The key to understanding the suggested prescription seems to lie in the WKB approximation. The temporal part of the wave function is

$$\psi(\vec{x}, t) \propto \exp\left(-i\omega t\right)\,. \tag{3.10}$$

Shifting the energy $\omega \to \omega \pm i\epsilon$ leads to

$$\psi(\vec{x}, t) \propto \exp\left(\pm\epsilon t\right)\exp\left(-i\omega t\right)\,. \tag{3.11}$$

For a wave function to describe decay, it is logical to assume its amplitude should decrease in time. This indeed corresponds to the choice of the minus sign in the shift in energy[3]. In the limit of $\epsilon \to 0^+$, the wave function describes a stable particle.

Regarding antiparticles, one should properly consider not only the case of a particle tunnelling from the inside of the black hole, but also tunnelling of

[2]What is more, after repeating the original argument [30] suggests that one should use $\omega \to \omega + i\epsilon$! This curious disagreement with the inaugural paper was probably meant to amend for a missing minus sign in (2.13), because otherwise the temperature would be negative. In fact, the authors apparently forgot to switch the limits of integration $r_{\text{in}} > r_{\text{out}}$ so that they could use the Sokhotski–Plemelj formula, which would lead to the positive sign of temperature only if the prescription $\omega \to \omega - i\epsilon$ was used.

[3]For antiparticles the opposite sign was proposed, presumably because they are thought to travel backwards in time. Indeed, $\lim_{t\to-\infty} ||\psi||^2 = 0$ only if the plus sign is used.

a nascent antiparticle into it, which is a classically forbidden process as well. However, it has been found [5] that considering both processes affects only the prefactor in Γ and has no effect on the resulting temperature whatsoever, meaning that in practical calculations antiparticles can be safely disregarded.

Furthermore, it is a well known fact that considering coordinates that are singular across the horizon (as we intend to do), one obtains half the correct inverse temperature. The reason is that for singular coordinates even the classically permitted trajectories of particles falling into the black hole produce a divergent action, which needs to be regularised in the same way as the action of the outgoing particles, leading to a non-vanishing imaginary part. The resulting tunnelling rate is then proportional to the quotient of the exponential factors [30, 40, 41], leading to

$$\Gamma \propto \exp\Big(-2(\operatorname{Im} S_{\text{out}} - \operatorname{Im} S_{\text{in}})\Big)\,, \tag{3.12}$$

where S_{out} and S_{in} are respectively the action for outgoing and incoming particles. Using regular coordinates, one obtains $\operatorname{Im} S_{\text{in}} = 0$ and the corresponding exponential factor is equal to one.

Before we continue further, it needs to be said that, as with most new theories, the method is not without its opponents, the most vocal of which appears to be Vladimir A. Belinski [42]. The main points of his criticism seem to be as follows:

- First, no geodesic can reach a future horizon from the inside and cross it. That is correct, but the method does not rely on analytic extension of the geodesic across the horizon. Instead, we end the classical geodesic below the horizon and continue it above, arbitrarily close to the horizon in both cases, connecting the two points via a full quantum-mechanical solution.

- Further, it is asserted that the used coordinate system should be irrelevant. We have already covered the difference between coordinates that are regular and singular across the horizon, but the request is more profound than that: we should be able to consider an arbitrary coordinate transformation that could lead to multiple parts of the action being complex. The original formula for the imaginary part of the action (3.5) is, however, manifestly non-covariant, as it assumes the only complex part is the one corresponding to the radial coordinate, which is indeed problematic[4]. To remedy this, a generalisation of the null geodesic method has been suggested [30, 40], replacing the original integral (3.5) with that of the full Liouville differential one-form

  $$\varpi = p_\mu \mathrm{d}x^\mu\,, \tag{3.13}$$

  providing us with a covariant formula. The generalised method gives the same results if the r component of the four-momentum is the only one gaining an imaginary part upon crossing the horizon.

- Next, there is a related question whether the temporal part of the action should be taken into consideration when evaluating the imaginary part, a problem more visible when angular momentum also comes into play. We shall briefly discuss that later.

[4] Take note that the other approach to tunnelling, the Hamilton–Jacobi method, is covariant, and it generally seems more robust [30].

- Finally, as any point of the horizon is a regular point of the space-time, the equivalence principle allows us to introduce locally flat coordinates with vanishing Christoffel symbols there, which supposedly means that no radiation should emanate from there, because that would mean there is a source of radiation in the Minkowski space-time as well. However, even in a globally flat space-time an accelerated observer would be immersed in a heat bath of a temperature given by his or her acceleration with respect to the (both locally and globally) flat space-time [43], a phenomenon called the Unruh effect. A static outside observer (perhaps trying to figure out the horizon's temperature) is accelerated with respect to the locally flat frame momentarily static with respect to the horizon, which results in the thermal radiation seen by the observer. With the last point, Belinski actually attacks not only the tunnelling methods, but the whole concept of the Hawking radiation itself!

From the perspective of what has been said, some points of the criticism do not appear entirely convincing, while some do, mainly the issue of covariance and the temporal part of the action. At any rate, most of the scientific community seems to have accepted the tunnelling approach as a valid perspective on the thermal aspects of the horizon.

Now, let us apply what has been said to the horizons in our space-time, in hopes of obtaining their temperatures...

3.2 Horizon temperatures

3.2.1 Horizons of multiplicity one

With the Kerr–Newman–(anti-)de Sitter space-time being an asymptotically non-flat stationary solution with multiple horizons, there are several pitfalls that may endanger our quest for horizon temperatures:

For one, while the θ coordinate was entirely ignored by radial geodesics in the static Schwarzschild solution, it does affect them in our space-time. However, the temperature (or, equivalently, surface gravity) should be constant on the whole horizon, as one must assume thermodynamic equilibrium in order to speak about temperature in the first place, which means a particular choice of θ in the geodesic should not affect the resulting temperature. Since we have already analysed null radial geodesics on the axis in section 2.5.1, we shall make use of our previous results and consider tunnelling of particles on the axis. The θ independence of the temperature in the Kerr family of black holes is also supported in the literature even if the temperature is obtained by the means of tunnelling [30, 37].

Further, as our space-time is not asymptotically flat, it does not have a well-defined ADM mass. Instead, we shall use the generalised Komar mass [44]

$$M = \frac{m}{\Xi^2}\,, \tag{3.14}$$

as it is equivalent to the ADM mass if both exist (in asymptotically flat stationary space-times). On the subject of the invariant mass there is a curious inconsistency in the literature, with some authors using the above value [34, 45, 46, 47] and

some m/Ξ [35, 48]. Interestingly, as it turns out the multiplicative factor eventually drops out during the evaluation, meaning neither set of papers necessarily contains erroneous results.

Next, using the full expression for $\hat{r}$ (2.86) would make it difficult to perform the regularisation, as the denominator in the full $1/\hat{r}$, $\Delta_r(r)$, is not in the form allowing for the use of the Sokhotski–Plemelj theorem. Instead, one must use the factorisation (2.94)[5]. At least for now, let us consider a horizon of multiplicity one only. Extremal horizons shall be discussed later. All things considered, the integral we want to evaluate is

$$\operatorname{Im} S^r_{\text{out}} = \operatorname{sgn}(\hat{r}) \operatorname{Im} \int_0^{+\omega} \int_{r_{\text{in}}}^{r_{\text{out}}} \frac{\mathrm{d}r}{\zeta_1(r)\,(r - R[m-\omega'])} \left(-\frac{\mathrm{d}\omega'}{\Xi^2}\right) , \tag{3.15}$$

where the index r stresses that we are dealing with the radial part of the action. One needs to include the sign of $\hat{r}$ to make sure that the particle indeed tunnels out of the horizon (e.g. considering the inner black hole horizon, a particle tunnels out towards smaller r, $\operatorname{sgn}(\hat{r}) < 0$). ω is the reduction of the space-time's mass parameter during the tunnelling process, the particle's energy is ω/Ξ^2. Here, it should be noted that in our treatise we assume that it is possible for a particle carrying a part of the space-time's energy to tunnel through any horizon, including the cosmological ones. We are not investigating the process of pair creation and its feasibility in the vicinity of any of the four horizons.

Using the factorisation, it is not immediately clear how the shift in energy $\omega' \to \omega' - i\epsilon$ translates into the integrand's denominator $r - R \pm i\epsilon$, because we do not have an expression for R for a general space-time[6]. Fortunately, having an explicit formula for R is not needed, as we can infer the sign of the dependence of R on ω' from looking at the derivative of Δ_r with respect to m,

$$\frac{\partial \Delta_r}{\partial m} = -2r\,. \tag{3.16}$$

As m decreases by ω', Δ_r increases in the area with $r > 0$ and decreases everywhere else. The change in the positions of the horizons is then clear: provided the space-time contains all of them, the outer black hole horizon moves towards smaller r, while the other three horizons move towards higher r. The situation for a generic $(-1 \oplus 1 - 1 + 1-)$ scenario is illustrated on the following page in figure 3.1, where a decrease in m corresponds to going from the red curve to the blue one. Corresponding horizons of multiplicity one in extremal or naked singularity space-times follow the same rules.

Knowing how the horizons change with a decreased mass parameter, one can see that the leading term in the Taylor series in ω' for the outer black hole horizon's position must be negative, while for the remaining three horizons it must be positive. Considering $\omega' \to \omega' - i\epsilon$, it is clear that the leading order in $i\epsilon$ must have the opposite sign. Ignoring the leading term coefficient's absolute value, as it is irrelevant in the limit of $\epsilon \to 0^+$, one must consider $R \to R + i\epsilon$ for the outer black hole horizon and $R \to R - i\epsilon$ otherwise. In the following, the sign of the appropriate shift in R shall be denoted $\operatorname{sgn}(\operatorname{Im} R)$.

[5] As it is actually the integral of a delta function, the imaginary term in the theorem makes it irrelevant whether one uses the first or the second expression in (2.94).

[6] In the extremal scenarios, however, we do know the horizons' positions explicitly.

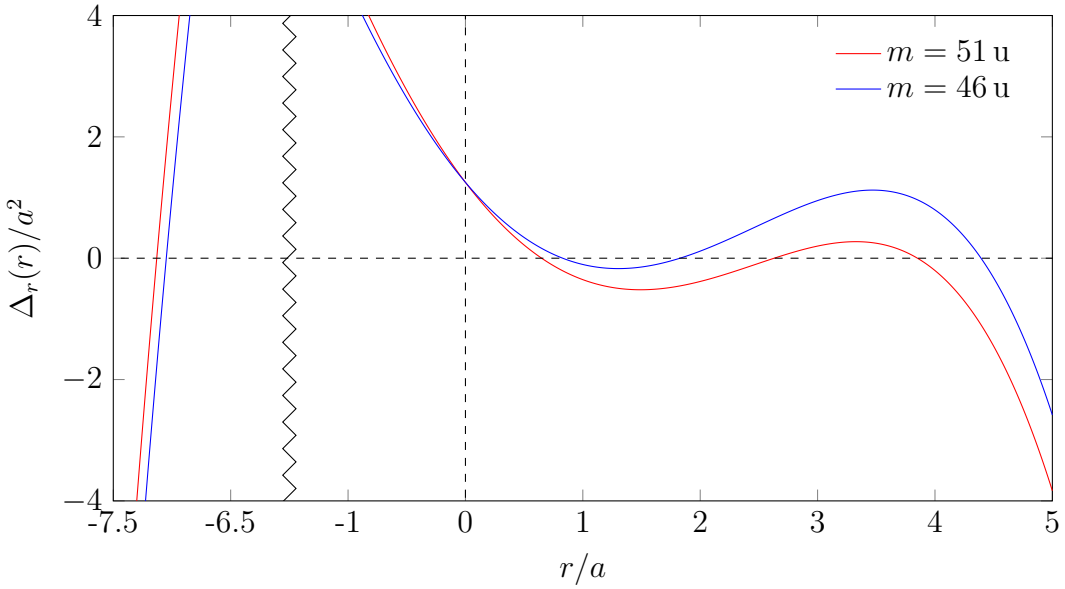

Figure 3.1: The course of $\Delta_r(r)$ in the vicinity of the horizons for two space-times with the same $\{\Lambda, a, q\} = \{5 \times 10^{-5}\,\mathrm{u}^{-2}, 40\,\mathrm{u}, 20\,\mathrm{u}\}$ but with different values of m, both corresponding to the most general horizon configuration. The quantities are expressed using a instead of m, as the value of a is the same for both curves.

The integration over r is then a trivial application of the Sokhotski–Plemelj theorem (3.9). One must only keep in mind that the regularised denominator contains $-R$ instead of $+R$ when selecting the sign of the imaginary part and add $\operatorname{sgn}(r_{\mathrm{out}} - r_{\mathrm{in}})$ to include the switch of the integration limits whenever $r_{\mathrm{in}} > r_{\mathrm{out}}$. We obtain

$$\operatorname{Im} S^r_{\mathrm{out}} = -\operatorname{sgn}(\hat{r}) \operatorname{sgn}(\operatorname{Im} R) \operatorname{sgn}(r_{\mathrm{out}} - r_{\mathrm{in}}) \frac{\pi}{\Xi^2} \int_0^\omega \frac{\Xi \rho_0^2(R[m-\omega'])}{\Delta_r'(R[m-\omega'])} \mathrm{d}\omega' \,, \quad (3.17)$$

where we further used the definition of ζ_1 (2.93) and (2.92) to replace δ_1 with Δ_r' now that the functions are evaluated on a horizon.

Next, we need to compute the integral over ω'. However, the lack of a general formula for R again proves to be an unwelcome complication. Instead, we shall perform a series expansion in ω to obtain the temperature. Unfortunately, the mentioned higher-order corrections shall be lost in the process. Seeing that for a well-behaved f we have

$$\int_0^\omega f(m-\omega')\,\mathrm{d}\omega' = \int_0^\omega \Big(f(m) + \mathcal{O}(\omega')\Big)\,\mathrm{d}\omega' = f(m)\,\omega + \mathcal{O}(\omega^2)\,, \quad (3.18)$$

we can write

$$\operatorname{Im} S^r_{\mathrm{out}} = -\operatorname{sgn}(\hat{r}) \operatorname{sgn}(\operatorname{Im} R) \operatorname{sgn}(r_{\mathrm{out}} - r_{\mathrm{in}}) \frac{\pi \rho_0^2(R[m])}{\Xi \Delta_r'(R[m])}\,\omega + \mathcal{O}(\omega^2)\,. \quad (3.19)$$

For classically allowed particles crossing the horizon in the opposite direction, one must take the opposite sign of $\hat{r}$ and, as the black hole's mass increases after swallowing a particle $m \to m + \omega$, the remaining two sgn functions in $\operatorname{Im} S^r_{\mathrm{out}}$ change their signs as well, correctly leading to the discussed factor two in

$$\operatorname{Im} S^r_{\mathrm{tot}} = \operatorname{Im} S^r_{\mathrm{out}} - \operatorname{Im} S^r_{\mathrm{in}} = \operatorname{Im} S^r_{\mathrm{out}} - (-1)^3 \operatorname{Im} S^r_{\mathrm{out}} + \mathcal{O}(\omega^2) = 2\operatorname{Im} S^r_{\mathrm{out}} + \mathcal{O}(\omega^2)\,. \quad (3.20)$$

Finally, omitting $\mathcal{O}(\omega^2)$ in the following, by comparing

$$\exp(-2\mathrm{Im}\, S^r_{\mathrm{tot}}) = \exp(-\beta\omega/\Xi^2)\,, \tag{3.21}$$

where we used that the particle's energy is ω/Ξ^2 (thus eliminating the factor $1/\Xi^2$ from $\mathrm{Im}\, S^r_{\mathrm{tot}}$ as promised), one arrives at the result

$$\beta_R = -\mathrm{sgn}(\hat{r})\,\mathrm{sgn}(\mathrm{Im}\, R)\,\mathrm{sgn}(r_{\mathrm{out}} - r_{\mathrm{in}})\,\frac{4\pi\Xi\rho_0^2(R)}{\Delta_r'(R)}\,. \tag{3.22}$$

Now we must check if the inverse temperature is positive for all the four possible horizons of multiplicity one in the space-time as it should be. If not, our procedure would be manifestly flawed. The sign of β_R is

$$\mathrm{sgn}(\beta_R) = -\mathrm{sgn}(\hat{r})\,\mathrm{sgn}(\mathrm{Im}\, R)\,\mathrm{sgn}(r_{\mathrm{out}} - r_{\mathrm{in}})\,\mathrm{sgn}(\Delta_r'(R))\,, \tag{3.23}$$

where $\mathrm{sgn}(\Delta_r'(R))$ can be easily read off figure 3.1 for each horizon. Inspecting table 3.1 below, where the signs of the sgn functions are written, one can see that our procedure gives $\beta_R > 0$ consistently for every horizon of multiplicity one, much to our delight.

R	$\mathrm{sgn}(\hat{r})$	$\mathrm{sgn}(\mathrm{Im}\, R)$	$\mathrm{sgn}(r_{\mathrm{out}} - r_{\mathrm{in}})$	$\mathrm{sgn}(\Delta_r'(R))$	$\mathrm{sgn}(\beta_R)$
$R_{\mathrm{C}-}$	$+$	$-$	$+$	$+$	$+$
R_{I}	$-$	$-$	$+$	$-$	$+$
R_{O}	$+$	$+$	$-$	$+$	$+$
$R_{\mathrm{C}+}$	$-$	$-$	$+$	$-$	$+$

Table 3.1: Signs of the inverse temperature for the four possible horizons of multiplicity one ($R_{\mathrm{C}-} < 0 < R_{\mathrm{I}} < R_{\mathrm{O}} < R_{\mathrm{C}+}$).

To sum up, the inverse temperature of a horizon of multiplicity one was found to be

$$\beta_R = \frac{4\pi\Xi\rho_0^2(R)}{|\Delta_r'(R)|}\,. \tag{3.24}$$

This result, however, is not in accordance with what seems to be a general consensus on the KN(a)dS horizon temperature, as the common result does not contain the Ξ factor[7] [35, 41, 45, 46, 47, 48, 49, 50]. Nonetheless, our result does occasionally appear in the literature as well, although it is indisputably in the minority [34]. It seems that this disagreement is a coordinate effect: the extra Ξ factor comes from the radial null geodesic $\hat{r}$ (2.86), which was obtained directly from the metric. The only paper in agreement with us uses the same metric as we do, but more commonly a rescaled time coordinate $\mathrm{d}T = \mathrm{d}t/\Xi$ is used. It then holds $\mathrm{d}r/\mathrm{d}T = \Xi\,\mathrm{d}r/\mathrm{d}t$, eliminating the Ξ factor in β_R in the end. The other coordinates appear to be preferred due to the normalisation of the Killing vector fields [35, 49], which is – as usual – considerably more complicated in space-times that are not asymptotically flat. The Killing vector corresponding to the time

[7] Alas, in the limit of vanishing Λ or a the difference disappears, as $\Xi \to 1$. Hence, we cannot check where the discrepancy arises from in an asymptotically flat space-time with clear interpretation of the quantities involved in the calculation.

coordinate is typically normalised to -1 at radial infinity. It can then be identified with the four-velocity of a static observer at flat radial infinity, which is the observer with respect to whom one defines surface gravity, and, equivalently, horizon temperature. This normalisation is not achievable for our space-time with a non-zero Λ, which means that the notion of temperature is ill-defined in space-times that are not asymptotically flat, as they lack a preferred observer in the definition of surface gravity. The two cited papers justified their choice of the normalisation by saying the conserved quantities then generate the so(3,2) algebra, which is apparently relevant in the context of the analogue of our space-time in supergravity [51]. Having said that, it is now clear that it is important to have a consensus on a preferred normalisation of the Killing vectors, as space-times that are not asymptotically flat lack an obvious choice of it. At any case, considering an unusual normalisation does not invalidate our derivation or our result, however, one needs to specify the coordinates which were used to obtain it.

The previous method can be generalised to include not only the conservation of energy but also angular momentum [34, 37, 38, 39, 52, 53, 54, 55]. A decrease in the space-time's energy also results in a decrease in its total angular momentum am/Ξ^2 if a is constant. As ϕ is a cyclic coordinate in the Lagrangian, it has been suggested that one should use the reduced action to eliminate this degree of freedom (as usual, we were not able to find an explanation anywhere in the literature). The corresponding reduction of the action yields a shift in the exponent of the tunnelling probability which is proportional to the conserved angular momentum of the particle and the angular velocity of the black hole horizon. This, however, has no effect on the temperature of the horizon and the above result still holds, as the same shift should be considered in the Boltzmann exponential as well. However, t also is a cyclic coordinate in the Lagrangian, and none of the cited papers seems to acknowledge that fact. This is related to one of the points of Belinski's criticism: that the imaginary contribution of the temporal part in the action tends to be ignored in the literature. Further, considering the reduced action seems incompatible with the covariant generalised null geodesic method integrating ϖ (3.13), as that would lead to an opposite sign of the angular part in the action.

The last two paragraphs discussed two encountered problems that were completely different in their nature. The first paragraph was about a problem with the definition of the horizon temperature that is unavoidable in any method trying to compute it. The second one, however, should be understood as a criticism of the very method of null geodesics, as we were not able to solve the issues at hand to our satisfaction. It almost appears that after seeing that a naive application of the formalism yields correct results, some problems with the method have been conveniently swept under the rug. The other approach, the Hamilton–Jacobi method, relies on reconstructing the entire action and it is devoid of the presented problems [30]. Using this method for performing computations concerning tunnelling is strongly recommended.

As a side note, the result (3.24) seems to imply that neighbouring horizons may not be of the same temperature, which means they are not in a thermodynamic equilibrium – which means that it is also inappropriate to speak about temperature in the first place, as it is meant to describe equilibria! A radiation flux from the hotter horizon towards the colder one could be, in theory, detected

by an observer living between them. This classical viewpoint, however, neglects the importance of observers in general relativity. While temperature is typically given with respect to a static observer in infinity, a different observer generally measures a different temperature [56]. Especially in our case, where it is unknown which observer can measure our result to begin with (because for space-times that are not asymptotically flat the notion of temperature is not considered with respect to a given observer but rather a particular normalisation of the Killing vectors, as discussed above), the conditions neighbouring horizons must satisfy in order to be in an equilibrium are unclear.

3.2.2 Extremal horizons

As far as the extremal horizons are concerned, performing a corresponding limit in β_R gives a divergent inverse temperature

$$\lim_{\Delta_r'(R)\to 0} \beta_R = \infty \,, \tag{3.25}$$

so the temperature of an extremal horizon is zero, as expected for the Kerr–Newman–(anti-)de Sitter solution[8] [47].

On the following page, figure 3.2 shows this divergence considering space-times with fixed $\{\Lambda, a, q\}$ but with varying m. In each subfigure, for one particular value of m the space-time becomes extremal and the inverse temperatures of the horizon of multiplicity two in 3.2a and of the horzion of multiplicity three in 3.2b diverge.

However, the problem of the extremal horizon temperature could be approached more thoroughly than by simply performing a limit in the temperature derived for horizons of multiplicity one. It is believed that no emission of neutral particles can occur for extremal space-times if it leads to a naked singularity [37, 57], which is the case for all possible horizons of multiplicity two in our metric as seen in the section on parametric perturbations 1.2.7. However, neutral tunnelling from the horizon of multiplicity three does not lead to a naked singularity but to a horizon of multiplicity one, which perhaps makes performing the above limit more justified for this horizon. In any case, it seems that the proper way to treat extremal horizons would be by considering emission of particles preserving the extremality [37]. Even though we shall not follow this path to its end we shall lay the groundwork for this approach, perhaps as a foundation for future research...

The Kerr–Newman–(anti-)de Sitter space-time is characterised by four parameters. Three of them – mass m, angular momentum per unit energy a and charge q – are properties of the black hole, while the last one – the cosmological constant Λ – is an attribute of the background[9]. A tunnelling particle cannot be expected to alter Λ, but it is able to take a portion of m, a and q with it. As extremality depends on a delicate combination of the space-time's parameters, it is necessary for the particle to carry more than just mass. In order to keep Λ fixed, it must be considered as one of the free parameters of the extremal scenario. Fortunately, upon inspecting our results summarised in section 1.2.6, one sees that

[8] Note that extremal horizons in different space-times can have non-zero temperatures [35].

[9] This distinction is somewhat arbitrary, as the parameters simply characterize the solution of the Einstein equations, but one usually considers the universe a collection of separate local sources and a shared cosmological background.

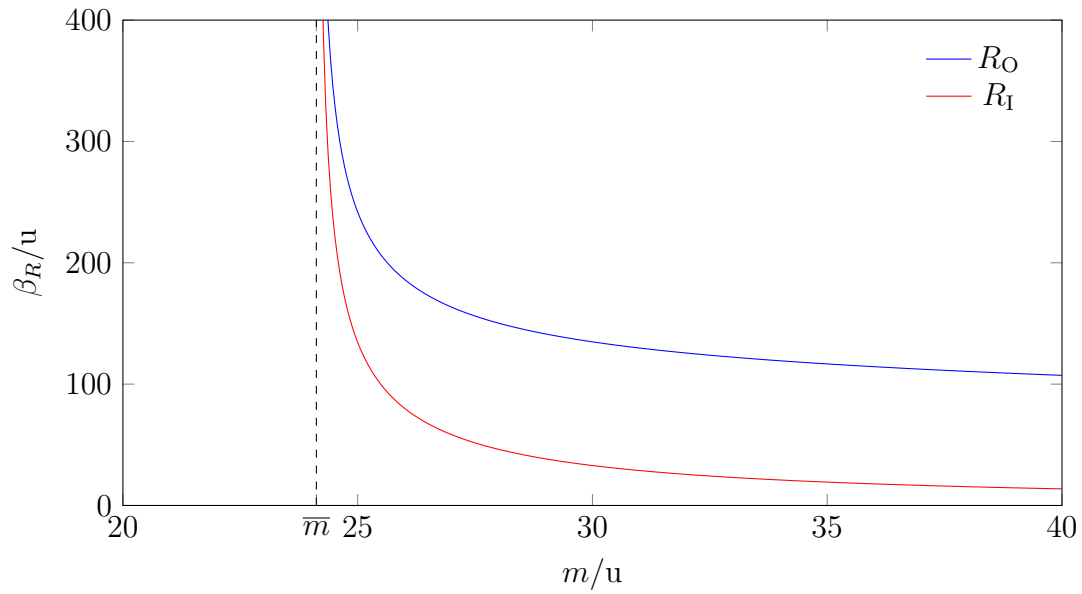

(a) Inverse horizon temperatures β_R for $\{\Lambda, a, q\} = \{-10^{-3}\,\mathrm{u}^{-2}, 10\,\mathrm{u}, 20\,\mathrm{u}\}$ as functions of m. For $\overline{m} = 24.12\,\mathrm{u}$, the extremal scenario $(\oplus 2+)$ separates the horizonless scenario $(\oplus)$ for $m < \overline{m}$ and the scenario with both black hole horizons $(\oplus 1 - 1+)$ for $m > \overline{m}$. The outer black hole horizon is denoted R_{O}, the inner R_{I}. As $\Lambda < 0$, there are no cosmological horizons.

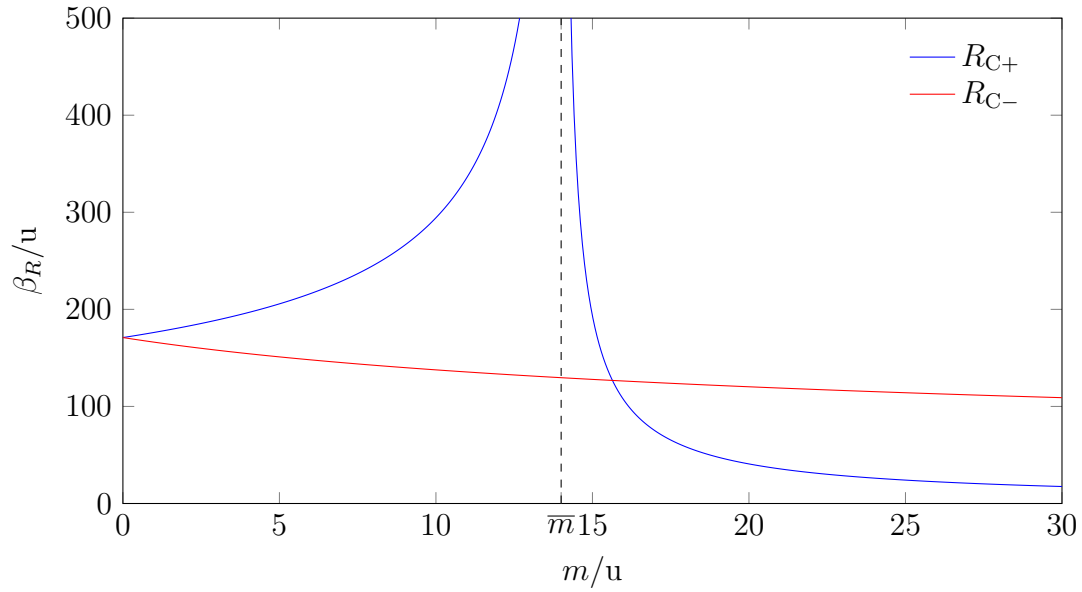

(b) Inverse horizon temperatures β_R for $\{\Lambda, a, q\} = \{10^{-3}\,\mathrm{u}^{-2}, 11.09\,\mathrm{u}, 10.34\,\mathrm{u}\}$ as functions of m. For almost every m in range the space-time is that of a naked singularity $(-1 \oplus 1-)$ with no black hole horizons, but with both cosmological horizons $R_{\mathrm{C}+} > 0 > R_{\mathrm{C}-}$. However, for $\overline{m} = 14\,\mathrm{u}$ the positive cosmological horizon is of multiplicity three, corresponding to scenario $(-1 \oplus 3-)$, and its inverse temperature diverges.

Figure 3.2: Inverse temperatures β_R (3.24) of extremal horizons.

every scenario has already been prepared with Λ as one of its free parameters. All the double-horizon scenarios were discovered using a and q as the remaining free parameters, which means the tunnelling particle does not need to carry away portions of both a and q along with a part of $m(\Lambda, a, q)$; it is possible (but not necessary) to ignore one of these parameters. The part of the black hole's mass the particle carries away is determined by the (arbitrary) portions of a and q it also takes so that extremality is preserved. For the triple-horizon scenario, there is only one other free parameter (we have chosen m), which means the particle needs to take away parts of all the three remaining parameters m, a and q.

Moreover, if the particle carries a portion of a and q, one should be more careful using the Hamilton canonical equations. Altering a may further convolute the already-troublesome issue with the angular part of the action mentioned in the previous section, and tunnelling charge seems to necessitate the introduction of a canonical momentum conjugate to the four-potential into the reduced action [53, 54].

As far as $\hat{r}$ is concerned, we already know that considering a charged massless particle changes nothing in $\hat{r}$, as the expression was derived from the normalisation equation, which does not contain the particle's charge-to-mass ratio κ. Considering our $\hat{r}$ for radial motion on the axis, it is questionable how such a particle could carry away part of the black hole's angular momentum, which would already be problematic if we wanted to include the conservation of angular momentum properly in the previous case of non-extremal horizons. There, the particle does not affect angular momentum *per unit energy* a, but as it decreases the black hole's energy it must somehow decrease the total angular momentum as well. On the other hand, a particle that decreases a in such a way that the *total* angular momentum is constant should definitely move on the already-used radial geodesic (2.86).

Another thing that would need to be examined is how the extremal horizon's position changes after performing an appropriate decrease in the values of the black hole's parameters. For scenario $(-1 \oplus 3-)$ it is clear that the horizon's radius decreases with decreasing m, but for the three double-horizon scenarios it is not immediately apparent.

Finally, in order to perform the integration over r in the near-horizon approximation of $1/\hat{r}$, one would not be able to use the Sokhotski–Plemelj theorem as presented (3.9). Instead, we would need to find analogous formulae with higher powers of x.

Conclusion

This thesis is a comprehensive review of the properties of a special class of solutions to Einstein-Maxwell equations involving a non-zero cosmological constant, namely the Kerr–Newman–(anti-)de Sitter family of space-times. After verifying compliance with the Einstein–Maxwell equations, we looked into their causal structure and presented all the four possible extremal scenarios. The conditions imposed on the parameters in the metric and the resulting positions of the horizons are compactly summarised in section 1.2.6 and the effects of parametric perturbations can be found in table 1.2 on page 25. We also gave the relevant Penrose diagrams for these solutions, beginning on page 28. After a brief comparison of the extremal Kerr–Newman–(anti-)de Sitter scenarios with those from the simpler Kerr space-time we concluded that the observed value of the cosmological constant does not allow real black holes to be over-rotating to a measurable degree. Next, we investigated the concept of frame-dragging and the related notion of ergosphere, proving that closed time-like curves must lie below the innermost ergosphere hidden under the first positive horizon (if applicable) in the process.

In the following and most extensive section, we dealt with the motion of test particles, both neutral and charged, in these backgrounds. Following our derivation of the equations and integrals of motion in the Lagrangian formalism, we showed that an equation of motion corresponding to a non-vanishing component of u_μ is interchangeable with the normalisation equation. Afterwards, we investigated static particles using the equations of motion. A charge-to-mass ratio allowing massive particles to stay at a given point in the used coordinates was discovered both on the axis (2.24) and in the equatorial plane (2.37). Moreover, we found out that static particles of arbitrary charge may be located on the axis at $r = \pm a$ for certain naked-singularity space-times with a negative cosmological constant. We also determined when these particles become zero angular momentum observers: a particle bound to the axis is always a ZAMO, and static particles in the equatorial plane must satisfy (2.40). Next, we focused on the equatorial plane, first specifying the necessary conditions the angular velocity of a particle must satisfy in order to stay in a stationary circular orbit with a given radius in section 2.4.1. However, after performing a few numerical experiments it became clear that the conditions are not sufficient, as we discovered some world lines satisfying the equations that have a negative time component of their four velocity, meaning these particles travel backwards through time, contrary to our common experience. The inability to distinguish between normal and antichronical particles was also detected in the effective potential, which we established after a short discussion of photon orbits. The effective potential was defined as $\dot{r}^2/2 = -V$ so that it behaved similarly as in classical mechanics for both massive particles (2.63) and photons (2.73). Unfortunately, we were unable to separate the characteristics of the particle and the dependence on the radial coordinate in V. Finally, we focused on radial motion on the axis. First, we examined radial null geodesics and performed the near-horizon approximation in section 2.5.1, which proved to be relevant in the following chapter on quatum tunnelling. Next, we performed a thorough analysis of the effective potential for charged massive particles (2.105). We were able to separate the integral of motion

classically corresponding to energy from the potential, defining the so-called lite potential (2.110) satisfying $W \leq E$ in the classically allowed areas. The lite potential was shown to be equivalent to the original one when examining the turning points, staticity and stability of static particles. Additionally, the lite potential was also found to ignore the problematic antichronical particles, for which one can derive an analogous lite potential (2.111). Using the effective potentials, we were able to reobtain our previous results for static particles both on the axis and in the equatorial plane. For static particles at $r = \pm a$ on the axis we were further able to show that their stability depends on their charge-to-mass ratio, which, interestingly, was irrelevant in the question of their staticity. The effective potential (2.141) showed there are no turning points for photons on the axis.

In the final chapter we introduced the null geodesic tunnelling method of calculating the temperature of horizons. We applied our previous results to find the inverse temperature of horizon R of multiplicity one (3.24), a result depending on the choice of coordinates due to the lack of a static observer in radial infinity in the examined space-time. We also summarized the inconsistencies present in the literature on the subject along with the issues arising from this approach and suggested ways of dealing with some of them. However, all things considered it should be noted that the method does indeed seem to have its flaws (most notably the lack of covariance and the inconsistent treatment of cyclic coordinates in the literature) and appears inferior to the Hamilton–Jacobi approach. We thoroughly recommend abandoning the null geodesic method of quantum tunnelling in favour of its more reliable sibling.

The thesis also comprises three appendices. Appendix A introduces an alternative Lagrangian and compares it with the one used in the second chapter. In the end, the obtained equations of motion were the same. Even though we know they hold for massive and massless particles alike, the alternative derivation strangely seemed to forbid massless particles. Appendix B shows how to deal with the electrogeodesic equations based on the Hamilton–Jacobi equation and calculates the corresponding conserved quantity, the Carter constant, for the general Kerr–Newman–(anti-)de Sitter space-time. Appendix C is a succinct look at the methods of determining the number of real roots of polynomials. We presented Descartes' rule of signs and Sturm's theorem and applied both to an appropriate polynomial from chapter 2, with both yielding the same result.

In the future, there are several ways in which our current work may be extended. Regarding particle motion, now that we have exhausted the Lagrangian formalism it seems logical to make use of the more robust Hamilton–Jacobi equation, germinating the seeds planted in appendix B. The papers that were among the sources of inspiration for this thesis [3, 4] took advantage of this equation to obtain a considerably more complete picture of motion (albeit in simpler scenarios) than we managed to do, and in principle the same could be performed for charged particles in the Kerr–Newman–(anti-)de Sitter space-time as well. Likewise, considering the Hamilton–Jacobi approach to quantum tunnelling seems preferable over the null geodesic method due to covariance of the former. However, the most immediate next step in following up on the thesis seems to be to thoroughly investigate the problem of extremal horizons in the tunnelling methods, based on the groundwork laid in section 3.2.2, albeit with the null geodesic method in mind.

Appendices

A. A tale of two Lagrangians

The Lagrangian of a system is not a unique function; any system may be represented be a number of Lagrangians yielding the same equations of motion. In particular, a free particle is commonly represented by two Lagrangian densities [17],

$$\mathcal{L}_0 = \frac{1}{2} g_{\mu\nu} \dot{x}^\mu \dot{x}^\nu \,, \tag{A.1}$$

$$\widetilde{\mathcal{L}}_0 = -\sqrt{-g_{\mu\nu} \dot{x}^\mu \dot{x}^\nu} \,. \tag{A.2}$$

For charged particles, an interaction part of the Lagrangian is to be added to the above [17, 58],

$$\mathcal{L}_{\text{int}} = \kappa \dot{x}^\mu A_\mu \,. \tag{A.3}$$

First, let us verify that the second Langrangian $\widetilde{\mathcal{L}} = \widetilde{\mathcal{L}}_0 + \mathcal{L}_{\text{int}}$ gives the same equations of motion: The partial derivatives of the Lagrangian are

$$\begin{aligned} \frac{\partial \widetilde{\mathcal{L}}}{\partial x^\alpha} &= \frac{1}{2} \frac{g_{\rho\sigma,\alpha} \dot{x}^\rho \dot{x}^\sigma}{\sqrt{-g_{\mu\nu} \dot{x}^\mu \dot{x}^\nu}} + \kappa \dot{x}^\beta A_{\beta,\alpha} \,, \\ \frac{\partial \widetilde{\mathcal{L}}}{\partial \dot{x}^\alpha} &= \frac{g_{\alpha\beta} \dot{x}^\beta}{\sqrt{-g_{\mu\nu} \dot{x}^\mu \dot{x}^\nu}} + \kappa A_\alpha \,. \end{aligned} \tag{A.4}$$

Inserting these into the Lagrange equations of the second kind,

$$\frac{\mathrm{d}}{\mathrm{d}p} \left(\frac{\partial \widetilde{\mathcal{L}}}{\partial \dot{x}^\alpha} \right) - \frac{\partial \widetilde{\mathcal{L}}}{\partial x^\alpha} = 0 \,, \tag{A.5}$$

and using

$$\sqrt{-g_{\mu\nu} \dot{x}^\mu \dot{x}^\nu} = \sqrt{-g_{\mu\nu} \frac{\mathrm{d}x^\mu}{\mathrm{d}p} \frac{\mathrm{d}x^\nu}{\mathrm{d}p}} = \frac{\mathrm{d}\tau}{\mathrm{d}p} \,, \tag{A.6}$$

we find

$$\frac{\mathrm{d}}{\mathrm{d}p} \left(\frac{\mathrm{d}p}{\mathrm{d}\tau} g_{\alpha\beta} \dot{x}^\beta + \kappa A_\alpha \right) - \frac{1}{2} \frac{\mathrm{d}p}{\mathrm{d}\tau} g_{\rho\sigma,\alpha} \dot{x}^\rho \dot{x}^\sigma - \kappa \dot{x}^\beta A_{\beta,\alpha} = 0 \,. \tag{A.7}$$

Knowing that

$$\frac{\mathrm{d}p}{\mathrm{d}\tau} \dot{x}^\mu = \frac{\mathrm{d}p}{\mathrm{d}\tau} \frac{\mathrm{d}x^\mu}{\mathrm{d}p} = \frac{\mathrm{d}x^\mu}{\mathrm{d}\tau} = u^\mu \,, \tag{A.8}$$

we multiply the previous equation by $\mathrm{d}p/\mathrm{d}\tau$ to obtain

$$\begin{aligned} &\frac{\mathrm{d}}{\mathrm{d}\tau} \left(g_{\alpha\beta} u^\beta + \kappa A_\alpha \right) - \frac{1}{2} g_{\rho\sigma,\alpha} u^\rho u^\sigma - \kappa u^\beta A_{\beta,\alpha} = \\ &\quad = g_{\alpha\beta} \frac{\mathrm{d}u^\beta}{\mathrm{d}\tau} + g_{\alpha\beta,\gamma} u^\beta u^\gamma + \kappa A_{\alpha,\beta} u^\beta - \frac{1}{2} g_{\rho\sigma,\alpha} u^\rho u^\sigma - \kappa u^\beta A_{\beta,\alpha} = 0 \,. \end{aligned} \tag{A.9}$$

We then get[1]

$$g_{\alpha\beta} \frac{\mathrm{d}u^\beta}{\mathrm{d}\tau} = \left(\frac{1}{2} g_{\rho\sigma,\alpha} - g_{\alpha\rho,\sigma} \right) u^\rho u^\sigma + \kappa F_{\alpha\beta} u^\beta \,. \tag{A.10}$$

[1]Please take note that, somewhat deceptively, $\mathrm{d}u^\mu/\mathrm{d}\tau$ is not the four-acceleration of the particle. Actually, it is not a tensor at all! The four-acceleration would, in fact, be $\mathrm{D}u^\mu/\mathrm{d}\tau$, where an absolute derivative is used instead of a total one. The presence of a non-covariant total derivative also means that we cannot carelessly lower the index in $\mathrm{d}u^\mu/\mathrm{d}\tau$ using the metric without a compensation of some sort.

It is evident that $u^\rho u^\sigma$ is symmetrical in ρ and σ. We can therefore take only the symmetrical part of $g_{\alpha\rho,\sigma}$ with respect to ρ and σ, which leads to

$$g_{\alpha\beta}\frac{\mathrm{d}u^\beta}{\mathrm{d}\tau} = -\Gamma_{\alpha\rho\sigma}u^\rho u^\sigma + \kappa F_{\alpha\beta}\,u^\beta\,. \tag{A.11}$$

Finally, by multiplying the equation by $g^{\mu\alpha}$, we rediscover the electrogeodesic equations,

$$\frac{\mathrm{d}u^\mu}{\mathrm{d}\tau} = -\Gamma^\mu{}_{\rho\sigma}u^\rho u^\sigma + \kappa F^\mu{}_\nu\,u^\nu\,, \tag{A.12}$$

or, equivalently,

$$\frac{\mathrm{D}u^\mu}{\mathrm{d}\tau} = \kappa F^\mu{}_\nu\,u^\nu\,. \tag{A.13}$$

The integrals of motion E and L become

$$\begin{aligned} -\widetilde{E} \equiv \frac{\partial\widetilde{\mathcal{L}}}{\partial\dot{t}} &= \frac{g_{tt}\dot{t} + g_{t\phi}\dot{\phi}}{\sqrt{-g_{\mu\nu}\dot{x}^\mu\dot{x}^\nu}} + \kappa A_t\,, \\ \widetilde{L} \equiv \frac{\partial\widetilde{\mathcal{L}}}{\partial\dot{\phi}} &= \frac{g_{t\phi}\dot{t} + g_{\phi\phi}\dot{\phi}}{\sqrt{-g_{\mu\nu}\dot{x}^\mu\dot{x}^\nu}} + \kappa A_\phi\,. \end{aligned} \tag{A.14}$$

Take note that unlike the original E and L these expressions cannot be used for massless photons. For massive particles parametrised by τ, the integrals of motion become the original ones (2.17).

Even though we have eventually obtained the same results as far as massive particles as concerned, there are some differences between the two Lagrangians. First, the computation was more straightforward with the original $\mathcal{L}$ and we obtained the affine form of the electrogeodesic equation rather effortlessly. However, nowhere during the derivation was there any indication that the only permissible affine parametrisation for massive particles was their proper time τ, as we managed to prove in the corresponding chapter. Here, keeping a general p was out of the question if we wanted to simplify the equations into the preferred form; for that we *needed* to eliminate the general parameter p from the equations in favour of the affine parameter τ. The chief reason for this move was the presence of the square root of the normalisation in the denominator of the partial derivatives of $\widetilde{\mathcal{L}}$, which also prohibits photons from being described by this Lagrangian, as these terms would diverge. Nonetheless, naively transferring from massive particles to photons in the result by simply swapping the corresponding quantities ($\tau \to \lambda$, $u^\mu \to \dot{x}^\mu$) and setting $\kappa = 0$ works fine despite the prohibitive derivation, as, in the end, we are still dealing with the same electrogeodesic equations as obtained originally.

B. The road not taken

The Hamilton–Jacobi equation and the Carter constant

In the part of the thesis dedicated to electrogeodesics we utilise the Lagrangian formalism. A frequently used alternative [3, 4] is the Hamilton–Jacobi equation, which can give us another constant of motion, the Carter constant. Even though we chose to proceed differently in the main body of work, let us, for the sake of completeness, derive the constant here, without further drawing any conclusions for particle motion from it.

The relativistic Hamilton–Jacobi equation reads

$$\mathcal{H}\left(x^\alpha, \frac{\partial S}{\partial x^\alpha}\right) + \frac{\partial S}{\partial \lambda} = 0\,, \tag{B.1}$$

where $\mathcal{H}$ is the Hamiltonian function of the system and S is the action, λ is the variable used to parametrise motion[1]. Notice that the components of the four-momentum p_α naturally appearing in the Hamiltonian $\mathcal{H}\left(x^\alpha, p_\alpha\right)$ are substituted for the derivatives of the action as an important application of canonical transformations of Hamiltonian mechanics.

First, let us derive the Hamiltonian

$$\mathcal{H} \equiv \dot{x}^\alpha p_\alpha - \mathcal{L}\Big|_{\text{Insert } \dot{x}^\alpha = \dot{x}^\alpha(p_\beta)}\,. \tag{B.2}$$

As the Lagrangian is not an explicit function of λ, neither is the Hamiltonian and its value is a constant of motion. The Lagrangian we shall use is

$$\mathcal{L} = \frac{1}{2} g_{\mu\nu}\dot{x}^\mu \dot{x}^\nu + \kappa \dot{x}^\mu A_\mu\,. \tag{B.3}$$

The generalised four-momentum is

$$p_\alpha \equiv \frac{\partial \mathcal{L}}{\partial \dot{x}^\alpha} = g_{\alpha\mu}\dot{x}^\mu + \kappa A_\alpha\,. \tag{B.4}$$

p_α defined in this way is primarily a transformation of $\dot{x}^\alpha$ and becomes the physical four-momentum only if $\dot{x}^\alpha = u^\alpha$, hence the word "generalised". To express $\dot{x}^\alpha$ as a function of p_α, let us multiply the previous equation by $g^{\alpha\beta}$, leading to

$$\dot{x}^\beta = p^\beta - \kappa A^\beta\,. \tag{B.5}$$

The Hamiltonian then becomes

$$\begin{aligned} \mathcal{H} &= \dot{x}^\alpha\left(g_{\alpha\mu}\dot{x}^\mu + \kappa A_\alpha\right) - \mathcal{L} = \frac{1}{2} g_{\mu\nu}\dot{x}^\mu \dot{x}^\nu = \\ &= \frac{1}{2} g_{\mu\nu}\left(p^\mu - \kappa A^\mu\right)\left(p^\nu - \kappa A^\nu\right) = \frac{1}{2} g^{\mu\nu}\left(p_\mu - \kappa A_\mu\right)\left(p_\nu - \kappa A_\nu\right)\,. \end{aligned} \tag{B.6}$$

[1] In order to avoid confusion with the four-momentum p_α, we avoid using p as the parameter in this section.

As it is proportional to the normalisation of (the used analogue of) the four-velocity, it is easy to see that the Hamiltonian of the charged particle is indeed constant. The Hamilton–Jacobi equation then becomes

$$\frac{1}{2}g^{\mu\nu}\left(\frac{\partial S}{\partial x^\mu}-\kappa A_\mu\right)\left(\frac{\partial S}{\partial x^\nu}-\kappa A_\nu\right)+\frac{\partial S}{\partial \lambda}=0\,. \tag{B.7}$$

As for the action, from section 2.1 we already know that two components of the generalised four-momentum are constant, as they correspond to cyclic coordinates in the Lagrangian,

$$\begin{aligned} -p_t &\equiv E=\text{const.}\,,\\ p_\phi &\equiv L=\text{const.}\,, \end{aligned} \tag{B.8}$$

meaning that the action is separated in these coordinates. Assuming further separability in the remaining two coordinates, the action becomes

$$S=-\frac{1}{2}\delta\lambda-Et+L\phi+R(r)+\Theta(\theta)\,, \tag{B.9}$$

where

$$\delta=g_{\mu\nu}\dot{x}^\mu\dot{x}^\nu\,. \tag{B.10}$$

The term with λ is separated too, as the Hamiltonian does not depend explicitly on λ. Its coefficient can be obtained by integrating (B.1) after substituting $\mathcal{H}=\delta/2$ from (B.6). For massive particles parametrised by their proper time, $\delta=-1$ is the normalisation of the four-velocity. Unlike the Lagrangian formalism, however, these equations do not coerce us into using the proper time, as a different (non-affine) parameter does not complicate the form of the Hamilton–Jacobi equation, it only changes the value of δ.

Next, we need to insert S into the Hamilton–Jacobi equation (B.7). After a straightforward computation, we separate the terms with r and θ and rewrite the equation as

$$\begin{aligned} &-\delta a^2\cos^2\theta+\Delta_\theta(\theta)\Big(\Theta'(\theta)\Big)^2+\frac{\Xi^2}{\Delta_\theta(\theta)\sin^2\theta}\Big(L-Ea\sin^2\theta\Big)^2=\\ &\quad=\delta r^2-\Delta_r(r)\Big(R'(r)\Big)^2+\frac{\Xi^2}{\Delta_r(r)}\left(La-E(a^2+r^2)+\frac{r}{\Xi}q\kappa\right)^2\equiv K\,. \end{aligned} \tag{B.11}$$

Due to the equation being separable, S is indeed separable in every variable as assumed originally and the values of both sides of the equation must be equal to a constant of motion K, called the Carter constant. To analyse motion itself, one must first obtain $R(r)$ and $\Theta(\theta)$ from the Carter constant, if only in an integral form, and, in doing so, the full expression for S. Then, derivatives of S with respect to the constants of motion δ, E, L and K are constants themselves, yielding a simpler set of equations to describe motion. But that is a story for another time perhaps...

After setting q or κ equal to zero, the Carter constant (B.11) reduces to the one derived in [4] with $\delta\to-\delta$, as the referred paper uses the opposite signature of the metric. Interestingly, our original result is then reobtained after substituting

$$\begin{aligned} E &\to E-\frac{r}{\Xi\rho^2(r,\theta)}q\kappa\,,\\ L &\to L-\frac{ar\sin^2\theta}{\Xi\rho^2(r,\theta)}q\kappa\,. \end{aligned} \tag{B.12}$$

The additional variable dependence gets subtracted on both sides of the equation.

C. Positive roots of polynomials

During the course of this thesis we encountered a significant number of polynomials. It is a well known fact that finding roots is easy for polynomials of degree up to two. For third-degree polynomials one can use Cardano's formulae, as we on one occasion did, but these are somewhat more complicated. The highest generic polynomials whose roots can be found analytically are those of degree four, but the resulting expressions are very convoluted and usually of no use to us. It is often said that before his untimely demise at age 20 due to a gunshot wound sustained in a duel, Évariste Galois managed to prove that there shall never be a radical formula for the roots of generic polynomials of degree five and higher. In reality, however, while parts of the Frenchman's work also concerned solvability of polynomials, the proof was discovered a couple of years prior in 1824 by Norwegian mathematician Niels Henrik Abel (who also died young at 26) [59].

Sometimes, however, we do not need to know the values of the roots, as we would be content simply knowing how many of them are positive. During our research, we came across two theorems that can aid us in our quest to determine this number. However, as it turns out, in most cases neither of these is of any assistance to us, as the older one only gives the upper bound on the number of positive roots and the newer one is quite difficult to apply in itself. Nonetheless, months after we first considered using them in more difficult situations, we obtained equation (2.40) for the roots of the polynomial

$$p(r) = 2\Lambda r^3 + \Lambda a^2 r + 3m \tag{C.1}$$

with $m > 0$, $a^2 > 0$ and $\Lambda \neq 0$, which happened to be the perfect candidate for both of these theorems to be put into practice, as we were mainly interested in the number of positive roots[1]. Now, without further ado, let us introduce the two theorems and demonstrate them on the polynomial in question. Proofs and additional information are to be found in the cited bibliography.

Descartes' rule of signs [60] was first published in *La Géométrie*, an appendix to 1637's *Discours de la méthode* by René Descartes[2]. The rule says that the number of sign changes in the sequence of the coefficients in polynomial $p(x)$ (omitting zeroes) gives the upper bound on the number of positive real roots (including multiplicities). Moreover, the exact quantity may be lower by an even number only. Thus, the rule does give the exact result if and only if there are less than two sign changes, which makes it more difficult for the rule to be useful for polynomials of higher degrees, where one can expect multiple sign changes. If needed, this rule can also give the upper bound on the number of negative real roots by considering polynomial $p(-x)$ instead of $p(x)$.

Now, for the currently studied polynomial (C.1), we need to consider two cases with respect to the sign of Λ. In table C.1 we wrote down the signs of the

[1] Recall that equation (2.40) gave the positions of static ZAMOs in the equatorial plane for space-times with $a > 0$. For space-times with $a = 0$ no such condition was necessary, as all static particles were ZAMOs automatically.

[2] As a short philosophical intermezzo, let us mention that the book is also the source of the famous quotation "I think, therefore I am" in its French original "Je pense, donc je suis". Interestingly, the Latin variant "Cogito ergo sum" did not appear until seven years later in Descartes' *Principia philosophiae*, which was written in Latin, unlike the previous work.

individual coefficients for a given sign of Λ. From the table one can immediately see that for a positive Λ the polynomial has no positive roots, while for a negative Λ it has one.

Term	$\Lambda > 0$	$\Lambda < 0$
r^3	$+$	$-$
r^2	0	0
r^1	$+$	$-$
r^0	$+$	$+$
Sign changes:	0	1

Table C.1: Descartes' rule applied on (C.1)

Sturm's theorem [61], first published by French mathematician Jacques Charles François Sturm in 1835 (almost 200 years after Descartes' work), gives the exact number of real roots in an almost arbitrary real interval $(a, b) \subset \mathbb{R}$, with the only condition that a and b are not roots of the polynomial themselves. The theorem is, therefore, much more robust than the rule of signs, which only estimates (not necessarily precisely) the number of roots on a half of the real axis, but it is also understandably more complicated, which excludes the use of the theorem in most of the thesis[3].

Before we present the theorem itself, we first need to introduce a so-called Sturm sequence of polynomials for $p(x)$. The standard sequence[4] begins with $p_0(x) = p(x)$ and $p_1(x) = p'(x)$, with the remaining polynomials defined as

$$p_{i+1}(x) = p_i(x)q_{i-1}(x) - p_{i-1}(x) = -\mathrm{rem}(p_{i-1}, p_i)(x) \tag{C.2}$$

for $i \geq 1$, with q_j being the quotient and $\mathrm{rem}(p_j, p_{j+1})$ the remainder of polynomial division of p_j by p_{j+1}. The degree of polynomials in the sequence is decreasing and the sequence ends with the last non-zero remainder. Further, let us denote $\delta(x_0)$ the number of sign changes in the standard sequence at $x = x_0$, again ignoring zeroes. The theorem then states that the number of distinct real roots (that is, excluding multiplicities) in real interval (a, b) satisfying $p(a) \neq 0$ and $p(b) \neq 0$ is equal to $\delta(a) - \delta(b)$. In order to obtain the number of positive roots, one should set $a = 0$ and formally $b = \infty$; for $\delta(\infty)$ one only needs to consider the leading terms in the polynomials of the Sturm sequence.

For (C.1) the standard sequence is

$$\begin{aligned} p_0(r) &= 2\Lambda r^3 + \Lambda a^2 r + 3m\,, \\ p_1(r) &= 6\Lambda r^2 + \Lambda a^2\,, \\ p_2(r) &= -\frac{2}{3}\Lambda a^2 r - 3m\,, \\ p_3(r) &= -\Lambda a^2 - \frac{243m^2}{2\Lambda a^4}\,. \end{aligned} \tag{C.3}$$

[3] If polynomials' coefficients were *numbers*, the theorem would be applied quite easily. Unfortunately, we want to deal with *letters*...

[4] A Sturm sequence is defined by the properties of the polynomials. The provided formulae are one way of constructing the sequence.

The results, consistent with Descartes' rule, are written in table C.2 for both signs of Λ.

	$\Lambda > 0$		$\Lambda < 0$	
Polynomial	Sign at 0	Sign at ∞	Sign at 0	Sign at ∞
p_0	$+$	$+$	$+$	$-$
p_1	$+$	$+$	$-$	$-$
p_2	$-$	$-$	$-$	$+$
p_3	$-$	$-$	$+$	$+$
Sign changes:	$\delta(0) = 1$	$\delta(\infty) = 1$	$\delta(0) = 2$	$\delta(\infty) = 1$
Positive roots:	$\delta(0) - \delta(\infty) = 0$		$\delta(0) - \delta(\infty) = 1$	

Table C.2: Sturm's theorem applied on (C.1)

Take note that considering the amount of information one can extract about the roots, there are other methods somewhere in between these two, such as the Budan–Fourier theorem [60], which gives the upper bound on the number of roots in an interval. We elected to examine the two methods only, as the former one represents the most effortless yet imprecise way of estimating the number of positive roots, while the latter one is the precise (and for our needs usually unusable) method.

Bibliography

[1] Maldacena, J. M. The Large N limit of superconformal field theories and supergravity. *Advances in Theoretical and Mathematical Physics* **2** (1998) 231.

[2] Aharony, O., Gubser, S. S., Maldacena, J., Ooguri, H., Oz, Y. Large N Field Theories, String Theory and Gravity. *Physics Reports* **323** (2000) 183.

[3] Hackmann, E., Xu, H. Charged particle motion in Kerr–Newmann space-times. *Physical Review D* **87** (2013) 124030.

[4] Hackmann, E., Lämmerzahl, C., Kagramanova, V., Kunz, J. Analytical solution of the geodesic equation in Kerr–(anti-) de Sitter space-times. *Physical Review D* **81** (2010) 044020.

[5] Parikh, M. K., Wilczek, F. Hawking Radiation as Tunneling. *Physical Review Letters* **85** (2000) 5042.

[6] Hawking, S. W. Black hole explosions? *Nature* **248** (1974) 5443.

[7] Hawking, S. W. Particle creation by black holes. *Communications in Mathematical Physics* **43** (1975) 199.

[8] Griffiths, J. B., Podolský, J. *Exact Space-Times in Einstein's General Relativity.* Cambridge: Cambridge University Press, 2009, xvii, 525 s. ISBN 978-0-521-88927-8.

[9] Planck Collaboration Planck 2015 results. XIII. Cosmological parameters. *Astronomy and Astrophysics* **594** (2016) A13.

[10] Lauer, T. R. et al. The Masses of Nuclear Black Holes in Luminous Elliptical Galaxies and Implications for the Space Density of the Most Massive Black Holes. *The Astrophysical Journal* **662** (2007) 808.

[11] Nielsen, A. B. On the distribution of stellar-sized black hole spins. *Journal of Physics: Conference Series* **716** (2016) 012002.

[12] Bambi, C. et al. *Astrophysics of Black Holes: From Fundamental Aspects to Latest Developments.* Berlin Heidelberg: Springer-Verlag, 2016, xi, 207 s. ISBN 978-3-662-52857-0.

[13] Gou, L. et al. The extreme spin of the black hole in Cygnus X-1. *The Astrophysical Journal* **742** (2011) 85.

[14] Gibbons, G. W., Shellard, E. P. S., Rankin, S. J. *The Future of Theoretical Physics and Cosmology: Celebrating Stephen Hawking's Contributions to Physics.* Cambridge: Cambridge University Press, 2003, xxvi, 879 s. ISBN 0-521-82081-2.

[15] Monroe, H. Are Causality Violations Undesirable? *Foundations of Physics* **38** (2008) 1065.

[16] Andréka, H., Németi, I., Wüthrich, C. A twist in the geometry of rotating black holes: seeking the cause of acausality. *General Relativity and Gravitation* **40** (2008) 1809.

[17] Blau, M., 2016. *Lecture Notes on General Relativity* [online]. Universität Bern. Last revision: 8 August 2016 [cit. 10 July 2017]. Available from: `http://www.blau.itp.unibe.ch/newlecturesGR.pdf`

[18] Luongo, O., Quevedo, H. Characterizing repulsive gravity with curvature eigenvalues. *Physical Review D* **90** (2014) 084032.

[19] Boshkayev, K., Gasperín, E., Gutiérrez-Piñeres, A. C., Quevedo, H., Toktarbay, S. Motion of test particles in the field of a naked singularity. *Physical Review D* **93** (2016) 024024.

[20] Berti, E., 2014. *A Black-Hole Primer: Particles, Waves, Critical Phenomena and Superradiant Instabilities* [online]. Bad Honnef School "GR@99". Last revision: 14 October 2014 [cit. 12 July 2017]. Available from: `https://arxiv.org/pdf/1410.4481v2.pdf`

[21] Stuchlík, Z., Bao, G., Østgaard, E., Hledík, S. Kerr–Newman–de Sitter black holes with a restricted repulsive barrier of equatorial photon motion. *Physical Review D* **58** (1998) 084003.

[22] Stuchlík, Z., Hledík, S. Equatorial photon motion in the Kerr–Newman spacetimes with a non-zero cosmological constant. *Classical and Quantum Gravity* **17** (2000) 4541.

[23] Cruz, N., Olivares, M., Villanueva, J. R. The geodesic structure of the Schwarzschild Anti–de Sitter black hole. *Classical and Quantum Gravity* **22** (2005) 1167.

[24] Grøn, Ø., Hervik, S. *Einstein's General Theory of Relativity: With Modern Applications in Cosmology.* London: Springer London, 2007, xx, 538 s. ISBN 978-0-387-69199-2.

[25] Stuchlík, Z., Slaný, P. Equatorial circular orbits in the Kerr–de Sitter spacetimes. *Physical Review D* **69** (2004) 064001.

[26] Barceló, C., Liberati, S., Visser, M. Towards the observation of Hawking radiation in Bose–Einstein condensates. *International Journal of Modern Physics A* **18** (2003) 3735.

[27] Belgiorno, F. et al. Hawking radiation from ultrashort laser pulse filaments. *Physical Review Letters* **105** (2010) 203901.

[28] Steinhauer, J. Observation of quantum Hawking radiation and its entanglement in an analogue black hole. *Nature Physics* **12** (2016) 959.

[29] Parikh, M. K. A Secret tunnel through the horizon. *International Journal of Modern Physics D* **13** (2004) 2351; *General Relativity and Gravitation* **36** (2004) 2419.

[30] Vanzo, L., Acquaviva, G., Di Criscienzo, R. Tunnelling methods and Hawking's radiation: achievements and prospects. *Classical and Quantum Gravity* **28** (2011) 183001.

[31] Zhang, J. Black hole quantum tunnelling and black hole entropy correction. *Physics Letters B* **668** (2008) 353.

[32] Kraus, P., Wilczek, F. Self-Interaction Correction to Black Hole Radiance. *Nuclear Physics B* **433** (1995) 403.

[33] Blanchard, P., Brüning, E. *Mathematical Methods in Physics: Distributions, Hilbert Space Operators and Variational Methods.* Boston: Birkhäuser, 2003, xxiii, 471 s. ISBN 0-8176-4228-5.

[34] Li, G. Q. Hawking radiation via tunneling from Kerr-Newman-de Sitter black hole. *Europhysics Letters* **76** (2006) 203.

[35] Angheben, M., Nadalini, M., Vanzo, L., Zerbini, S. Hawking Radiation as Tunneling for Extremal and Rotating Black Holes. *Journal of High Energy Physics* **0505** (2005) 014.

[36] Ali, M. H., Sultana, K. Tunneling of Charged Massive Particles from Taub-NUT-Reissner-Nordström-AdS Black Holes. *International Journal of Theoretical Physics* **53** (2014) 1441.

[37] Kerner, R., Mann, R. B. Tunnelling, Temperature and Taub-NUT Black Holes. *Physical Review D* **73** (2006) 104010.

[38] Wu, X., Gao, S. Tunneling effect near a weakly isolated horizon. *Physical Review D* **75** (2007) 044027.

[39] Lin, H. C., Soo, C. Generalized Painlevé–Gullstrand descriptions of Kerr-Newman black holes. *General Relativity and Gravitation* **45** (2013) 79.

[40] Vanzo, L. On tunneling across horizons. *Europhysics Letters* **95** (2011) 20001.

[41] Ma, Z. Z. Hawking temperature of Kerr-Newman-AdS black hole from tunneling. *Physics Letters B* **666** (2008) 376.

[42] Belinski, V. A. On tunnelling through the black hole horizon. *Physics Letters A* **376** (2012) 207.

[43] Unruh, W. G. Notes on black-hole evaporation. *Physical Review D* **14** (1976) 870.

[44] Aliev, A. N. Electromagnetic Properties of Kerr–anti-de Sitter Black Holes. *Physical Review D* **75** (2007) 084041.

[45] Sekiwa, Y. Thermodynamics of de Sitter Black Holes: Thermal Cosmological Constant. *Physical Review D* **73** (2006) 084009.

[46] Dehghani, M. H., KhajehAzad, H. Thermodynamics of a Kerr Newman de Sitter black hole. *Canadian Journal of Physics* **81** (2003) 1363.

[47] Caldarelli, M. M., Cognola, G., Klemm, D. Thermodynamics of Kerr-Newman-AdS Black Holes and Conformal Field Theories. *Classical and Quantum Gravity* **17** (2000) 399.

[48] Li, H. et al. Hawking radiation of Kerr-Newman-de Sitter black hole. *European Physical Journal C* **63** (2009) 133.

[49] Hawking, S. W., Hunter, C. J., Taylor-Robinson, M. M. Rotation and the AdS/CFT correspondence. *Physical Review D* **59** (1999) 064005.

[50] Jiang, Q. Q., Wu, S. Q. Hawking radiation from rotating black holes in anti-de Sitter spaces via gauge and gravitational anomalies. *Physics Letters B* **647** (2007) 200.

[51] Kostelecký, V. A., Perry, M. J. Solitonic black holes in gauged N=2 supergravity. *Physics Letters B* **371** (1996) 191.

[52] Wu, S. Q., Jiang, Q. Q. Remarks on Hawking radiation as tunneling from the BTZ black holes. *Journal of High Energy Physics* **0603** (2006) 079.

[53] Jiang, Q. Q., Wu, S. Q., Cai Xi. Hawking radiation as tunneling from the Kerr and Kerr–Newman black holes. *Physical Review D* **73** (2006) 064003.

[54] Zhang, J., Zhao, Z. Charged particles' tunnelling from the Kerr-Newman black hole. *Physics Letters B* **638** (2006) 110.

[55] Wu, S. Q., Deng, G. M., Wu, D. Hawking radiation from rotating AdS black holes in conformal gravity. *Astrophysics and Space Science* **352** (2014) 751.

[56] Stotyn, S., Schleich, K., Witt, D. M. Observer Dependent Horizon Temperatures: a Coordinate-Free Formulation of Hawking Radiation as Tunneling. *Classical and Quantum Gravity* **26** (2009) 065010.

[57] Kraus, P., Wilczek, F. Effect of Self-Interaction on Charged Black Hole Radiance. *Nuclear Physics B* **437** (1995) 231.

[58] Pugliese, D., Quevedo, H., Ruffini R. Motion of charged test particles in Reissner–Nordström spacetime. *Physical Review D* **83** (2011) 104052.

[59] Alekseev, V. B. *Abel's theorem in problems and solutions: Based on the lectures of Professor V. I. Arnold.* Dordrecht: Kluwer Academic Publishers, 2004, xiv, 269 s. ISBN 1-4020-2186-0.

[60] Curtiss, D. R. Recent Extensions of Descartes' Rule of Signs. *Annals of Mathematics* **19** (1918) 251.

[61] Cohn, P. M. *Basic algebra: groups, rings and fields.* London: Springer London, 2003, xii, 465 s. ISBN 978-0-85729-428-9.